The morphological, physiological, and anatomical responses of temperate trees to climate change and their greenhouse gas emissions

Abdulrazaq Iliya Abubakar, B.Sc., M.Sc.

July 2024

Thesis submitted to the University of Nottingham for the degree of Doctor of Philosophy

Acknowledgements

I would like to express my deepest gratitude to my main supervisor, Prof. Sofie Sjögersten, for her invaluable guidance, support, and encouragement throughout the course of my research and thesis writing. I am also profoundly grateful to my second supervisors, Dr. Guillermina Mendiondo, Dr Nick Girkin and to Professor Barry Lomax and Professor Colin Osborne for their continuous support, constructive criticism, and invaluable contributions.

I would also like to all the staff at the University of Nottingham, particularly John Corrie for his help with the growth rooms, John Alcock and Matthew Tovey for logistical support, and Laura Holt for her help with gas analysis and lab assistance. Thanks to Becky Graham for her help analysing data and Dr Umar Mohammed for his invaluable help in the lab and providing advice during the project.

I sincerely thank all my friends for or creating a supportive and stimulating academic environment, without the support and care of my friends the journey would have not been a memorable one. I owe a special debt to my lovely wife for supporting me and always being there for me all these years. Also, my parents and brothers for their continued support and prayers. I thank you all for being there for me.

This work was supported by Yobe State Government, Nigeria and Petroleum Technology Development Fund (AIA/1865/2020PHD172).

Table of Contents

List of Figures

List of Tables

Abbreviations and Symbols

A	Photosynthesis
aCO_2	Ambient Carbon dioxide
eCO_2	Elevated Carbon dioxide
AFWL	After waterlogging
AR	Adventitious root
AT	Ambient temperature
ATP	Adenosine triphosphate
BWLG	Before waterlogging
CH_4	Methane
CO_2	Carbon Dioxide
DWLG	During waterlogging
E	Transpiration
ET	Elevated temperature
Gs	Stomatal conductance
GHG(s)	Greenhouse gas(es)
N_2O	Nitrogen oxide
O_2	Oxygen
PVC	Polyvinyl chloride
ROS	Reactive oxygen species
SE	Standard Error
WUE	Water use efficiency

Chapter 1: General introduction

1.1 Introduction

This research uses extensive ex-situ and mesocosm experiments to examine the physiology, morphology, and anatomy of saplings to the impact of climate change in wooded temperate forest and assess their greenhouse gas emissions. This introductory chapter provides context for the research, explains the knowledge gap, presents the research objectives, and outlines the thesis structure.

1.1.1.1 Temperate forest and global climate change

Forest provides ecosystem services such as timber, biomass, carbon, litter decomposition, soil fertility and regulating carbon, water and nitrogen cycles (Jager et al. 2015; Hao et al. 2020). Temperate forest covers 16% geographical area (665.8 million ha) of the world's forest (FAO 2020) and is the second largest biome distributed in eastern North America, North eastern Asia, Western and Central Europe (Gilliam 2016), yet plays an important role in global biogeochemical cycling of greenhouse gases (GHGs). GHGs particularly methane (CH_4), carbon dioxide (CO_2) and nitrous oxide (N_2O) and most of their global emissions have been attributed to anthropogenic sources (Fig. 1.1). Over the past decades, there has been continuing growth in emissions and atmospheric concentrations of GHGs, although at different rates (IPCC 2022). The largest absolute growth in emissions comes from CO_2 in fossil fuels and industry followed by CH_4 (Fig 1.1). GHGs are emitted from both natural and human-made sources, and the increased concentration of GHGs in the atmosphere over the past century are caused by human activities such as burning fossil fuels, deforestation, industrial process, and agriculture.

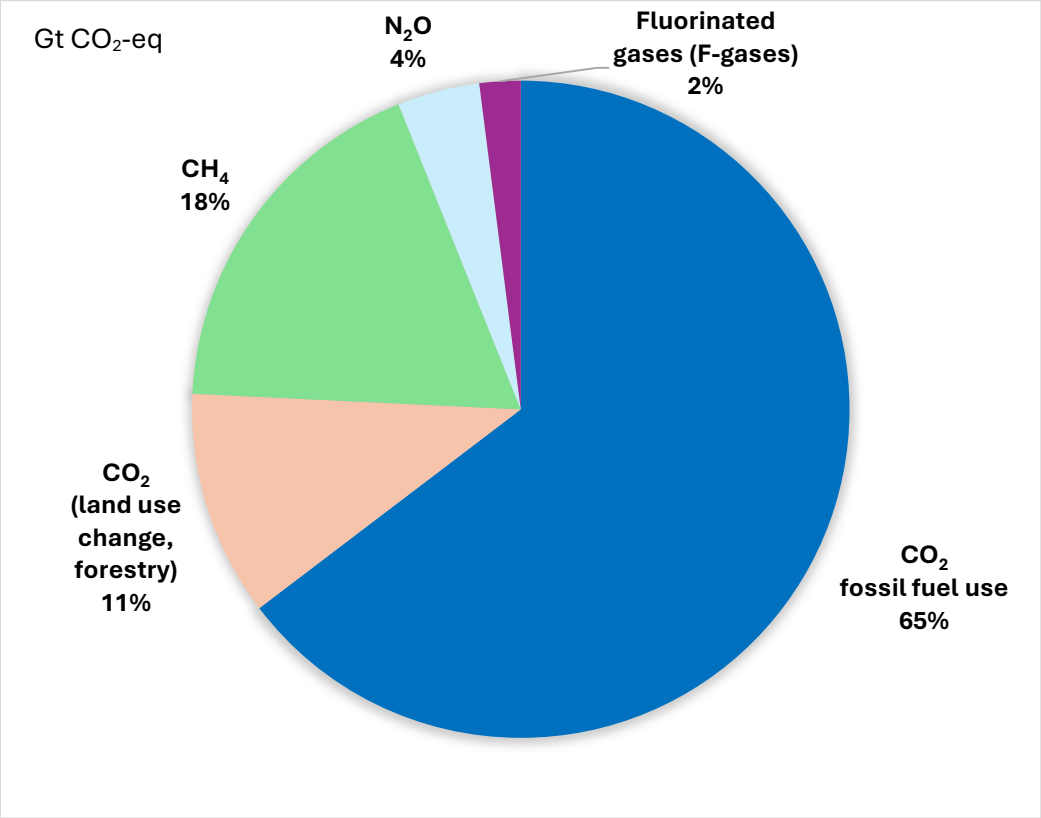

Figure 1:1 Global anthropogenic greenhouse gas emissions in 2019. Source IPCC, Sixth Assessment Report (AR6), (Source: Climate Change, 2022).

1.1.1.2 Impacts of global climate change on temperate trees

Global climate change as a result of increasing concentration of GHGs, mainly CO_2, CH_4 and N_2O has warmed the Earth's climate by 0.6°C from 1990 to 2022 and is expected to increase warming by another 1.5-3.2 °C by the year 2100 (IPCC 2022; Liu et al. 2023). In addition to the unprecedented rising of mean annual temperatures, there will also be recurrence of flooding, drought, heat waves and fire (Wagner 1996; Bowles et al. 2020). As a consequence, temperate saplings in the future will not only be exposed to elevated levels of CO_2, but will also likely experience severe warmth as a result of elevated temperature, which can result in negative ecosystem productivity (Saxe et al. 1998) and biodiversity (Thomas et al. 2004). In this regard, it has been reported that 30 years of warmer temperatures have greatly impacted the geographic distribution of species, seasonal timing, and community composition and dynamics (Walther et al. 2002). Consequently, the length of growing season for plants has increased over the decade and has occurred progressively since the 1960s (Walther et al. 2002).

In this regard, temperate regions have experienced a decadal increase of 0.5-1% in precipitation which mostly occurs in autumn and winter (EEA 2012).

1.1.1.3 Impacts of elevated CO_2 on temperate trees

Increasing emissions of CO_2 in the atmosphere can impact ecophysiological processes. Previous studies have demonstrated that raising CO_2 promotes tree development and the results from short-term studies with saplings, field studies using saplings and longer term free-air CO_2 enrichment (FACE) experiments have been previously evaluated (Medlyn et al. 1999; Norby et al. 2006; Gardner et al. 2022). Growth improvement resulting from CO_2 enrichment typically happens when net photosynthesis rates increase by 40-80% which is followed by an increase in leaf area (Saxe et al. 1998; Medlyn et al. 1999). These short-term studies with saplings have been shown to increase photosynthesis more than the long-term responses. The main cause of the downward acclimation with time of photosynthesis appears to be N concentration (Ellsworth et al. 2012). In young trees with expanding canopies, increased leaf production has been linked to elevated CO_2 (Ainsworth and Rogers 2007). Furthermore, the physiological responses of large, mature forest trees to increased CO_2 are similar to the younger trees employed in the majority of investigations (Bader et al. 2010).

1.1.1.4 Impacts of precipitation on temperate trees

Due to the changes in global atmospheric carbon dioxide and temperature, there will also be increases in the severity duration and frequency of flooding events (Bowles et al. 2020). In North Europe, annual precipitation is likely to increase whereas it will decrease in other regions of the world (Christensen et al. 2007). However, winter precipitation is expected to increase in the future, but summer precipitation will be lower resulting in a droughts during summer months (Palmer and Räisänen 2002). As a result of such intense rainfall events, terrestrial ecosystems in North Europe will face more and probably longer waterlogging periods during

winter and spring and more severe short term flooding periods during summer (Christensen and Christensen 2003).

Waterlogging of soils can have various impacts on temperate trees such as reduced oxygen supply, root rot, nutrient imbalance, and disruption of mycorrhizal associations (Kreuzwieser et al. 2002; Dolman et al. 2018a). Moreover, the majority of temperate forest species are sensitive to waterlogging because it greatly reduces the rates at which oxygen and carbon dioxide diffuse through the roots and stems of the plants, inhibiting photosynthesis and respiration. During waterlogging, trees endure environmental distresses such as decreased access to atmospheric CO_2 and O_2, hindered outward diffusion of plant evolved ethylene (C_2H_4) (Colmer and Voesenek 2009b), electrochemical soil changes leading to higher concentrations of toxic elements including sulfide (H_2S, HS^-. S^{2-}), manganese (Mn^{2+}) and iron (Fe^{2+}) (Voesenek and Bailey-Serres 2015) and reduction in available light (Glenz et al. 2006). As a result, tissues and cells are subjected to a distinct difference in CO_2 and O_2 and increase in ethylene as well as reactive nitrogen and reactive oxygen species (ROS). ROS are formed at the beginning of flooding induced O_2 deprivation as a consequence of the inhibition of mitochondrial electron transport and generation of superoxide that in converted to hydrogen peroxide by dismutation (Colmer and Voesenek 2009a). However, superoxide and hydrogen peroxide both decline upon reaeration (Jaeger et al. 2009) (Fig. 1.2).

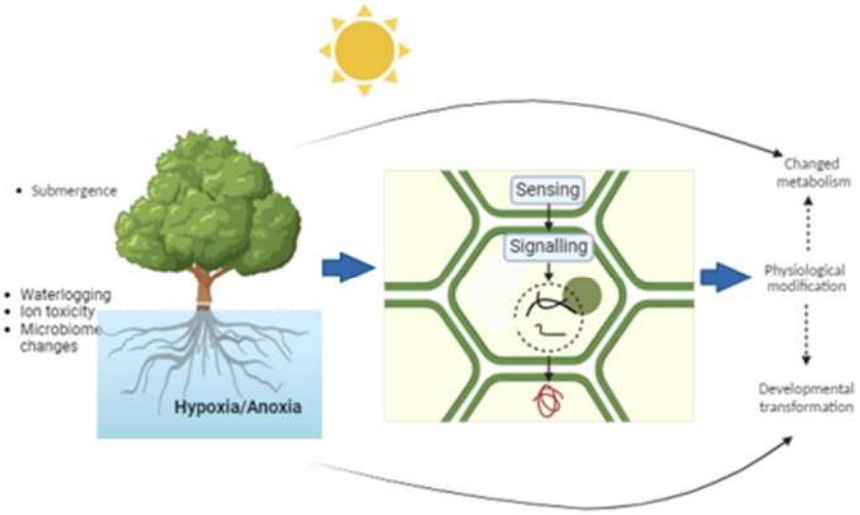

Primary event	Secondary effect	Signalling	Key responses	Reaeration
Prolong complete submergence	low CO_2 in light low O_2 in dark reduced C and N	ethylene reduced light low O_2 NO ROS	**Low oxygen Quiescence strategy (LOQS)** Quiescence of metabolism and growth; meristem or organ protection	ROS dehydration
Partial submergence	low CO_2 in light low O_2 in dark	ethylene reduced light	**Low-oxygen Escape Strategy (LOES)** Escape by elongation of aerial organs	ROS
Root waterlogging	Low O_2 toxic ions reduced C and N	ethylene ROS low O_2	Increased ventilation via aerenchyma or adventitious roots; reduced O_2 loss by barrier formation	ROS

Figure 1:2: Overview of flooding stimuli that trigger plasticity in plant physiology and development. The low-O_2 quiescence strategy (LOQS) is associated with plants that endure prolonged complete submergence. The low-O_2 escape strategy (LOES) is also triggered by submergence but is generally characterized by stimulated elongation of submerged organs, ultimately increasing gas exchange between aerial and submerged tissues.

1.2 Adaptation of waterlogging tolerance in trees

Plant adaptation to waterlogging hypoxia/anoxia includes a switch in physiological, morphological and anatomical changes commonly observed when O_2 availability becomes limiting (Visser and Voesenek 2005) which comprise the formation of hypertrophied lenticels, the initiation of adventitious roots and the development of aerenchyma.

1.2.1 Physiological adaptation

When trees are partially waterlogged, one of the physiological processes that is most frequently researched is leaf gas exchange, specifically net CO_2 assimilation. Assimilation rates generally tend to decline in conditions of waterlogging stress, as temperate (Pezeshki 2001; Jaeger et al. 2009; Ferner et al. 2012) and tropical (Ojeda et al. 2004; Hasper et al. 2017) trees demonstrate. The species ability to tolerate low soil oxygen levels determines the extent of a decline that will occur. While less tolerant or sensitive species' net CO_2 assimilation is significantly reduced, highly tolerant trees maintain very high rates of photosynthesis or are completely unaffected by the stress (Vu and Yelenosky 1991; Parent et al. 2008).

Waterlogging results in the impairment of photosynthesis and there is a strong indication that both stomatal and non-stomatal limitation are involved. Waterlogging causes stomatal closure, which has been reported in several studies as the main reason for reduced photosynthesis in numerous trees (Wang and Kellomaki 1997; Gravatt and Kirby 1998; Du et al. 2012; Zúñiga-Feest et al. 2017). It is assumed to be related to decreased root hydraulic conductivity, which lowers the roots' ability to absorb water, or it could be as a result of chemical signals which are transported from waterlogged roots to the shoot through transpiration stream. On the other hand, non-stomatal limitations are linked with lowered pigment concentrations in leaves of waterlogged trees (Kreuzwieser et al. 2002), decreased activity (Vu and Yelenosky 1991) and abundance (Pires et al. 2018) of ribulose-1,5-bisphosphate carboxylase (Rubisco) and

accumulation of soluble carbohydrates which might lead to feedback inhibition of photosynthesis (Vu and Yelenosky 1991; Ferner et al. 2012).

1.2.2 Morphological and anatomical adaptation

Trees have developed diverse morphological modifications that alleviate root respiratory depression and damage caused by disrupted energy metabolism during waterlogging. The production of adventitious root (AR) upward bending of leaves (hyponasty), enhanced shoot elongation, induction of barriers to radial O_2 loss (ROL), hypertrophied lenticels at the stems base and the formation of aerenchyma are the primary morphological alterations (Kozlowski 1997; Jackson and Armstrong 1999b; Glenz et al. 2006). Among these traits, the developmental plasticity that promotes the creation of aerenchyma and AR formation as well as elongation of aerial organs is becoming increasingly studied. All include ethylene, but the first two also involve ROS, whereas the latter is controlled by a hormonal network including abscisic acid (ABA) and gibberellin (GA).

Adventitious roots are formed in the hypocotyl internodes or at the base of the stem after prolonged waterlogging, where they facilitate gas exchange and the uptake of water and nutrients. To a certain extent, AR formation can substitute the primary roots that die due to waterlogging stress, and provide normal growth and development as well as maintain metabolic cycles (Dong et al. 2015; Wang et al. 2015b). Compared to the primary roots, the newly generated ARs have more aerenchyma, which improves their capacity to absorb and diffuse oxygen (Visser and Voesenek 2005).

Another response of trees to waterlogging is rapid extension of their apical meristems. Tender stems and internodes quickly elongate to allow for quick escape from the anoxic environment and bring contact with the air as soon as possible, which permits normal respiration (Bailey-Serres et al. 2012). This response is called low oxygen escape syndrome (LOES) (Fig. 1.2).

Internodes of submerged parts of the trees elongate quickly: waterlogging produces ethylene and promotes synthesis of gibberellins, thereby resulting in internode elongation (Voesenek and Bailey-Serres 2015).

Formation of aerenchyma as a result of waterlogging occurs via programmed cell death and degradation in cortical cells of plant root under hypoxia, creating tissue cavities. Aerenchyma not only can transport O_2 from non-waterlogged tissue to the root system, but also discharge CO_2 and toxic volatile substances from waterlogged tissue. It is therefore possible for aerenchyma to provide the possibility of gas exchange within plants and is necessary for upholding the normal physiological metabolism in the cells of waterlogged roots (Drew et al. 2000a; Evans 2003; Yamauchi and Nakazono 2022).

1.2.2.1 Lysigenous versus Schizogenous aerenchyma

There are two types of aerenchyma which can be distinguished, although intermediate forms do occur. Lysigenous aerenchyma are most abundant in roots and rhizomes and are initiated by the death of cells in the cortex, leading to gas-filed voids between the living cells that remain (Figure 1.3A). Schizogenous aerenchyma, which may also be found in roots, stems and petioles of wetland plants and are formed through the separation of cells from each other in an early stage of development (Figure 1.3B). In both aerenchyma types, Justin and Armstrong (1987), have shown a large variation in the actual cell position and cell remnants in their extensive screening of root anatomy of wetland, intermediate and non-wetland species.

Lysigenous aerenchyma form in both newly developed and matured roots of most plants through a process determined by environmental stimuli. In contrast, schizogenous aerenchyma are a constitutive trait within the root which does not change in those roots that are already present at the beginning of waterlogging. New roots may develop instead that contain a large proportion of schizogenous aerenchyma (Visser and Voesenek 2005). Many trees species, such as *Alnus glutinosa* (Rusch and Rennenberg 1998), *F. excelsior* (Frye and Grosse 1992), *Salix*

pentandra, *Salix fragilis*, and *Salix myrsinifolia nigricans* (Gill 1975) form lysigenous aerenchyma.

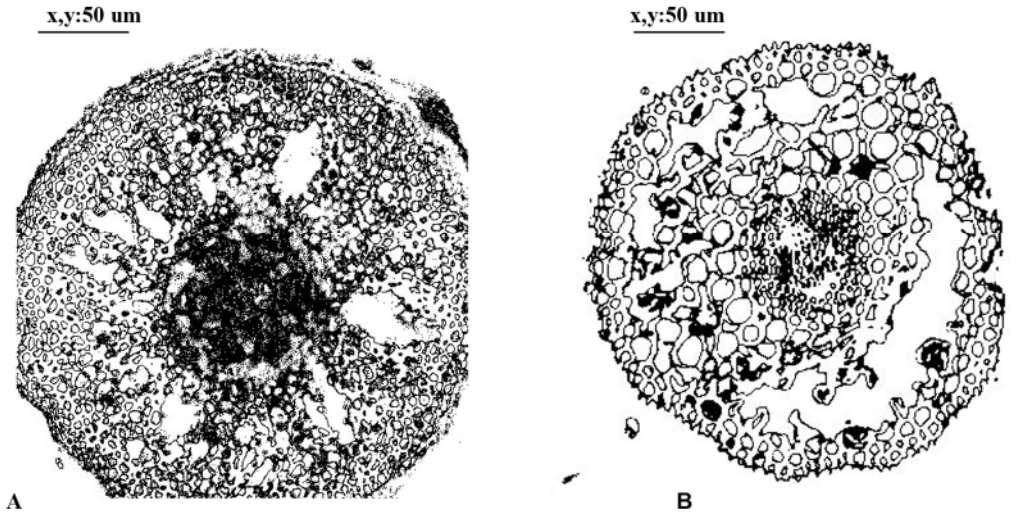

Figure 1:3: A. Cross-section of the aerenchymatous root of a waterlogged *Alnus glutinosa*. Large lysigenous aerenchyma has developed in the cortical parenchyma. B. Cross-section of an adventitious roots of a 60-day waterlogged *Salix aurita* sapling containing lysigenous aerenchyma.

1.2.2.2 Lenticles

Hypertrophied lenticels are enlarged cells that protrude from the bark of plants in response to waterlogging. Hypertrophied lenticels grow around the stem, usually in the area where stomata occur. They turn into pathways for gases to diffuse through the living cells of the bark, especially oxygen. Through the lenticels, potentially toxic substances related to anaerobiosis—such as acetaldehyde, ethanol, and ethylene—are released (Glenz et al. 2006). Similarly, lenticels on the saplings of different woody plant saplings have shown to provide access to O_2 (Topa and McLeod 1986). Hence, species with smooth bark (e.g. *F. sylvatica, Acer spp., F. excelsior*) are more sensitive to the effect of waterlogging than species with a coarse bark (e.g. *Salix spp., Populus spp., Ulmus spp., Quercus spp.*) as prolonged oxygen retention is possible under rough bark (Glenz et al. 2006).

1.2.3 Photosynthetic adaptation

During waterlogging, stomatal conductance of leaves lowers their stomatal conductance rises, their stomata close, and their absorption of CO_2 reduces (Li et al. 2010). However, in order to maintain growth and development, trees require light and CO_2 for photosynthesis. Long-term waterlogging inhibits the activities of enzymes involved in waterlogging; leaves' capacity to synthesis chlorophyll declined, resulting in senescence, peeling and yellowing of leaves; the development of new leaves was impeded; and finally, the photosynthetic rate decreased, ultimately resulting in the death of the plant (Visser and Voesenek 2005; Du et al. 2012).

Plant photosynthesis is based on photosynthetic pigments, and variations in the pigment's composition and content have an immediate impact on the rate of photosynthetic activity (Pan et al. 2021). In addition to catalysing the initial phase of the photosynthetic carbon cycle and photorespiration, the enzyme rubisco is essential for converting inorganic carbon into organic form that plant can use. Sucrose and starch are the essential products of photosynthesis in most plants. The primary transport of carbohydrate from source to sink is via sucrose, and this mechanism is very sensitive to waterlogging. In cotton, increased gene expression and enzyme activity of sucrose synthase during waterlogging were linked to extending the period of rapid accumulation of seed fibre weight, which tended to mitigate the phenomenon of boll weight decline caused by waterlogging (Fig. 1.4). The enzyme sucrose synthase is essential to the metabolic breakdown of sucrose required for cellulose biosynthesis (Kuai et al. 2014).

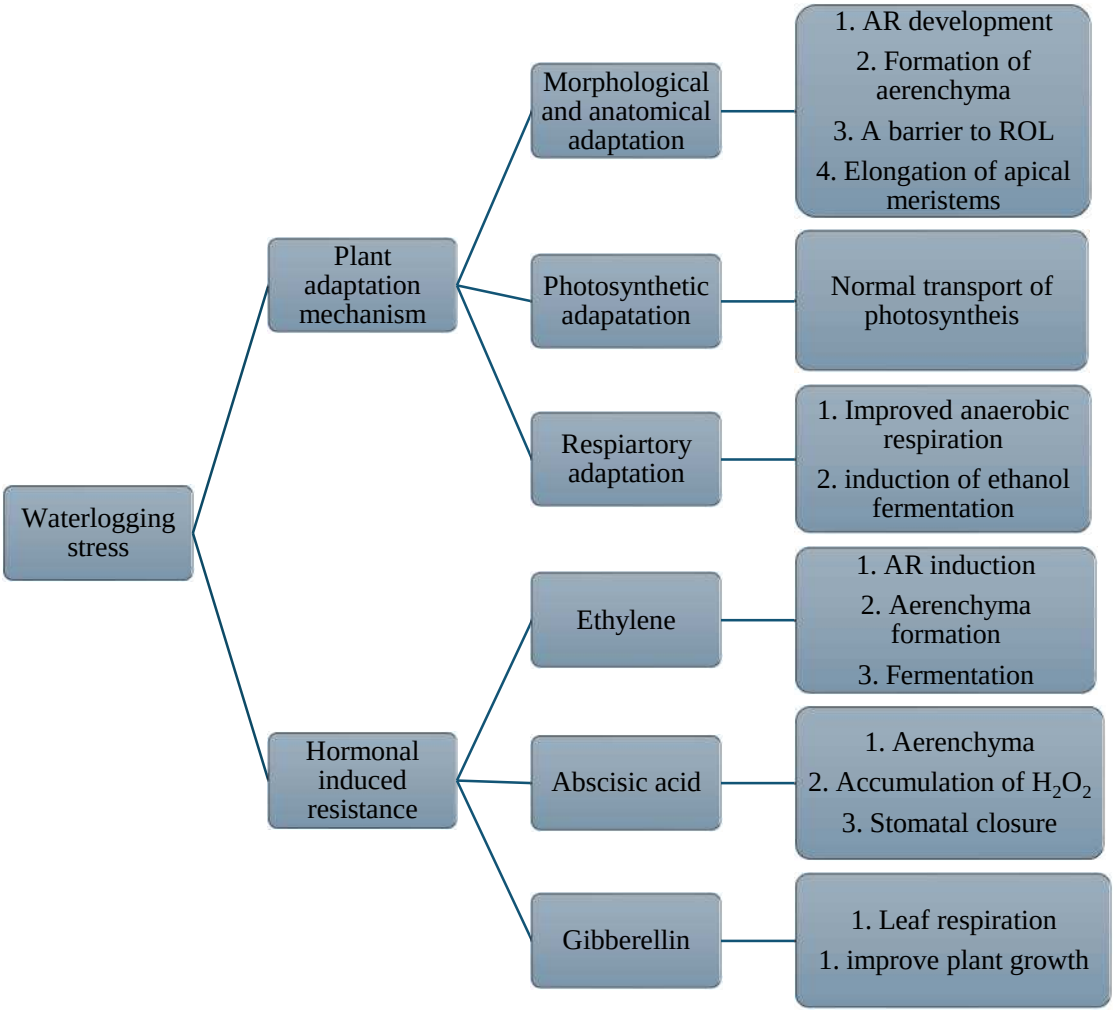

Figure 1:4: Schematic overview of plants response to waterlogging and hormonal effects resistance in plants (Source: (Evans 2003)). AR- Adventitious root

1.2.4 Respiratory adaptation

Energy production is essential to the growth and development of plants. One of the most significant problems plants under waterlogging encounter is the lack of energy brought on by hypoxia and the subsequent suppression of root respiration (Kozlowski 1997). The concentration of dissolved oxygen in water under waterlogged conditions is less than 0.05 mmol/m^3, in cultivated soil the value is typically around 0.23 mol/m^3. In waterlogged soil, the rate of O_2 diffusion is only 1/10,000 of that in the atmosphere. Reduced oxygen availability interferes with the electron transport chain, which stops mitochondrial respiration and quickly suppresses the synthesis of adenosine triphosphate (ATP) (Bailey-Serres et al. 2012). Plants must utilise glycolysis and ethanol fermentation to acquire the required energy while facing

energy deficiency due to waterlogging stress (Voesenek and Bailey-Serres 2015). Through the carboxylic acid cycle, 1 mol of glucose can yield 36–38 mol of ATP, however glycolysis and ethanol fermentation can only yield 2 mol of ATP. Therefore, in order for plants to produce the requisite amounts of ATP needed to maintain life, they must speed up the processes of glycolysis and ethanol fermentation.

1.3 The role of temperate trees in greenhouse gas emissions

Temperate forest can act as both a net source and a net sink of atmospheric methane and nitrous oxide, two greenhouse gases with potentials for global warming that are 23 and 296 times greater than those of carbon dioxide (IPCC 2001). Due to seasonal, interannual, and site-to-site changes, estimations of the global CH_4 sink and N_2O source strength for forest soils are largely unknown (Covey et al. 2012). The dynamics of CH_4 and N_2O fluxes may be explained by changes in soil temperature, moisture content, gas permeability, and freeze-thaw cycles, while a variety of other site-specific factors may be involved in regulating site-to-site variation (Covey et al. 2012; Pangala et al. 2015).

Forest ecosystems have received global research focus due to their potential as carbon sinks (Vesterdal et al. 2012; Dolman et al. 2018a). This is especially true for younger forest ecosystems, where net primary production greatly exceeds the rate of decomposition, leading to net atmospheric CO_2 uptake (Addo-Danso et al. 2016). In recent years, the increase in above-ground biomass resulting from net carbon accumulation has been taken into account in national greenhouse gas inventories (Curtis and Wang 1998; Bowles et al. 2020). Although, many studies have examined C pools in different forest types (Saxe et al. 1998; Ceulemans et al. 1999; Morison et al. 2012), understanding the role of temperate trees is required to support the potential of these ecosystems as sources or sinks of greenhouse gases and their response to changing climate.

1.4 Sources and sinks of greenhouse gas in temperate trees

In recent years, there has been rising interest over the potential contribution of trees, especially, to the emissions of methane, and, to a lesser extent, nitrous oxide. CH_4 and N_2O emission have been reported from stems and leaves of trees via transport from soil e.g. (Rusch and Rennenberg 1998; Terazawa et al. 2007; Rice et al. 2010; Covey et al. 2012; Pangala et al. 2015; Machacova et al. 2016) and because of the microorganisms living inside the tree (Covey et al. 2012). Similarly, if there is entry of O_2 in the rhizosphere then CH_4 can also enter the plant aerenchyma system and afterwards be emitted into the atmosphere (Laanbroek 2010).

Previous research has focused on many herbaceous species (Rusch and Rennenberg 1998; Carmichael et al. 2014; Pangala et al. 2015; Carmichael and Smith 2016) regarding the roles of plants especially wetland adapted species as conduits for CH_4 emissions, and for N_2O in a few species such as rice and rushes (Reddy et al. 1989). According to Rusch and Rennenberg (1998), plant-mediated gas efflux that contributes to overall emissions for most natural ecosystems is unknown and is dependent on the plant community and the soil. For instance, Thomas et al. (1996), reported in a Sphagnum dominated bogs where plants have no or only small roots, their ecosystem importance is minimal because of low vegetation. However, according to recent research, woody plants with larger root systems and more gas-occupying spaces in the stem xylem sapwood and heartwood (Gartner et al. 2004) can contribute significantly to both CH_4 and N_2O fluxes e.g., (Rusch and Rennenberg 1998; Gauci et al. 2010a; Rice et al. 2010; Pangala et al. 2013; Dolman et al. 2018a; Maier et al. 2018) (Fig. 1.5). They are also arguably one of the least researched and understood emission pathways (Carmichael et al. 2014; Pangala et al. 2015).

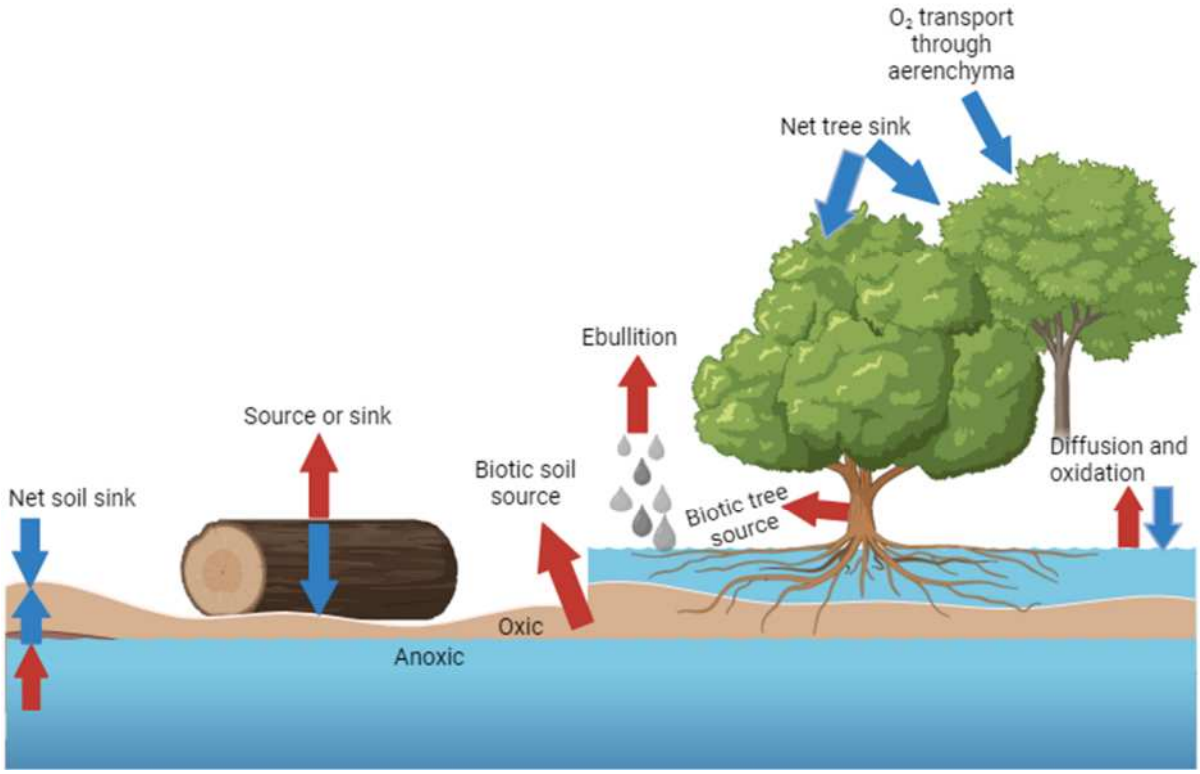

Figure 1:5: Sources and sinks of greenhouse gas in temperate trees. Red arrows, GHG sources; blue arrows, sinks. (Source: Carmichael et al. (2014)).

Rice et al. (2010) measured the CH_4 emission from three woody riparian tree species grown in mesocosms: willow, ash, and poplar. They scaled it up globally using a leaf area normalised mean emission rate for flooded forest regions and estimated the amount to be 60 ± 20 Tg yr^{-1}, or about 10% of the global CH_4 source. This provides an example of the potential magnitude of CH_4 and N_2O fluxes. In order to provide a thorough estimate of the overall scale of vegetation in the global CH_4 budget, Carmichael et al. (2014) reported the degradation of coarse woody debris and litter, heartwood rot in trees, plant cisterns—water-filled hollows and organs—that function as cryptic wetlands, and the transport of CH_4 through herbaceous and woody plants. They calculated, though with a great deal of uncertainty, that plant-based CH_4 emissions would account for as much as 22% of the entire global CH_4 budget, or roughly 32–143 Tg yr−1, with trees contributing 6-42% (2–60 Tg CH_4 yr−1) of these emissions (Carmichael et al. 2014). In order to close the much-discussed gap in the global methane

budget, they therefore highlighted the importance of better understanding the function of vegetation in the biogeochemical cycle of CH_4. Similar to this, tree stems and leaves have the potential to be a major source of emissions of N_2O (Pihlatie et al. 2005; Machacova et al. 2016) and as much as 30% more than previously believed (Barba et al. 2019). According to the most recent report on GHG emissions estimation from the Committee on Climate Change (IPCC 2022), sectors like waste, agriculture, and land use, land use change, and forestry that involve complex biological processes or diffuse sources have higher levels of uncertainty and should therefore receive priority attention for additional research. However, because of uncertainty in global emissions, plants are not included as a separate category of CH_4 and N_2O flux to the atmosphere in global budget reports (e.g., (IPCC 2013; Saunois et al. 2016).

1.5 Consequences of climate change on temperate trees species' morphology, physiology, and anatomy

It has been established for decades that anthropogenic activities such as uncontrolled deforestation and rising GHG emissions have led to a number of environmental issues that have significantly altered the complex climate dynamics all over the world. Increases in the global average temperature and the atmospheric CO_2 concentration are two examples of these changes (IPCC 2022). Several climate models indicate that these elements will intensify in the coming decades in addition to the changes that have already been observed. This could lead to an increase in the frequency of extreme weather occurrences (Bai et al. 2010). These models predict that certain places will see sharp drops in rainfall while others will see higher volumes of rainfall, leading to more frequent and severe drought and flood events, respectively (IPCC 2013b). Changes in thermic regimes are also anticipated in many parts of the world in addition to pluviosity patterns, which might intensify and increase the frequency of extreme temperature occurrences like heat waves and late-spring frost episodes (IPCC 2013b).

Two major factors that affect the development, distribution, and survival of plant species worldwide are temperature and the availability of water (Teskey and Hinckley 1981; Delatorre et al. 2008; Zhen et al. 2020). Therefore, as reported by climate model projections, the frequency, intensity and duration of extreme weather events may cause significant alterations in a number of plant communities, leading to large dieback of forest, which may ultimately result in a massive loss of biodiversity (Wiens 2016; Menezes-Silva et al. 2019). According to some research, climate change may cause some species in some biomes to become extinct and be replaced by others that are better suited to withstand harsh weather conditions. For instance, a number of studies have reported the impacts of climate change on temperate areas (Orsenigo et al. 2014; Walsh et al. 2020), with the occurrence of extreme weather events may causing plant mortality or 'browning' (Bokhorst et al. 2011). A similar pattern of alterations in the species composition is anticipated for various other types of vegetation, including grasslands, tropical, boreal forests (Boulanger et al. 2017; Barros et al. 2018). However, these extreme weather events are predicted to intensify over the coming decades, but their harmful impacts are already being observed. In fact, an increasing amount of data link temperature and water stressors such as floods and drought to rising death of forest species (Menezes-Silva et al. 2019) and the observations are concerning considering the percentage of plants species that could go extinct as a result of increase of such pressures (Wiens 2016).

The significant disturbances brought about by climate change-related factors in plant communities are indicative of their influence on nearly every level of plant organisation. A number of studies conducted in recent years have shown the variety of defence mechanisms and techniques used by plants subjected to extreme weather events, as well as the elements that contribute to tree mortality in such circumstances (Bokhorst et al. 2011; Orsenigo et al. 2014; Walsh et al. 2020). Nonetheless, despite significant advancements in our understanding of the consequences of climate change on temperate trees, there is still a great deal of fragmentation

in our knowledge of this subject. Therefore, there is need to provide a broad and integrated understanding of the primary physiological, morphological, and anatomical traits linked to exposure to stress factors caused by extreme weather events (primarily flooding and global warming), which may jeopardize the survival and overall health of tree species and forest ecosystems in the temperate.

1.6 Mechanism of gas transport in temperate trees

Transport of gas in trees occurs through internal air spaces in the tree bodies and at lower stem height as reported by several researchers (Rusch and Rennenberg 1998; Terazawa et al. 2007). They observed that the primary mechanism for gas transport in trees is diffusion, which is triggered when soil gas concentrations are higher than atmosphere concentrations. This gradient in concentration makes it possible for gases to be transported from soil to the atmosphere. More evidence supporting diffusive gas transport of CH_4 is shown by (Garnet et al. 2005). They argue that the non-hysteretic CH_4 emission response curve and the absence of a mid-morning CH_4 emission peak support the diffusion driven CH_4 transport over pressurised gas transport.

The transport of gases through transpiration is another route of transport that is frequently mentioned. An actively transpiring tree may transport gases by transpiration stream from the roots to the leaves and emitted to the atmosphere through the stomata (Schröder 1989), or stem surfaces (diffusing laterally and radially through intercellular spaces of aerenchyma tissues) as shown for variety of wetland plant species (Sorrell and Brix 2015). However, Conrad (2009) argued that because CH_4 is comparatively insoluble in water, the transpiration stream's capability for transporting the gas may be lower in magnitude than that of the other routes. These results suggest that there are two major processes for which gas transport by trees: diffusion gradient-driven emissions and transpiration stream-driven emissions (Gauci et al.

2010). The current understanding of the mechanisms underlying gas emissions mediated by CO_2 transport in temperate trees, herbaceous plants-mediated gas emission, and oxygen transports in wetland trees is substantial and may provide important insight into the likely mechanism underlying tree-mediated gas emissions transport.

1.6.1 Carbon dioxide transport in temperate trees

Recent research has focused on the internal transport of dissolved CO_2 from below ground, which is mostly produced via root respiration, absorption, and subsequent release in trees (Medlyn et al. 1999; Aubrey and Teskey 2009; Ashraf and Harris 2013; Carmichael and Smith 2016). These investigations show that the transpiration stream, which is already thought to be the mechanism for tree-mediated gas emissions, carries root-respired CO_2 internally upward in the tree and diffuses it to the atmosphere. Moreover, such transport is caused by CO_2 concentrations in the xylem that are many times higher than those in the atmosphere (Aubrey and Teskey 2009) and high CO_2 concentrations around the base of tree stems suggest that a large portion of the CO_2 in stem xylem comes from underground sources (Teskey and Mcguire 2007). Given the amount detected at the base of tree stems, the estimated contribution of dissolved inorganic carbon received by roots from the soil is significantly smaller, indicating that a large portion of it originates inside the root system (Teskey and Mcguire 2007). Therefore, because not all of the CO_2 that is respired by roots diffuses into the soil atmosphere, it is possible that the rates of belowground respiration that are measured using conventional methods may be underestimated.

1.6.2 Plant-mediated gas emissions

Gas circulation is crucial to plants survival especially for aquatic plants since their lower parts exist in a water-saturated, frequently organic-rich anaerobic environment (Crawford 1992). These plants must transport oxygen below ground to enable root respiration (Jackson and Armstrong 1999a). The movement of reduced gases, most notably methane, from the sediments

into the atmosphere is one example of the gas circulation process. Plants allow CH_4 produced within the anaerobic sediments to bypass the sediments-water interface via convective through flow. This diffusion driven CH_4 transport, in which CH_4 flows from area of high pressure to lower pressure has been reported in wetland species such *Typha spp.*, *Phragmites australis* and *Equisetum fluviatile* (Whiting and Chanton 1996; Kankaala et al. 2005). In addition, other wetland plant species such as *Oryza sativa*, *Carex gracilis*, and *Peltandra virginica* employ molecular diffusion driven CH_4 transport- another gas transport mechanisms (Whiting and Chanton 1996; Colmer 2003). However, plants with higher rates of CH_4 transports employ the convective gas transport and/or both convective and molecular diffusion transport than those that only employ molecular diffusion (Whiting and Chanton 1996).

1.6.3 Oxygen transport in temperate trees

During the growing season, stem tissue respiration might be increased (Teskey et al. 2015) and bark, wood and cambium may present barriers to gas diffusion. Oxygen can either be taken up by the roots and carried upwards with the transpiration stream, or it can diffuse radially through periderm, phloem, cambium, and wood to supply live cells in the sapwood. Certain tree species that have adapted to waterlogged soils have cambium with tiny intercellular gaps that allow oxygen to pass through the bark (Buchel and Grosse 1990), while in other species with no intercellular spaces, the cambium and bark both seem to be impermeable to gases- and the transpiration stream is considered to be the primary supply of oxygen to the xylem (Hook et al. 1972; Sorz and Hietz 2006).

The mechanisms involved in O_2 transport in the aerenchyma are closely related to plant mediated GHG transport, except the gas transport is in the opposite direction. These mechanisms include: i) O_2 diffusion induced by photosynthesis (Frye and Grosse 1992); ii) transport via pressure gradient: thermo-osmotic and humidity-induced diffusion (Justin and Armstrong 1987; Jackson and Armstrong 1999a) and iii) Diffusion-based O_2 transport

according to Fick's law (Brix et al. 1992). Release of oxygen during photosynthesis and respiratory consumption in the rhizosphere, together produce an O_2 concentration gradient that diffuses O_2 downward in the aerenchyma along the concentration gradient and permits O_2 transportation (Armstrong and Webb 1985; Jung et al. 2008), while the concentration gradient caused by this drives humidity induced diffusive O_2 transport (Brix et al. 1992) and the temperature difference between the stem and ambient air drives thermos-osmotic O_2 transport (Brix et al. 1992; Jackson and Armstrong 1999a).

1.7 Environmental regulation of greenhouse gas fluxes

Several environmental factors are known to influence plant-mediated gas transport. The three critical factors—air temperature, hydrology, and vegetation — are thought to be significant for tree-mediated CO_2, CH_4 and N_2O emissions.

1.7.1 Air temperature and soil

Vegetations is known to be influenced by temperature, and it has been suggested that trees emissions of GHG emissions are influenced by temperature. For instance, some studies have asserted that the metabolic rates of methanogens and methanotrophs are directly impacted by temperature, and temperature can also indirectly affect CH_4 emissions through a variety of mechanisms, such as changes in plant physiology and net ecosystem productivity (NEP), as well as changes in plant communities, density, and composition. These processes are known to increase substrate availability and microbial activity, which in turn increases CH_4 production (Gauci et al. 2010b; Sjögersten et al. 2018, 2020a). Similarly, CO_2 emission rates can double with a 10 °C increase in temperature, according to laboratory incubations utilising samples from peatlands (Brady 1997). On the other hand, there have also been reports of diurnal fluctuation in CO_2 fluxes; efflux decreases overnight may be caused by a drop in CO_2 derived from roots or a fall in decomposition rates due to lower temperatures (Wright et al. 2013b).

1.7.2 Water-table depths

It has previously been shown that the height of the water table may directly or indirectly affect tree-mediated CO_2 and CH_4 emissions, mainly through indicating whether aerobic or anaerobic decomposition predominates at any particular depth. Joabsson et al. (1999) reported that the level of anaerobic conditions and the depth of the aerobic layer are influenced by water-table depths, which in turn affects the ratio of CH_4 production and oxidation. As such, they are crucial in controlling CH_4 production (Grünfeld and Brix 1999; Turetsky et al. 2014; Hoyos-Santillan et al. 2019).

Water-table depth can also affect tree-mediated gas emissions due to its ability to alter assimilation, root distribution, and growth. For example, a study has shown that drier soil conditions enhance below-ground productivity of plants resulting in stimulating CH_4 emissions through increased labile carbon substrates in soil and increasing CH_4 transport to the surface due to shifting rooting zones (Henneberg et al. 2012; Maier et al. 2018). Also, water-table depth can present a distinct seasonality because of changes in precipitation. For example, CO_2 has been found to increase during periods of both lower rainfall and intense rainfall (Wright et al. 2013a).

1.7.3 Wetland vegetation

The contribution of vegetation to the global flux of gases especially CO_2 and CH_4 has been reported many times in literature (Covey et al. 2012; Carmichael et al. 2014; Carmichael and Smith 2016; Dolman et al. 2018a). Vegetation influences both the production and consumption of methane via different pathways. For instance, plants have the ability to affect soil carbon dynamics both directly and indirectly. Directly, they can do this through releasing carbon molecules into the rhizosphere, which in turn promotes methanogenesis (Chanton et al. 1995; Weiss et al. 2005) or indirectly through the quality and quantity of litter (Upton et al. 2018).

Additionally, plants can affect methane-oxidation through rhizosphere oxygenation (Colmer 2003), thus suppressing methanogenesis and increasing below-ground oxidation (Joabsson et al. 1999) and oxidation of other electron acceptors (Garnet et al. 2005). Plants can act as conduits in transporting methane to the atmosphere (Rusch and Rennenberg 1998), that avoids the role of soil and/or aquatic microorganisms in attenuation.

Different species have varying effects on wetlands' CH_4 emissions. For instance, a number of studies have shown that the removal of wetland vegetation reduces CH_4 emissions, and the emissions response is usually consistent across studies; however, reports of a reduction in CH_4 emissions in the presence of wetland vegetation have also been reported, and in both cases, the magnitude varied both within and between studies (Joabsson et al. 1999; Hirota et al. 2004; Terentieva et al. 2019). On the other hand, some studies have found contrasting evidence of a relationship between plant biomass, net ecosystem and CH_4 emission attributing these differences to plant-root-microbial consortium (Johansson 1992), root depth, architecture and morphology (Megonigal et al. 2005), morphological adaptation (Kozlowski 1997), assimilation (Whiting and Chanton 1996), and vegetation height and biomass (Joabsson et al. 1999).

1.8 Research aims and objectives

In order to understand the physiological, anatomical, and morphological modifications connected with exposure to the stress factors caused by extreme weather events on tree saplings, as well as their significance in the GHG budget, this study aims to assess the potential impact of elevated temperature, elevated CO_2 and waterlogging on the survival and growth of growth-room grown temperate tree saplings in an attempt to understand and identify their responses to future climate change. Previous studies have shown GHG emissions from mature and young trees (e.g., Rusch and Rennenberg 1998; Vann and Megonigal 2003; Gauci et al. 2010b; Pangala et al. 2013; Sjögersten et al. 2020) and the adaptive responses of trees saplings

to climate change especially morphological and anatomical changes (e.g.,Yamamoto et al. 1995; Tanaka et al. 2011; Oliveira et al. 2015; Wang et al. 2015) but the interactive effects of elevated temperature and waterlogging or elevated CO_2 and waterlogging on physiology, anatomy and morphology have been less well studied.

1.9 Research objectives

Objective 1: To evaluate the physiological acclimatization responses of leaf physiological acclimation to increasing temperature to thirty-days waterlogging and increasing CO_2 to sixty-days waterlogging. The objective and associated hypotheses are addressed in Chapter 3: "Physiological responses of temperate trees species: Interactive effects of elevated temperature, CO_2, and waterlogging".

1. Elevated temperatures lead to an increase in transpiration rates, resulting in reduced carbon assimilation and growth while stomatal conductance decreases under elevated CO2 conditions, reducing transpiration rates and improving water use efficiency.
2. Increased atmospheric CO2 levels will lead to higher rates of photosynthesis and greater carbon assimilation in water-tolerant species only but stomatal conductance under waterlogged conditions lead to decreased transpiration rates but could also hinder CO2 uptake.
3. Interactive effects of elevated temperature and waterlogging will result in reduced photosynthetic efficiency and decreased below-ground biomass accumulation while CO2 enrichment mitigates the negative impacts of waterlogging by enhancing photosynthetic rates and improving energy availability for stress recovery.

Objective 2: To examine the anatomical root traits and the leaf physiological traits associated with water use efficiency of five temperate tree species in a 2-year growth room manipulating temperature, CO_2 and precipitation change. The objective and associated hypothesis are

addressed in chapter 4: “Exploring the influence of Root anatomical traits on leaf-level physiology and their responses to climate change in woody temperate trees species”.

i. Do temperate woody species differ in their root anatomical traits, physiological traits and water use efficiency?
ii. How are root anatomical traits, leaf physiological traits and intrinsic water use efficiency related in temperate woody species?
iii. How do root anatomical traits and leaf physiological traits as well as intrinsic water use efficiency respond to global change in temperate woody species?
iv. How do root anatomical traits influence how leaf physiological traits and water use efficiency react to global change?

Objective 3: To understand how these environmental factors influence the release of greenhouse gases, such as carbon dioxide (CO_2) and methane (CH_4) from the soil-plant-atmosphere continuum. The work focuses mainly on how the interactive effect of waterlogging, elevated temperature and CO2 enrichment impacts on CO2 and CH4 emission from temperate tree saplings. We explored net GHG exchange, soil and stem emissions. This research contributes to our understanding of how future climate change scenarios may impact greenhouse gas dynamics in terrestrial ecosystems, specifically in relation to temperate tree species.

1.10 Thesis structure

There are six chapters in this thesis. The background information for the main research topics covered in the thesis is presented in Chapter one, along with the knowledge gaps and the goals and objectives of the study. Chapter two describes the growth room used during the research

and general methods used. Also, specific methods and materials description are included within each chapter.

Chapters three, four, and five are written in paper format, and include introduction, specific methods, results, and discussions connected with each of the aspects investigated. Chapter three tackles the core aim of the thesis by identifying the adaptive response of physiological and morphological acclimatization to elevated temperature and 30 days waterlogging and is currently under review, Chapter four identifies the anatomical responses to elevated CO_2 and 60 days waterlogging. Chapter five assesses the effect of increasing temperature and CO_2 levels, combined with periods of waterlogging stress, on greenhouse gas emissions from temperate tree saplings. Finally, chapter six provides a brief overview of the three preceding data chapters' findings, highlights their outcomes, placing the findings in a global context, summarises the study's key conclusions, and makes recommendations for further research.

Chapter 2: Methodology

2.1 Introduction

This chapter describes the plant material and experimental design, growth room facilities, and the generic methods used throughout the investigation such as instrumentation used (SPAD, Fluorpen, LI-6800 portable photosynthesis system, scanning laser electron microscope), static chambers, samples collection, flux calculations and statistical analyses. Each experimental chapter discusses the more specific methodologies that are designed to address certain research objectives.

2.2 The growth room facility

The growth room facility is a controlled environment facility located on the Sutton Bonington Campus of the University of Nottingham (52^{o} 50' N, 1^{o} 15' W) (Fig.2.1). The facility is designed to have precise control over factors such as temperature, humidity, light intensity, photoperiod (the duration of light exposure), and can simulate elevated CO_2 concentrations. The rooms have an internal dimension (L x W x H) 3200mm x 3692mm x 2620mm with a height adjustable lighting box containing 58W colour 84 fluorescent lamps with Far Red supplementation. The facility is also equipped with a ceiling mounted evaporator, a humidifier (55%- 80% lights on and 60-90% lights off) as well as a CO_2 delivery system to about 3500ppm with max air change rate of 4 per hour. The growth room facility is fitted with an aspirated temperature sensor that delivers between (10-25°C) range. It is also equipped with a monitoring and control systems that tract these environmental parameters that help ensure that conditions remain within the desired range.

Figure 2:1: Growth room facility site.

2.3 Experimental design

Two growth room experiments were conducted, one in each of 2021-22 and one in 2022-23 (referred to hereafter as 2021 and 2022). The experimental design was a fully factorial design for both experiments. For the experiments, the factorial design comprised of a combination of two [temperature] treatments (ambient temperature (aT) and (eT)) with two waterlogging treatments (control and waterlogged) for experiment 1 and two [CO_2] treatments ambient CO_2

(aCO_2) and elevated CO_2 (eCO_2) with two waterlogging treatments (control and waterlogged), for experiment 2. The plants were randomly allocated into eight blocks (n = 12 per species) There were four blocks per treatment in each of the growth room resulting in twelve replicates per treatment combination per species per. Out of the 12 plants of each species in each growth room, six were randomly allocated for a waterlogging treatment. The remaining six plants were controls (Fig. 2.2).

For the waterlogging treatments, all pots (10-L) assigned a waterlogging treatment were inserted into 15-L buckets and filled with tap water and water-level was maintained daily. The 30-day waterlogging was set to stimulate a waterlogged soil concentration comparable to commonly occurring peatland soils and natural habitats for these plants. The 30- and 60-days waterlogging was to determine the stress response of these plants as investigating both 30-day and 60-day waterlogging periods helps distinguish between short-term stress responses and long-term survival strategies.

For temperature treatment, saplings were subjected to the temperature treatment in March 2021, well before leaf flushing. Following the emergence of leaves, waterlogging was then initiated in late August 2021. The rationale for the temperature treatment is to stimulate future climate conditions and assess how different species will respond in terms of growth, survival and physiological changes. For the CO_2 experiment, saplings were transferred into the growth room in May 2022 and CO_2 treatment was initiated on the same day. Thirty days after, when leaves have emerged, saplings were subjected to waterlogging in July 2022

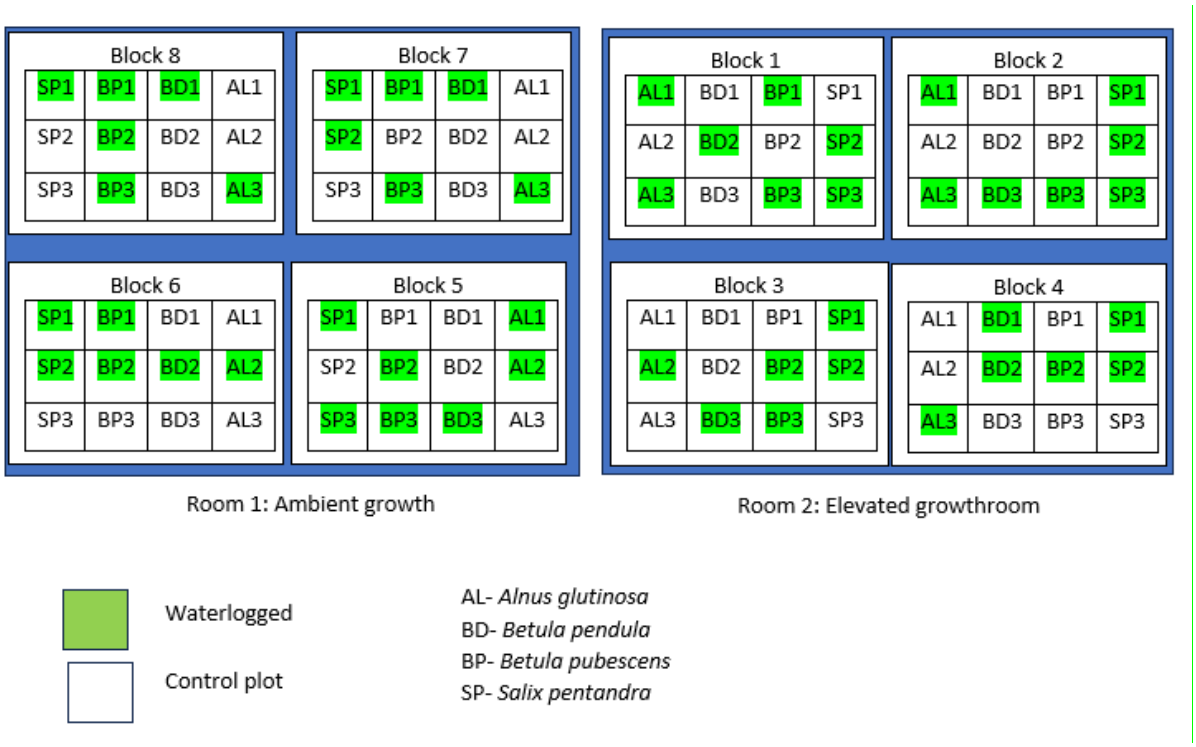

Figure 2:2: Growth room layout showing the four experimental blocks in each treatment.

2.4 Instrumentation

2.4.1 Leaf chlorophyll concentration

2.4.1.1 SPAD readings

Measurements of chlorophyll content can be used to indicate the physiological state of the leaves, hence the plant as chlorophyll content tends to decline rapidly when plants are under stress or during leaf senescence (Wang et al. 2017). Here, a portable chlorophyll meter (SPAD-502; Minolta, Osaka, Japan) was used to determine leaf greenness, which is directly linked to the concentration of chlorophyll present in leaves (Piekielek et al. 1995). The SPAD meter provides rapid non-destructive estimates of relative chlorophyll content in the leaves of a wide range of plant species (Wang et al. 2017). Leaf relative chlorophyll content was measured for the newest fully emerged leaf on the main shoot. For each plant, three leaves were selected at random from the upper part of the main shoot and chlorophyll content was measured at three points of the leaf. SPAD readings were taken by inserting a fully expanded leaf into the sensor head of the instrument (Fig 2.3).

Figure 2:3: SPAD 502 meter for determining leaf greenness in plants.

An area of 2 x 3 mm (12.57 mm^2) of every leaf selected was measured for its chlorophyll content and three SPAD readings per leaf were averaged to take account of local variation within individual leaves.

2.4.2 Leaf chlorophyll fluorescence

2.4.2.1 Quantum yield

The leaf chlorophyll fluorescence as the quantum yield (QY) was measured by a Fluorpen 9 FP 100 fluorometer (PSI, Czech Republic) for the newest fully emerged leaf on the main shoot (Fig 2.4). It is used to provide insight into the physiological condition of plants, particularly their photosynthetic activity and stress responses. The Fluorpen are invaluable tool for studies of photosynthesis activities of plants as they provide non-destructive *in situ* method of quantifying various parameters related to the photosynthetic activity and stress responses of the plant, such as the maximum quantum yield of PSII (Fv/Fm). Measurements were taken from one leaf selected at random from the upper part of the shoots and quantum yield (QY) was measured at three points on the leaf to calculate the mean

Figure 2:4: Fluorpen FP 100 fluorometer for determining quantum yield (QY).

2.4.3 Photosynthetic gas exchange measurements

2.4.3.1 Leaf gas exchange

Leaf gas exchange measurements were measured using a LI-6800 Portable Photosynthesis System (LI-COR, Lincoln, NE, USA). This instrument is capable of simultaneous fluorescence and gas exchange measurements over the same sample area. The LI-6800 measures gas exchange of leaves under ambient or controlled light. For leaves that do not fill the apertures, the opening features 1-mm graduations around the perimeter to simplify leaf area estimation. It included interchangeable apertures for 2 cm^2 or 6 cm^2 leaf area. The LI-6800 has a combined light source and chamber which provides a highly uniform light field over the leaf area capable of saturation flash intensities up to 16, 000 μmol $m^{-2}s^{-1}$. To take the measurements, the leaf is inserted into the aperture and the average photosynthetic carbon assimilation rate recorded (Fig 2.5).

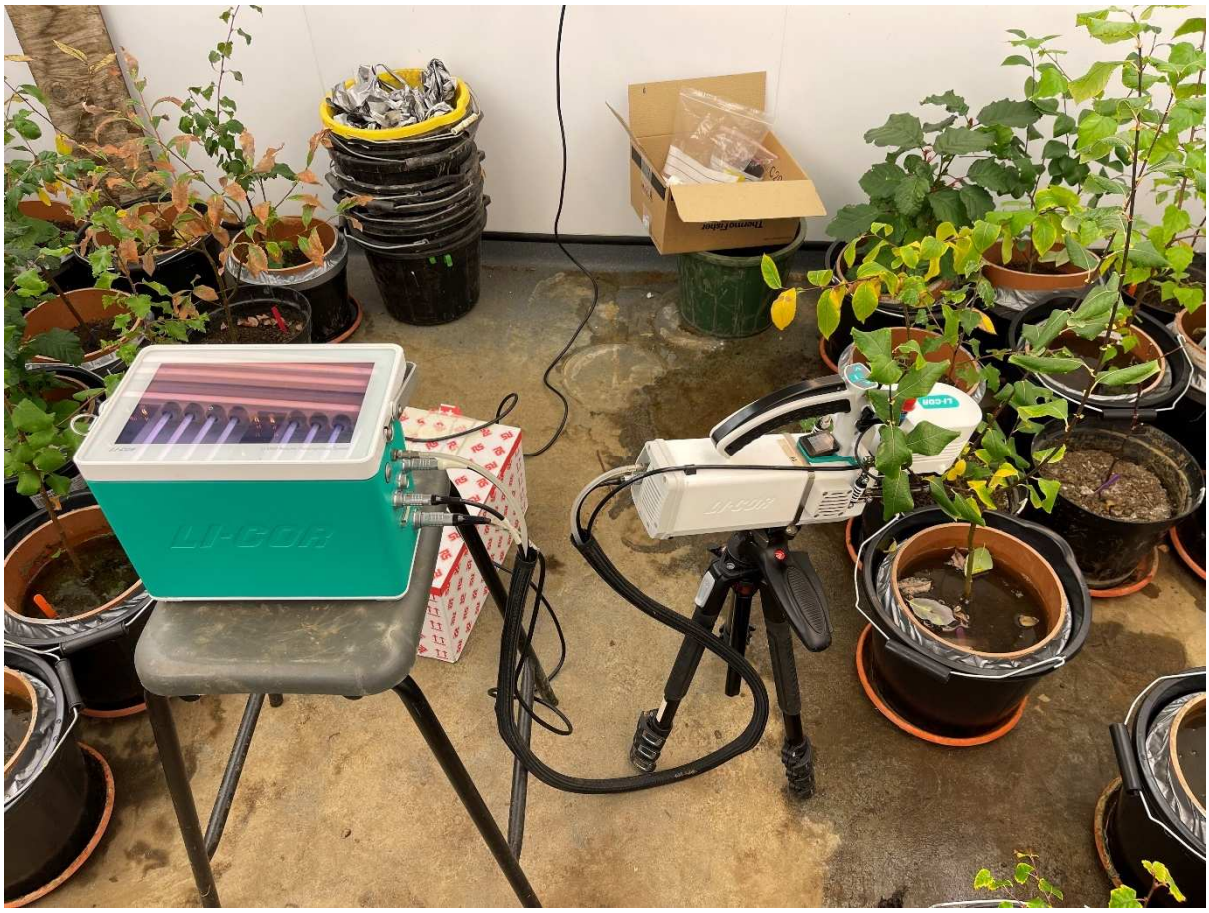

Figure 2:5: LI-COR 6800 used to measure detailed physiological and photosynthetic parameters.

2.4.4 Anatomical measurements

2.4.4.1 Sample collection and storage

Sections of saplings root were collected from soil at a depth of 5 cm and were carefully rinsed in water to remove excess soil. Direct contact with the samples at the point to be sectioned was avoided where possible, to prevent sample damage. All samples collected were ~3.5 cm in length. Samples were stored in undiluted methanol until sectioning day (Atkinson and Wells 2017).

2.4.4.2 Sample embedding, sectioning and staining

Root samples identified for sectioning were taken 15 cm from the base and consisted of a 15 cm long samples with root lateral removed by scissors. The lowest part (5 cm) of the roots were cut from randomly selected, most distal segments of fully acquisition roots. Root was visually determined by presence of root cortex and fully formed vascular tissue. Root samples were

placed directly from the wash media into custom designed 3D polylactic acid (PLA) molds in preparation for embedding. The mold can embed five roots in each block (Fig.2.6) and consist of a lower section with recesses for locating root samples, which suspends the roots over a well which is filled with agarose. The molds are assembled by fitting an upper section to clamp the samples prior to pouring the embedding medium. 5% (w/v) Agarose (Sigma Aldrich, Co. Ltd) was prepared in a microwave before placing the molds. Molds were sealed with pressure-sensitive tap and filled before leaving agarose to cool to 39°C, close to the temperature of solidification (Fig 2.7A).

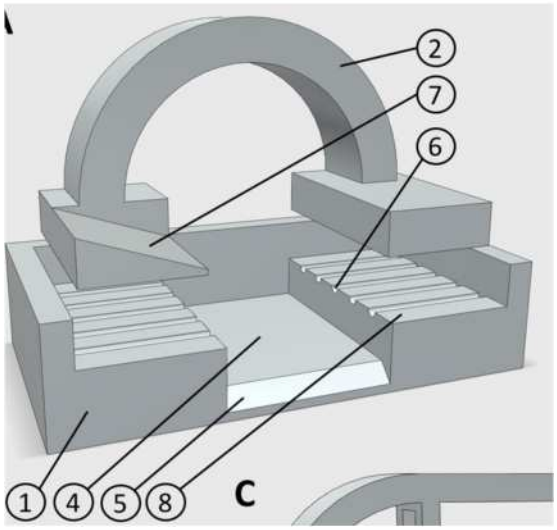

Figure 2:6: 3D printed embedding mold. (1) Mold base (2) lid/root clamp (3) mid sections for additional sample layers (4) embedding media well (5) chamfer for block orientation (6) 0.5 mm guide groves for positioning root material (7) embedding media chute (8) sample recess. Adopted from (Atkinson and Wells 2017)

A vibrating microtome (7000smz-2, Campden Instruments Ltd UK) was used to achieve fast, reliable sections of between 20 and 250 μm. Agarose blocks were trimmed using razor blade (Wilkinson Sword, United Kingdom), to cut off excess sample material and agarose following removal from the molds (Fig 2.7B). Samples were fixed to the vibratome using a Loctite (Cyanoacrylate adhesive). Vibratome was set to section between 200-250 μm thickness from the samples.

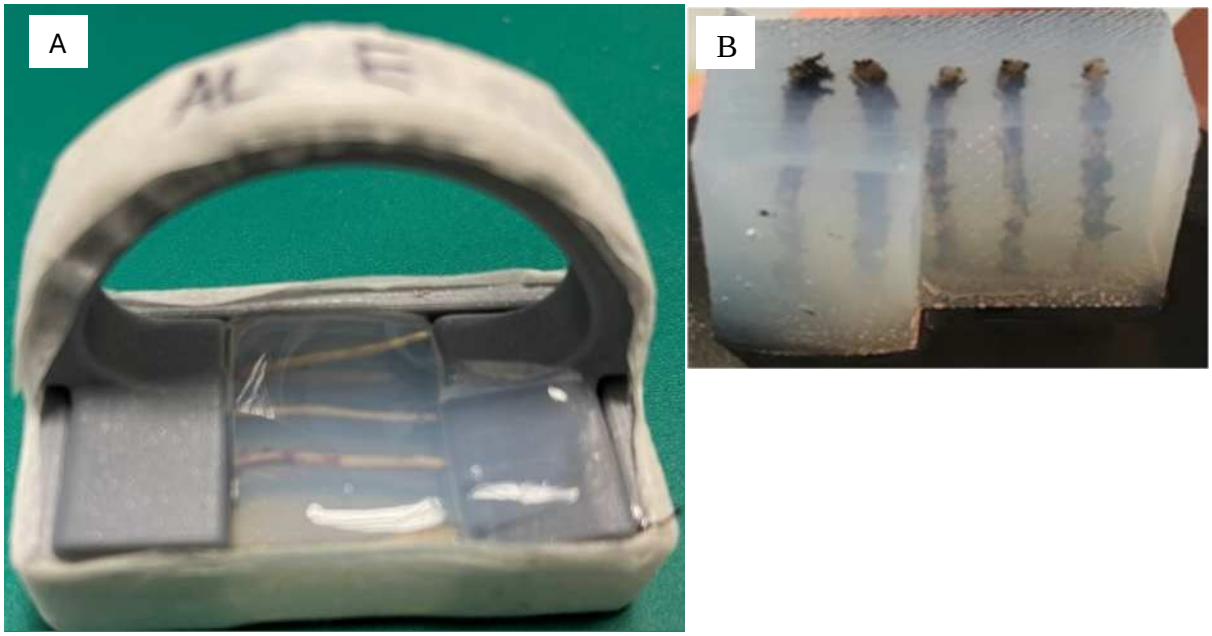

Figure 2:7: A) Mold containing five roots clamped into lace and the mold is sealed with pressure-sensitive tape ready for embedding B) Agarose block prepared for sectioning.

Root sections were removed from the vibratome bath and incubated in calcofluor white (Sigma-Aldrich, Co. Ltd) solution before rinsing in deionised water. Sections were rapidly mounted using a drop of water onto a slide without a coverslip.

2.4.4.3 Image collection

Anatomical imaging was made from all root samples from the different treatments in the present study to produce a clear image of the root anatomical traits. They were observed using an Eclipse Ti CLSM confocal laser scanning microscope (Nikon instruments) (Fig 2.8). The microscope has three excitation lasers (405/35, 515/30 and 605/75), and four detectors. Root anatomical traits such as xylem, phloem, exodermis, and endodermis detection will be achieved using a sequential combination of lasers and detectors to collect three image channels. The images were acquired by IMAGEJ and analysed by RootScan.

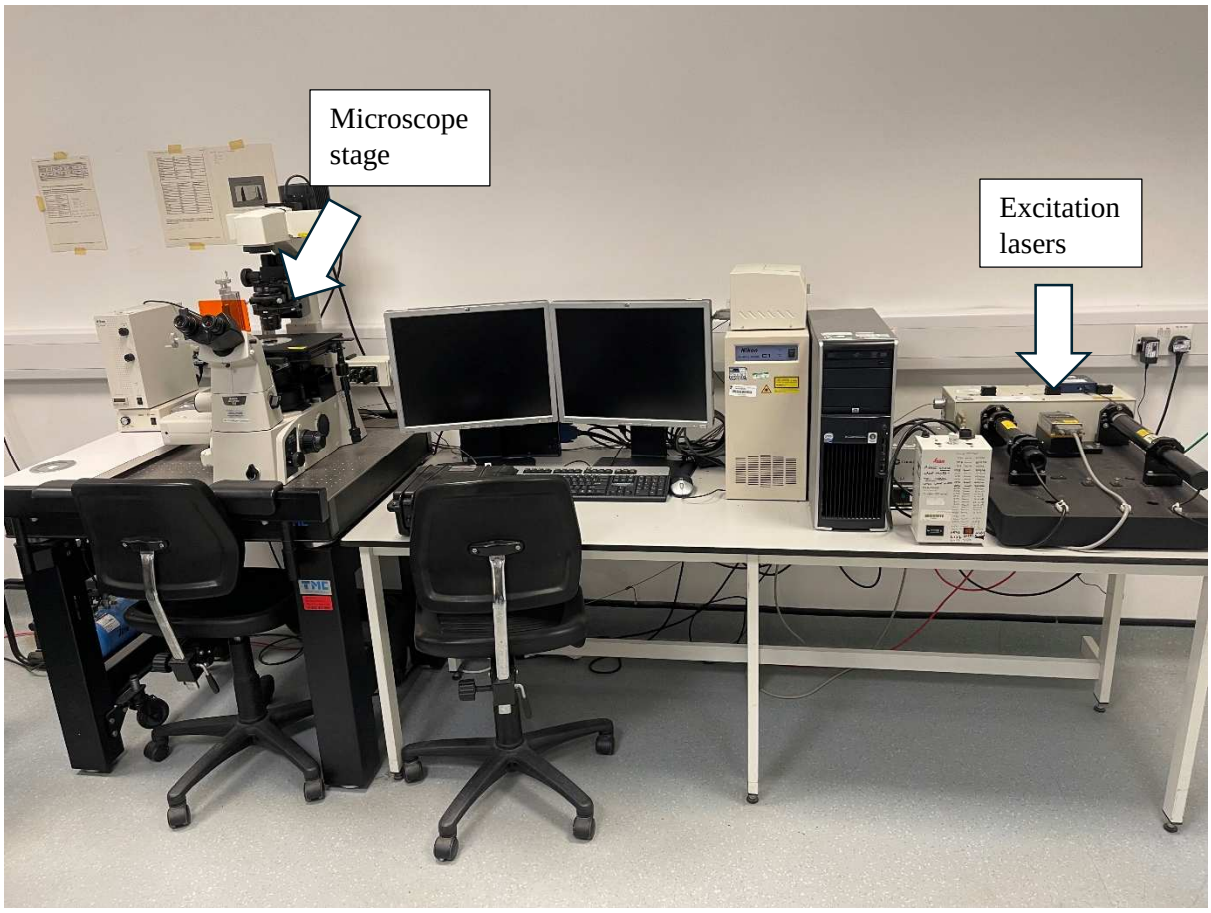

Figure 2:8: Confocal laser scanning microscope for root image collection

2.5 Mesocosm experiment

2.5.1 Static chambers

To measure the net ecosystem exchange (NEE) of CO_2 and CH_4, samples were collected from the soil and plants using transparent chambers. Permanent gas samplings collars (10 cm long) were installed in each pot (Fig 2.9) at the depth of 5 cm. The collars were secure with gaffa tape near the lower end.

Figure 2:9: Gas sampling collars installed to a depth of 5 cm in the pots.

Static chambers constructed from transparent chambers with an internal diameter of 24 mm and height of 105 cm were mounted on the collars (Fig 2.10) for an hour through which the gas sampling took place at the intervals of 0, 3, 20 and 60 min. Each chamber was fitted with fans to mix the air inside the chamber. The samples were taken using a 20 ml syringe and a hypodermic needle from the top of the chamber through a rubber septum.

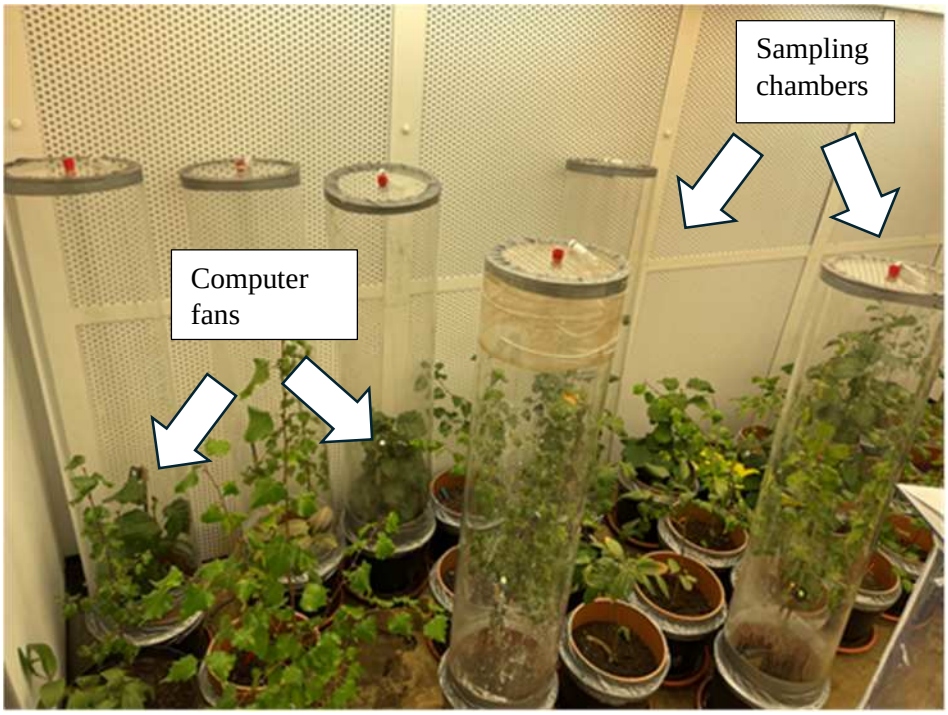

Figure 2:10: Static chambers used to measure the whole-mesocosm gas emissions.

Concentrations of CO_2 and CH_4 were measured using a gas chromatograph (GC) (GC-2014, Shimadzu). The GC measures the concentration of atmospheric greenhouse gases using a single injection system with 1 ml sample loop using hydrogen (H_2) as a carrier gas and measures CH_4 and CO_2 at the flame ionisation detector (FID) and thermal conductivity detector (TCD) respectively (Hoyos-Santillan et al. 2016). Line 2 uses nitrogen (N_2) as a carrier gas and measures N_2O with an electron capture detector (ECD). CO_2 and CH_4 concentrations were measured using a single injection system with a 1 ml sample loop using N_2 as a carrier gas through a non-polar methyl silicone capillary column (CMP1-W12-100, 0.53 mm 1.D., 12 m, 5mm; Shimadzu UK LTD, Milton Keynes, UK) and a porous polymer packed column (HayeSep Q 80/100). Time series data was used for obtaining a linear response used for calculation. The gas data was converted from volume per volume (ppm) to mass per weight using molecular weight of each gas and the ideal gas equation (Denef et al. 2007).

2.5.2 Soil static chambers

For measuring the soil gas fluxes, samples were collected from soil using a transparent chamber (diameter: 7 cm and height: 30 cm) which were inserted into the soil surface down to 2 cm

depth (inner volume of every chamber was around 580 dm^3). Gas sampling took place at the intervals of 0,3,20 and 60 min. The plastic chambers were moved from one plot to another after collecting samples. The samples were taken from the top of the chamber through a sealed rubber septum fixed for this purpose.

Chapter 3: Physiological responses of temperate saplings: Interactive effects of elevated temperature, CO_2, and waterlogging.

3.1 Abstract

The exchange of carbon, water, and energy between land and atmosphere is driven by plant physiological processes yet few studies have examined temperate tree saplings' physiological responses to climate change. Here we assessed the response of plant physiology and biomass of tree sapling waterlogging and either the interaction between elevated temperature and elevated CO_2 in a two-year growth room experiment with saplings of *Alnus glutinosa*, *Betula pendula*, *Betula pubescens*, *Salix pentandra* and *Salix aurita*. In the temperature experiment, waterlogging increased photosynthesis, stomatal conductance, and transpiration rates in *A. glutinosa* and *S. pentandra*. Elevated temperature increased the photosynthesis, stomatal conductance, and transpiration rates for *Betula pendula* but *Alnus glutinosa* decrease photosynthesis, stomatal conductance and transpirations rates. In the CO_2 experiment, there was a contrasting response to waterlogging among the species. Photosynthesis, transpiration and stomatal conductance increased for *B. pendula* but decreased for *B. pubescens*. Elevated CO_2 increased photosynthesis, transpiration and stomatal conductance *A. glutinosa* and *B. pubescens*. There was increase in total dry root biomass specifically under waterlogging in both species under elevated temperature and CO_2. Our results suggest that rising temperatures, CO_2 levels, and waterlogging will differentially impact plant physiology across tolerant and sensitive species, with significant implications for future vegetation dynamics and ecosystem functioning in temperate systems under climate extremes.

3.2 Introduction

Global atmospheric carbon dioxide (CO_2) concentration and air temperature, two essential factors influencing plant growth, development, and function, have changed considerably since 1750 and are expected to continue to do so as a result of human activities. According to the Intergovernmental Panel on Climate Change (IPCC), the global mean temperature is likely to increase by 1.5°C between 2030 and 2052 due to anthropogenic activities (Bowles et al. 2020) and an estimated 3.2°C increase by 2100 (IPCC 2022) which are attributable to rising atmospheric concentrations of CO_2 and other greenhouse gases. In many regions, and especially in Europe, the average temperature has continued to rise with seasonally different rates of warming being greatest in Northern Europe's high latitudes (EEA 2012). Further, high temperature extremes have become more common and annual precipitation has increased (up to +70 mm per decade; (EEA 2012).

In combination with the rising mean annual temperatures, and an increase in CO_2, it is expected that the magnitude and duration, will also increase in the future (Hennessy et al. 2008). Future projections in precipitation has been reported for Northern Europe with extreme precipitation in all seasons (EEA 2012). As a consequence, future vegetation will be exposed to waterlogging, elevated CO_2, and severe heat stress, which can impact significantly on ecosystem functions and diversity (Lawson et al. 2017).

Temperate forests provide many ecosystem services, including the regulation of water, nitrogen, and carbon cycles, biomass, carbon, soil fertility, litter decomposition, and timber production (Kumar et al. 2016; Hao et al. 2020). According to the FAO (2020), temperate forest occupies 16% (or 665.8 million ha) of the world's forest and is the second largest biome, with distribution in eastern North America, North-eastern Asia, and Western and Central Europe (Gilliam 2016). Temperate forest is deteriorating primarily as a result of human

activities, environmental disturbances, diseases, pest, fire and severe weather events (Rawat et al. 2022).

Rising atmospheric CO_2 concentration can stimulate plant growth and physiology through increased photosynthesis and water-use efficiency in angiosperm forest (Long et al. 2004; Gardner et al. 2023) and can affect carbon balance and macronutrient utilisation (Reich et al. 2014). Through increased photosynthesis (*A*) and decreased stomatal conductance (gs), plants respond to an increase in the concentration of CO_2 in the atmosphere (Morison and Lawlor 1999). These two fundamental responses are the source of all other effects that eCO_2 has on ecosystems and trees (Long et al. 2004). The physiological responses of individual species may differ when subjected to eCO_2 (Saxe et al. 1998). For example, Ainsworth and Rogers (2007) reported a reduction in stomatal conductance during elevated CO_2 (+208 μmol mol $^{-1}$) by an average of 19% and increased water-use efficiency in trees species growing in free-air CO_2 enrichment (FACE) experiments. Similarly, (Medlyn et al (2001) reported that stomatal conductance was reduced by 21% in European forest trees when exposed to eCO_2 (+250 μmol mol-1) within four types of CO_2 exposure facilities. However, for tree species, stomatal responses to eCO_2 experiments has been observed to induce reductions in stomatal conductance in gymnosperms species than in angiosperm species (Saxe et al. 1998; Medlyn et al. 2001), which implies that stomatal activity to eCO_2 may vary with phylogeny (Hasper et al. 2017).

Waterlogging stress can be more harmful to woody species during their growth season than during their dormant phase (Kozlowski 1997). Plants can experience hypoxia, anoxia, or re-oxygenation depending on the duration of water saturation during waterlogging and can also be exposed to varying soil oxygen concentrations (Colmer and Voesenek 2009a). Waterlogging can limit growth of plants either by modifying the metabolic structures in the root or by indirectly reducing nutrient availability in plants, especially soil nitrogen (Bailey-Serres et al.

2012; Nguyen et al. 2018). Other effects of waterlogging include decreased in stomatal conductance, transpiration, respiration, hydraulic conductance, and decreased soil oxygen (O_2) in the soil and roots. According to Pezeshki (2001), stomatal closure-related diffusional and non-stomatal limitations are linked to decreases in photosynthesis. In addition, re-oxygenation of roots and subsequent production of reactive oxygen species in roots and shoots may increase stress during intermittent rather than continuous waterlogging (Geigenberger 2003). Some species, on the other hand, exhibit four months tolerance (Megonigal et al. 2005) or 10 weeks acclimatisation to waterlogging (Piper et al. 2008). After a period of acclimatization, some woody species with tolerance to waterlogging can maintain the water potential and photosynthetic activity of leaves during period of water stress (Kogawara et al. 2006).

The interactive relationship of elevated CO_2 or elevated temperature and waterlogging on the physiology of temperate trees remain less understood. Interactive effects of waterlogging and eCO_2 on physiological response of *Cauarina cunninghamiana* and *Eucalyptus tereticornis*, two Australian riparian tree saplings (Lawson et al. 2015), revealed a species-specific effects of atmospheric CO_2 concentration and waterlogging on growth and gas exchange. Elevated CO_2 increased growth of *Casuarina cunninghamiana* but this effect was removed by waterlogging (Lawson et al. 2015). The physiological acclimation to elevated temperature and atmospheric CO_2 in mature boreal Norway spruce (Lamba et al. 2018) means that eCO_2 decreased photosynthetic carboxylation capacity and increased shoot respiration while warming had no significant effect. The interaction between eCO_2 and waterlogging has been investigated (Huang et al. 1997; Pérez-López et al. 2009; Shimono et al. 2012a; Lawson and Leishman 2017) but, findings are variable among studies. For example, Megonigal et al. (2005) reported that elevated CO_2 in juveniles of the flood tolerant tree species *Taxodium distichum* in waterlogged (water-table -10 cm) stimulated biomass production but not when inundated (water-table at +5 cm). Under elevated CO_2, inundation had no effect on the increased

photosynthesis but rather due to enhanced metabolic activity of roots under low O_2 conditions. In contrast, a well-adapted flood tolerant Amazonian tree grown in an open top chamber, showed that biomass of waterlogged *Senna reticulata* under elevated CO_2 increased (Arenque et al. 2014). These variable responses means that further studies are needed to assess the impact of eCO_2, elevated temperature and waterlogging on the physiology of temperate trees to better understand how they respond to these environmental changes in future climate.

To reduce uncertainties in the physiological response of temperate trees to climate change, the current study investigates the physiological responses of the interactive effect between waterlogging and elevated temperature or elevated CO_2 on leaf gas exchange function, and behaviour as well as biomass accumulation and allocation of temperate trees saplings. Previous work has shown that plants alter their physiological processes in short-term adaptations to waterlogging; For instance, they decrease the net photosynthetic rate (*A*) and stomatal conductance (*gs*) (Jacobsen et al. 2007), or increased their dry weight under elevated temperature (Shimono et al. 2012b). However, the physiological responses underlying sapling acclimation responses to leaf gas exchange parameters used to model carbon and water fluxes in earth systems models have not been thoroughly investigated. Here, we evaluated the physiological responses of leaf physiological acclimation to increasing temperature to thirty-days waterlogging and increasing CO_2 to sixty-days waterlogging. The aim of the study was to test the following hypotheses:

i. Elevated temperatures lead to an increase in transpiration rates, resulting in reduced carbon assimilation and growth while stomatal conductance decreases under elevated CO_2 conditions, reducing transpiration rates and improving water use efficiency
ii. Increased atmospheric CO_2 levels will lead to higher rates of photosynthesis and greater carbon assimilation in water-tolerant species only but stomatal conductance under

waterlogged conditions lead to decreased transpiration rates and could also hinder CO_2 uptake.

iii. Interactive effects of elevated temperature and waterlogging will result in reduced photosynthetic efficiency and decreased below-ground biomass accumulation while CO_2 enrichment mitigate the negative impacts of waterlogging by enhancing photosynthetic rates and improving energy availability for stress recovery.

3.3 Materials and method

3.3.1 Plant material and Experimental design

Three temperate forested wetland tree species and one common in well-drained sites were chosen for the study. The species used in experiment 1 (elevated temperature) were *Alnus glutinosa* (Common Alder) (Betulaceae), *Salix pentandra* (Bay Willow) (Salicaceae), *Salix aurita* (Eared willow) (Salicaceae) and *Betula pubescens* (Downy Birch) (Betulaceae) which are typically able to withstand in floodplain sites while *Betula pendula* (Silver Birch) (Betulaceae) typically is associated with well-drained sites. In experiment 2 (elevated CO_2), *Salix pentandra* was replaced with *Salix aurita* due to unavailability of the saplings. These species' biology and ecology are further described in Table 3.1.

Table 3-1: The study species' biological and ecological characteristics

Species Common name	***Alnus glutinosa* Common alder**	***Betula pendula* Silver birch**	***Betula pubescens* Downy birch**	***Salix pentandra* (Bay willow)/*Salix aurita* (Eared willow)**
Family	Betulaceae	Betulaceae	Betulaceae	Salicaceae
Distribution	Continental Europe (except for both the extreme north and south) as well as the United Kingdom and Ireland[a]	Native to Europe and some parts of Asia. Only found in higher latitudes in southern Europe[a]	Native and abundant throughout northern Europe and northern Asia, growing farther	Native to northern Europe and northern Asia[a]

			north than any other broadleaf tree[a]	
Habitat	It thrives in damp, cool areas like marshes, wet woodland, and streams, where its roots assist in preventing soil erosion. Its natural habitat is moist ground close to rivers, ponds, and lakes[a]	Thrives best in dry, acidic soils, needs a lot of light, and grows on heathland, mountainsides, and crags[a]	Saplings are intolerant of shady conditions, this allows other woodland trees to become established, displacing the birch, a short-lived tree but grows in damper areas with poor drainage and peatlands[a]	Grows beside rivers and streams and on marshy ground in wet woodland[a]
Morphology	Medium-sized, short-lived tree, 30m (98 feet)[a]	Deciduous tree, typically reaches 15 to 25m (49 to 82 feet)[a]	Deciduous tree, growing to 10 to 20m (33 to 66 feet) tall[a]	A small tree, 14m (46 feet) tall[a]
Community status	Dominant[a]	Common[a]	Common[a]	Common[a]
Biogeomorphic effects	It is a pioneer species, colonizing undeveloped land and establishing mixed forests alongside other trees.	It is most common in mountainous areas. It is a pioneer species, one of the first trees to sprout on bare land or after a forest fire, and its light seeds are easily carried by the wind[b]	It is a pioneer species that thrives in new environments away from its parent tree[b]	The plant cannot reproduce itself, it is pollinated by bees[d]
Nitrogen fixing ability	Nodulated with *Frankia*[c]	Nodulated with *Frankia*[c]	Nodulated with *Frankia*[c]	None[d]

[a]Royal Botanic Gardens and the woodland Trust (2023),

[b] Hynynen et al., (2010),

[c](Pawlowski et al. 2007),

[d](Sommerville 1991)

The experiment took place over a period of two years. For the first year in 2021 (Experiment 1), we stimulated elevated temperature and thirty-days waterlogging while for the second year in 2022 (Experiment 2), we stimulated elevated CO_2 and sixty-days waterlogging in a growth

room. For this, saplings were purchased in 2021 and 2022 from an online nursery (https://www.treesbypost.co.uk/) and transported to the University of Nottingham (Sutton Bonington Campus) (52º 50' N, 1º 15' W) bare rooted, 1-2 years old and between 30-70 cm tall (Fig. 3.1).

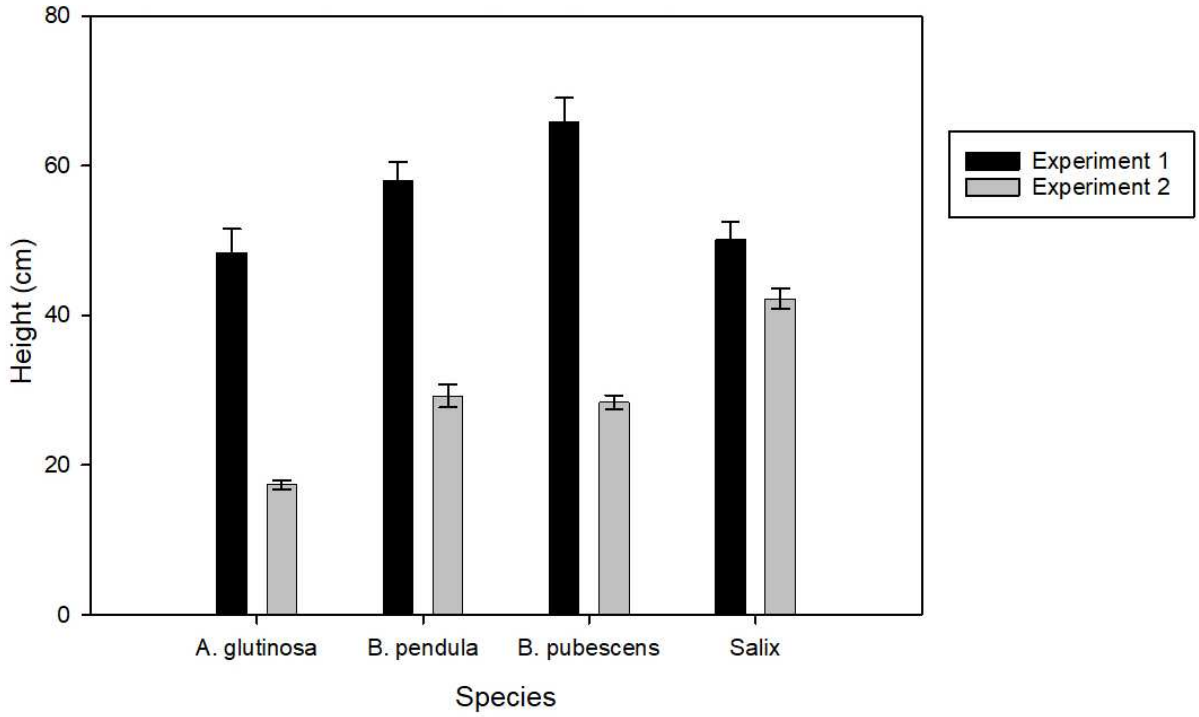

Figure 3:1: Height of saplings at the beginning of experiment 1 (Temperature experiment) and experiment 2 (CO_2 experiment)

Saplings were stored until March 2021 for the temperature experiment and May 2022 for the CO_2 experiment. During the storage period before the start of the experiment, the saplings were placed in a cold room (-4°C). They were moved into the growth rooms at the beginning of spring 2021 and 2022 for the temperature and CO_2 treatments, respectively, a few days before the start of experiment to allow adaptation to the growth room conditions. Saplings were planted individually in a 10-L bucket containing a mixture of loamy soil and topsoil which were obtained from submerge wetlands in Diamond Jubilee wood off Pasture Lane, Sutton Bonington Village, Nottinghamshire (https://www.nottingham.ac.uk/sustainability/grounds/diamondwoods.aspx) Loughborough.

The rationale for the temperature treatment is to stimulate future climate conditions and assess how different species will respond in terms of growth, survival and physiological changes. For temperature treatment, saplings were subjected to the temperature treatment in March 2021, At the peak of biomass, waterlogging was then initiated in late August 2021 (hottest month) for 30 days, in order to stimulate a significant waterlogging and elevated temperature. The 30 days period was chosen to allow for morphological adaptation to manifest and reflect a common period of flooding occurring (Hennessy et al. 2008).

The rationale for the CO_2 treatment is to understand how elevated CO_2 can influence photosynthesis, water use, growth rates and overall plant physiology. For the CO_2 experiment, saplings were transferred into the growth room in May 2022 and CO_2 treatment was initiated on the same day. Thirty days after the start of the experiment, i.e. when leaves have emerged, saplings were subjected to 60 days of waterlogging in July 2022. This longer flood exposure period was chosen to in order to identify tolerance traits (development of specialized root structures like aerenchyma), physiological adaptations and to assess growth and biomass accumulation to waterlogging during the main growth period. The two waterlogging treatments where different in order to access the initial stress response (30 days) and extended stress response (60 days) on plant physiology, growth and survival.

Ninety-six saplings of trees $n = 96$ (24 per species) were used for each experiment. We used a fully factorial design for both experiments. For both experiments, the factorial design comprised of a combination of two [temperature] treatments (ambient temperature (aT) and (eT)) with two waterlogging treatments (control and waterlogged) for experiment 1 and 2 [CO_2] treatments ambient CO_2 (aCO_2) and eCO_2 with two waterlogging treatments (control and waterlogged), for experiment 2. There were four blocks per treatment in each of the growth room resulting in twelve replicates per treatment combination per species. Out of the 12 plants

of each species in each growth room, six were randomly allocated for a waterlogging treatment. The remaining six plants were controls.

For the waterlogging treatments, all pots (10-L) assigned a waterlogging treatment were inserted into 15-L buckets and filled with tap water and water-level was maintained daily. The 30-day and 60-day waterlogging was set to stimulate a waterlogged soil concentration comparable to commonly occurring wetland soils and natural habitats for these plants.

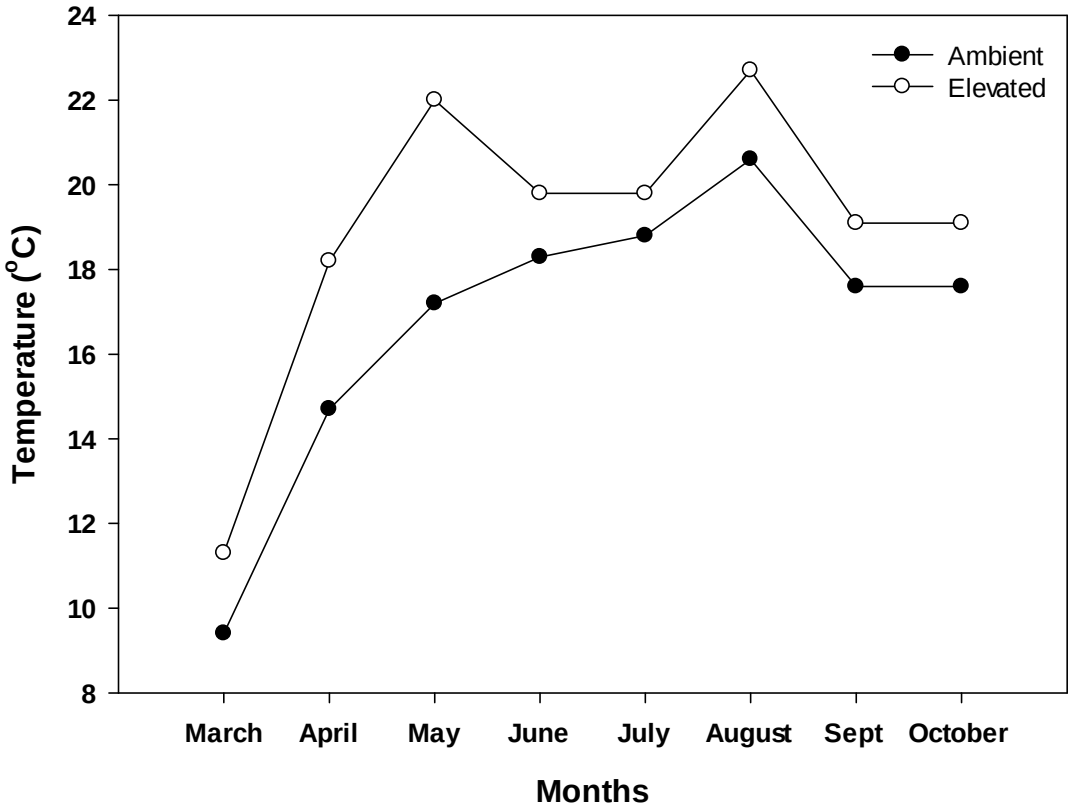

Figure 3:2: Monthly temperatures for growth rooms during the span of the temperature experiment (Experiment 1). The ambient temperature treatment was based on monthly mean temperatures recorded by the Sutton Bonington Meteorological station from 2015-2020.

For the first experiment, saplings were subjected to two temperature regulated growth rooms. Growth room one is the aT while growth room two is the eT growth room. The increase in temperature is to mimic global warming and natural increase in temperature projected within the range of 1.2°C to 3.2°C in the region by 2100 (IPCC 2022) (Fig. 3.2). We investigated four

treatments in each experimental year. For the first experiment, we investigated control+aT, WL+aT, control+eT and WL+eT. The temperature elevation goal was modified on a monthly time step following the Met office predictions with a monthly temperature increase above the actual aT of +2.4 ℃ (March-October) resulting in an increase during the growing season (Met office 2021). Therefore, the temperature treatment was set to target ambient +2.4℃. For the second experiment, saplings were placed in two growth rooms. Growth room one was the eCO_2 and was set to target 700 ppm while growth room two was the aCO_2 and was set to target 420 ppm, however the growthroom fluctuated between (700-800 ppm) in the eCO_2 and (420-500 ppm) for the ambient CO_2. Temperature for this experiment were set at ambient temperature for each month. We investigated four treatments in each experimental year. For the second experiment, we investigated control+aCO_2, WL+aCO_2, control+eCO_2 and WL+eCO_2.

Water-level before commencing the experiments were irrigated as in Wang et al (2015), briefly, the saplings that were not subjected to waterlogging treatment were irrigated three times during dormancy and two times a week during the growing season. During waterlogging, water-level was kept constant in both the first and second experiment and water was added when necessary to achieve even shoot submersion. In both growth rooms, before waterlogging, air relative humidity was 70/80%, photoperiod was 12/12 h (day/night), and the photosynthetically active radiation (PAR) ranges between 129 to 266 µmol m^{-2} s^{-1} with a mean of 210 µmol m^{-2} s^{-1}. During waterlogging, air relative humidity was 90%, photoperiod was 10/14 (day/night), photosynthetically active radiation ranges from 138 to 284 µmol m^{-2} s^{-1} with a mean of 212 µmol m^{-2} s^{-1}. At the end of each treatment, height and diameter were recorded. We also determined the below-ground biomass accumulation and distribution and root biomass of each plant species.

3.3.2 Gas exchange measurements and water use efficiency

Leaf gas exchange measurements for photosynthesis rate (*A*), Stomatal conductance (*gs*) and transpiration (*E*) were measured on the newest fully developed leaves between 9 a.m. to 2 p.m., using an LI-6800 Portable Photosynthesis System (LI-COR, Lincoln, NE, USA). The Li-cor was set to measure at one light intensity (Qin) in the Multi Control Loops, where the measure to be obtained with Qin= 2000 μmol m^{-2} $s^{-}1$ and temperature was held at the temperature of the growth room, growth (CO_2) (400 μmol m^{-2} $s^{-}1$), leaf-to-air vapour pressure deficit (VPD) and RH of 0.2 kPa and of 60% respectively. Measurements were taken after leaves were equilibrated for 10-15 mins. Gas exchange was measured during the three phases of the experiment (before, during and after waterlogging). For the first experiment, the first measurement was taken 30 days before the commencement of waterlogging, and the second measurement 30 days into waterlogging. The third measurement was taken 5 days after the termination of waterlogging treatment. For experiment 2, the first measurement was taken 10 days before the start of waterlogging and the second measurement 60 days into waterlogging. No 'after' measurement was taken in experiment 2. The *A/E* ratio was then used to calculate water-use efficiency (WUE). For each species and for both treatments.

3.3.3 SPAD measurements

Measurements of chlorophyll content can be used to indicate the physiological state of leaves, and hence, the plant. A portable chlorophyll meter (SPAD-502; Minolta, Osaka, Japan) was used to determine the leaf greenness, which is directly related to the concentration of chlorophyll present in leaves (Piekielek et al. 1995). Leaf relative chlorophyll content (SPAD) was measured during week 4, 5, 6, 17 and 29 for the newest fully emerged leaf on the main shoot in experiment 1 using a chlorophyll meter. For the second experiment, measurements were taken during week 4 and 11 only. For each plant, one leaf was selected at random from the upper part of the main shoot and chlorophyll content index (CCI) was measured at one

point of the leaf. CCI measured using the SPAD meter is a relative value that comprises of the ratio of transmittance of two wavelengths, 931 and 653 nm and indicates the amount of chlorophyll present in the leaf.

3.3.4 Chlorophyll fluorescence

The chlorophyll fluorescence as the quantum yield was measured during week 4, 5, 6, 17 and 29 for the newest fully emerged leaf on the main shoot in experiment 1and 2 using a Fluorpen FP 100 fluorometer (PSI, Czech Republic). These measurements were taken from one leaf selected at random from the upper part of the shoots and quantum yield (QY) was measured at three points on the leaf to calculate the mean. Measurements were taken on the same dates as the leaf SPAD measurements.

3.3.5 Biomass accumulation and distribution

To determine the biomass accumulation and distribution, height (new meristem growth during the treatments), diameter was measured, and roots of each plant species were destructively harvested at the end of the experiment. Thereafter, the fresh and dry weight was determined by drying the material to constant mass in an oven at 80ºC for 48 hours and then weighing using an analytical balance.

3.3.6 Statistical analysis

GENSTAT (21st edition) was used to run a mixed linear model using residual maximum likelihood (REML) method to test the impact for the main effects of and interactions between species, elevated temperature or elevated CO_2 and high-water level on physiology photosynthesis assimilation (*A*), stomatal conductance (*gs*), transpiration (*E*), chlorophyll fluorescence (Quantum yield (Qy)) and SPAD. The model has species (*Alnus glutinosa, Betula pendula, Betula pubescens and Salix pentandra/Salix aurita*), timepoints (before and during waterlogging) and temperature or CO_2 (ambient and elevated) as fixed effects and block as the random effect. All data were log-transformed to meet assumptions of normality. Standard error

of the differences was predicted from the mixed linear model and used to assess which specific differences were significant at $p \leq 0.05$. Full ANOVA tables are reported in Appendix A.

3.4 Results

3.4.1 Impacts of elevated temperature and waterlogging

Among the four species *A. glutinosa* has the greatest values for the physiological parameters i.e. *A*, *E*, and *gs*, followed by *B. pubescens* (Fig. 3.3) while *B. pendula* and *S. pentandra* consistently had the lowest values. *A. glutinosa* also had the highest for the chlorophyll content and chlorophyll fluorescence, followed by *B. pubescens* and *S pentandra* (Fig. 3.4), *B. pendula* again had the lowest values.

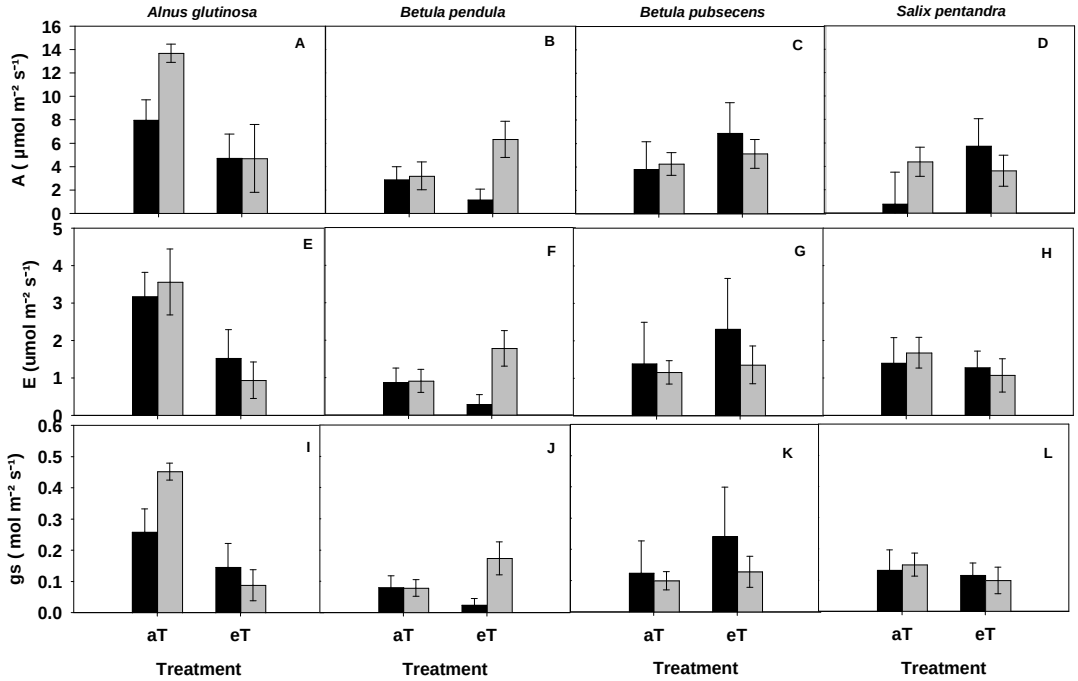

Figure 3:3: Leaf gas exchange measurements of *A. glutinosa*, *B. pendula*, *B. pubescens*, and *S. pentandra* saplings exposed to the temperature treatment (ambient +2.4°C) with 30 days waterlogging. Dark shaded columns represent control, and light shaded columns represent waterlogged measurements. Error bars represent the standard mean error.

At the end of the experiment *S. pentandra* followed by *B pubescens* had the greatest extension growth while *A. glutinosa* and *B. pendula* had the lowest extension growth. In contrast *B.*

pendula and *A glutinosa* had the greatest root biomass (Fig. 3.5) while the root biomass of *S. pentandra* and *B. pubescens* were the lowest.

The waterlogging treatment increased *A* across all four species but had no impact on the other physiological parameters measured, or root biomass. For the extension growth there was a significant species × waterlogging interaction (Tab. 3.2) with reduced extension growth in the waterlogging treatment for *A glutinosa, B pendula* and *S pentandra***.** In contrast *B. pubescens* had greater extension growth in the waterlogging treatment.

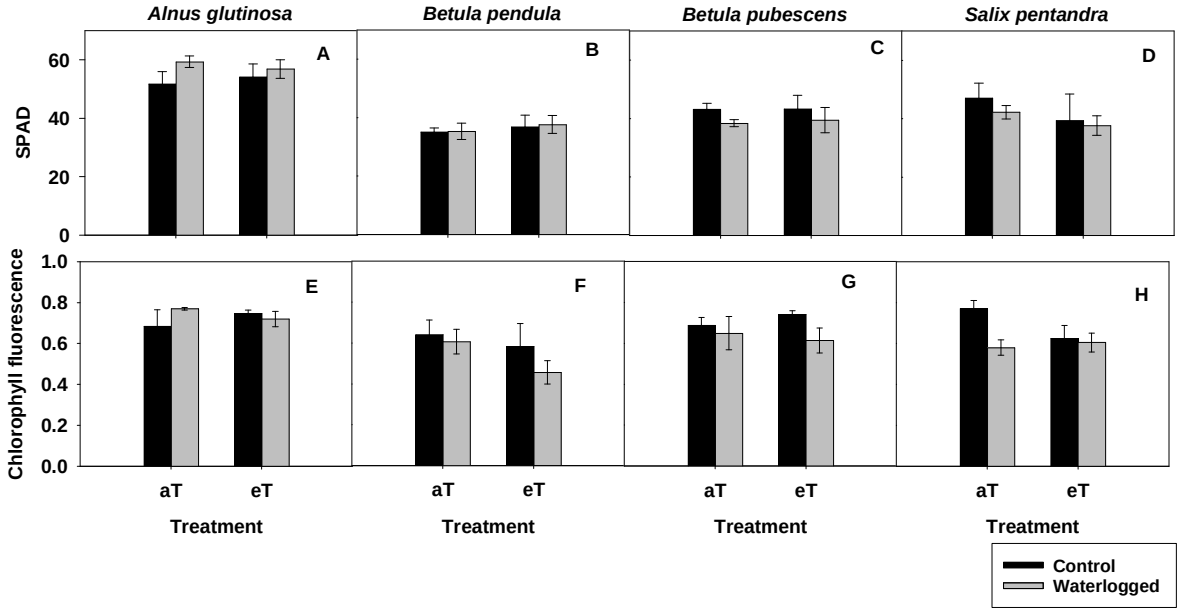

Figure 3:4: SPAD and chlorophyll fluorescence measurements of *A. glutinosa, B. pendula, B. pubescens*, and *S. pentandra* saplings exposed to the temperature treatment (ambient +2.4°C) and 30 days waterlogging. Dark shaded columns represent measurements before waterlogging and light shaded columns represent measurements during waterlogging. Error bars represent the standard error of mean.

The saplings had greater extension growth and root biomass in elevated than in ambient temperature ($P < 0.05$; Tab. 3.2) but there was no significant effect of temperature on any of the physiological parameters measured ($P > 0.05$; Tab. 3.2).

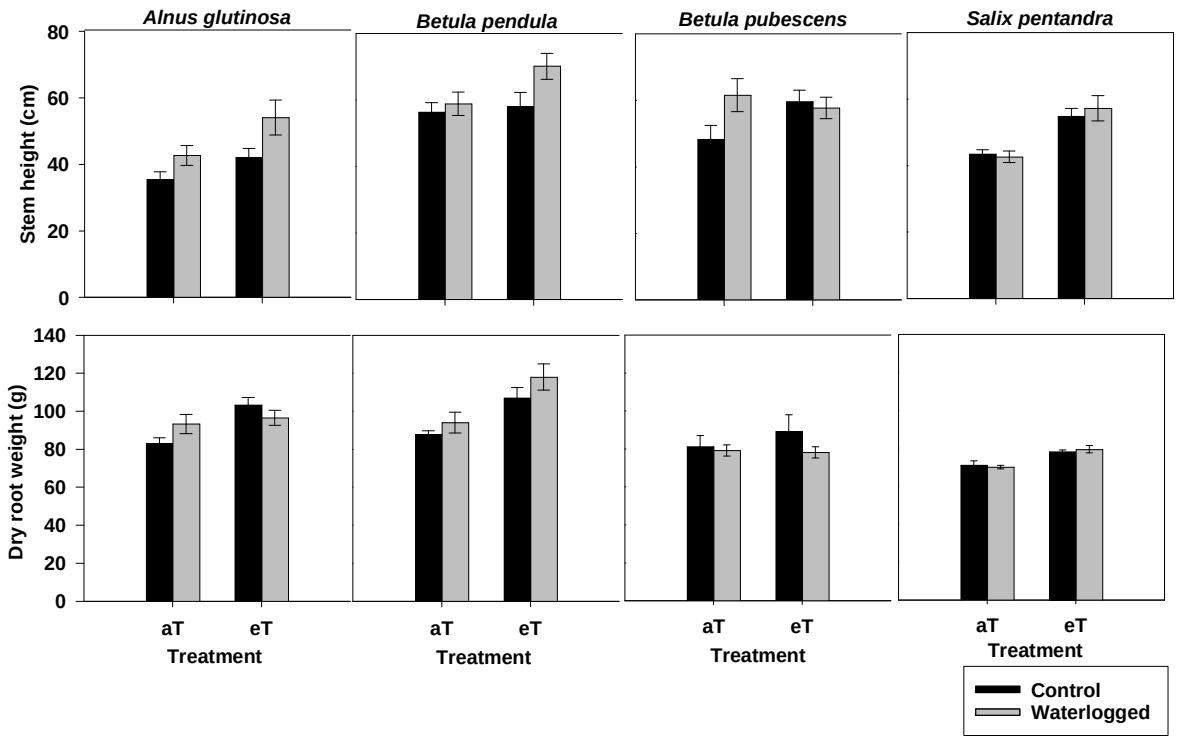

Figure 3:5: Biomass allocation measurements *of A. glutinosa, B. pendula, B. pubescens,* and *S. pentandra* saplings exposed to the temperature treatment (ambient +2.4°C) with 30 days waterlogging. dark shaded columns represent control measurements and light shaded columns represent waterlogged treatment. Error bars represent the standard error of mean.

With regards to the temperature, this interacted with species for the physiological, growth and biomass data (Tab. 3.2). Specifically, there was a species × temperature interaction for *A* where *A. glutinosa* had the lowest *A* under elevated treatment while the *A* of *B. pendula* did not differ between the temperature treatments, in contrast both *B pubescens* and *S. pentandra* had higher *A* in the elevated temperature treatment (Fig. 3.3). The transpiration and gs also showed species specific responses to temperature. The transpiration rate for *A. glutinosa* was lowest in the elevated treatment, for the two *Betula* species there was no significant effect of the temperature treatment, and only *S. pentandra* responded positively to the elevated treatment. For *gs*, *A. glutinosa* had the highest values in the ambient temperature, *B. pendula* and *S. pentandra* did not response significantly and only *B. pubescens* responded positively to elevated temperature. The overall extension growth was highest in the elevated temperature for *A. glutinosa*, *B pendula*, and *B. pubescens* while for *S. pentandra* extension growth was lowest in the elevated temperature (Fig. 3.5). The root biomass at the end of the experiment was highest in the

elevated temperature treatment for *A. glutinosa*, *B. pendula*, and *S. pentandra* while *B. pubescens* has the lowest root biomass in the elevated temperature.

3.4.2 Impacts of elevated CO_2 and waterlogging

A. glutinosa had the highest *A*, *E* and gsw followed by *B. pendula* (Fig. 3.6) while *S. aurita* and *B. pubescens* had the lowest. *Betula pubescens* had the highest chlorophyll content while *B. pendula* had the lowest chlorophyll content and chlorophyll fluorescence (Fig. 3.7).

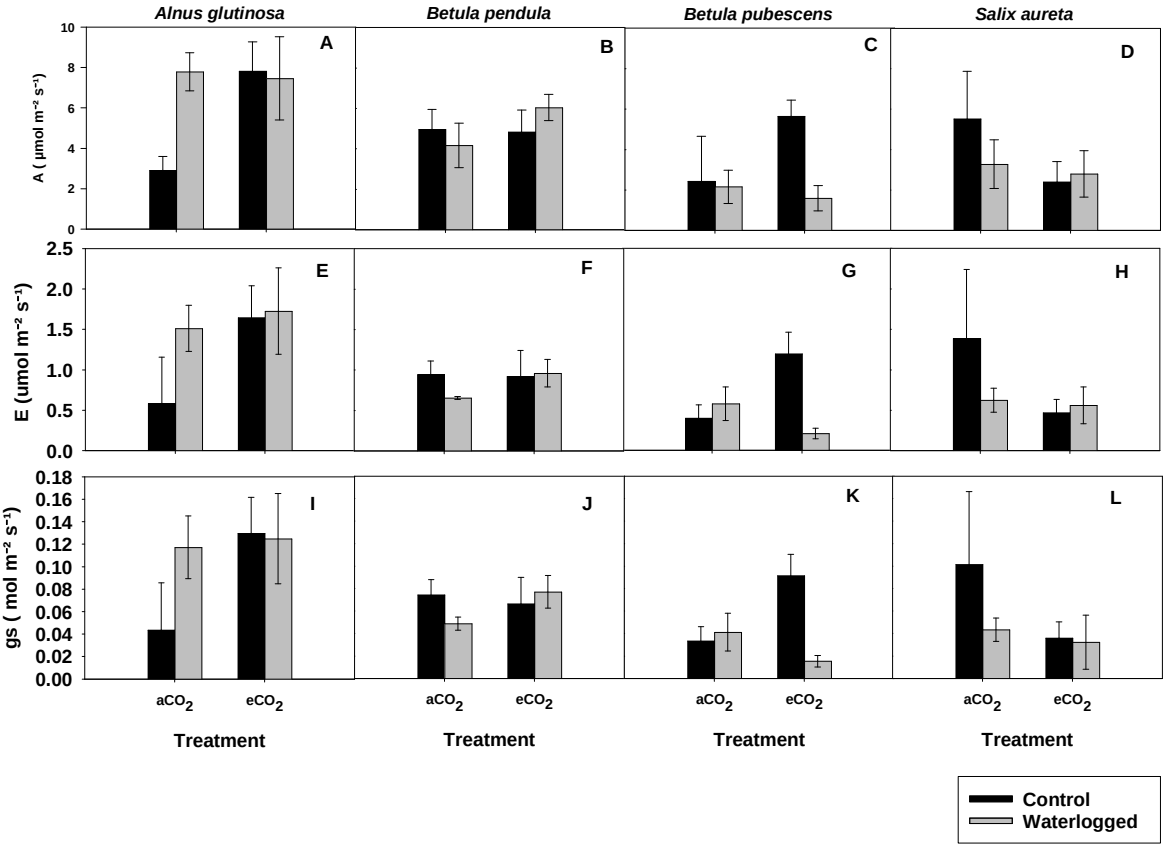

Figure 3:6: Leaf gas exchange measurements of *A. glutinosa, B. pendula, B. pubescens* and *S. aurita* saplings exposed to ambient CO_2 (420 ppm) and elevated CO_2 (700 ppm) with waterlogging. Each combination of CO_2 treatments and waterlogging. Dark shaded columns represent control, and light shaded columns represent measurements waterlogged treatments. Error bars represent the standard mean error

At the end of the experiment *S. aurita* had the greatest extension growth followed *B. pendula* and *B. pubescens* while *A. glutinosa* had the lowest extension growth (Fig 3.8). Similarly, *S.*

aurita and *A. glutinosa* had the greatest root biomass and stem diameter while the root biomass and stem diameter of *B. pendula* and *B. pubescens* were the lowest (Fig. 3.8).

The Waterlogging treatment had no significant impact on any of the physiological parameters measured across all species (*P > 0.05*; Tab. 3.2). overall, the saplings had greater chlorophyll content in ambient than elevated CO_2 (Fig. 3.7) but there was no significant effect of CO_2 on any of the physiological parameters measured (*P > 0.05*; Tab. 3.2).

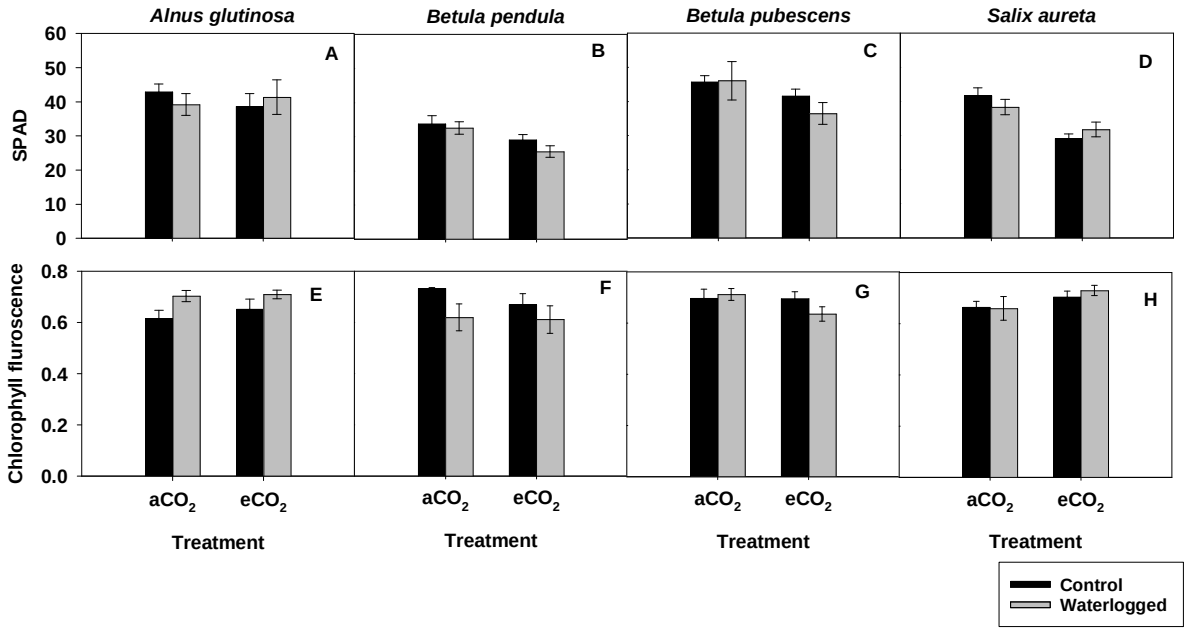

Figure 3:7: SPAD and chlorophyll fluorescence measurements of *A. glutinosa*, *B. pendula*, *B. pubescens*, and *S. aurita* saplings exposed ambient CO_2 (420 ppm) or elevated CO_2 (700 ppm) with 60 days waterlogging. Dark shaded columns represent measurements control and light shaded columns represent measurements waterlogging. Error bars represent the standard error of mean.

However, there was a species × elevated CO_2 interactive effect on stem (*P < 0.05*, Tab. 3.2). More specifically, *S. aureta* had the highest values in the elevated treatment (Fig. 8), while *A. glutinosa*, *B. pendula* and *B. pubescens* did not response significantly to elevated CO_2 (*P > 0.05*, Tab 3.2).

There was also a species × CO_2 × waterlogging interaction for *A* (*P < 0.05;* Tab. 3.2). More specifically, *A. glutinosa* had the lowest *A* rates in the ambient CO_2 under no waterlogging. For *B. pendula*, waterlogging facilitates a positive response to elevated CO_2, while in *B. pubescens*,

elevated CO_2 increases photosynthesis under no waterlogging treatment only, and *S. aureta* has the highest assimilation rate under no waterlogging and ambient CO_2 treatment (Fig 3.6).

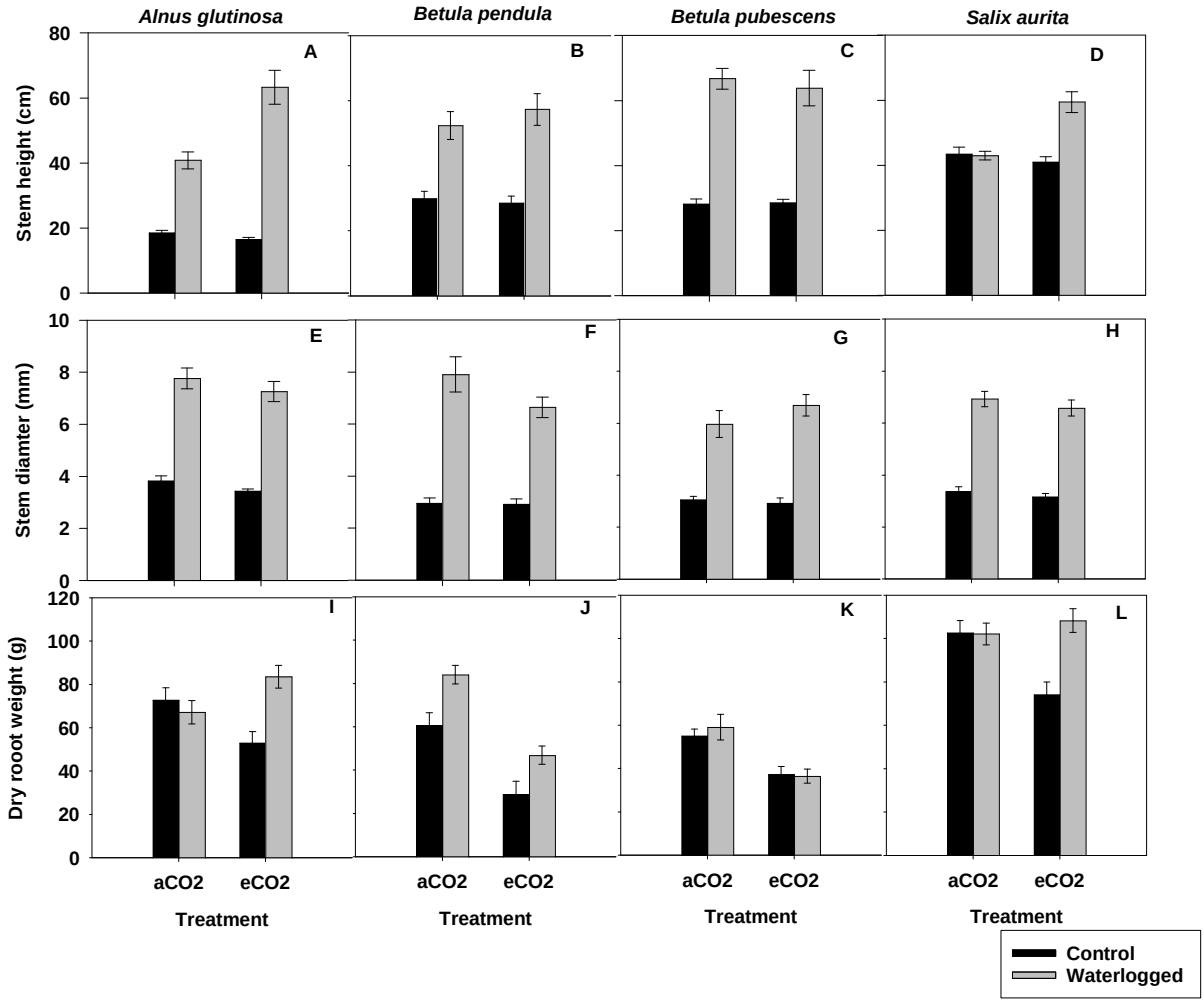

Figure 3:8: Stem height, diameter expansion and root biomass measurements of *A. glutinosa*, *B. pendula*, *B. pubescens*, and *S. aurita* saplings exposed to ambient CO_2 (420 ppm) or elevated CO_2 (700 ppm) with 60 days waterlogging. Dark shaded columns represent control measurements and light shaded columns represent waterlogged measurements. Error bars represent the standard error of mean.

Table 3-2: Statistical analysis summary of the main effects and interactions of species, temperature, CO2, and waterlogging

	Temperature (Experiment 1)					**CO_2 (Experiment 2)**				
Parameters	**Treatment effects *(P)***					**Treatment effects *(P)***				
	Species (S)	**Temperature (T)**	**Waterlogging (W)**	**S × T**	**S × W**	**Species (S)**	**CO_2**	**Waterlogging (W)**	**S × CO_2**	**S × CO_2 × W**
Photosynthesis CO_2 assimilation *A* ($\mu mol^{-2}s^{-1}$)	**0.002**	0.747	**0.035**	**0.009**	0.412	**<0.001**	0.408	0.537	0.175	**0.049**
Transpiration *E* ($mol\ m^{-2}s^{-1}$)	**0.016**	0.167	0.712	0.02	0.462	**0.006**	0.817	0.326	0.303	0.145
Stomatal conductance *gs* ($m\ mol\ m^{-2}s^{-1}$)	**0.008**	0.134	0.356	0.009	0.264	**0.006**	0.777	0.271	0.346	0.214
SPAD	**<0.001**	0.693	0.751	0.558	0.307	**<0.001**	**0.002**	0.256	0.37	0.455
Chlorophyll fluorescence	**0.002**	0.484	0.085	0.498	0.356	0.544	0.87	0.626	0.466	0.761
Stem height (cm)	**0.009**	**0.01**	-	**0.004**	-	**<0.001**	0.2	-	0.85	-
Stem diameter (mm)	-	-	-	-	-	**0.001**	0.204	-	**<0.001**	-
Dry root biomass (g)	**<0.001**	**0.016**	0.625	**0.033**	0.206	**<0.001**	0.272	0.071	0.957	0.562

Species, waterlogging and temperature or CO_2 was used as fixed effect, while blocking structure was utilized as a random effect. Bold numbers indicate significant effect at $P \leq 0.05$.

3.5 Discussion

In our experiments, we have shown that the anticipated increases in future temperature and CO_2 levels, along with waterlogging, exert control over the growth and physiology in 2–3-year-old saplings of *Alnus glutinosa, Betula pendula, Betula pubescens, Salix pentandra and Salix aurita*.

3.5.1 Effects of waterlogging on leaf greenness, chlorophyll fluorescence, gas exchange and water use efficiency

In this study, leaf greenness which is linked to (chlorophyll content) of waterlogged saplings significantly reduced irrespective of species during waterlogging. Similar reduction of chlorophyll content has been observed in other trees species after prolonging flooding and the reduction in photosynthetic pigments was viewed as a protective mechanism for the photosynthetic structures of waterlogged plants, as it minimized the absorption of sunlight and helped prevent photooxidation (Kreuzwieser et al. 2002). Chlorophyll fluorescence (F_v/F_m), an indicator of the photochemistry of photosynthesis, were negatively affected by waterlogging in all species. We also observed a more significant decrease in *B. pubescens*. Greater reduction in F_v/F_m in non-flooding species demonstrated a significant injury and greater photosynthetic inhibition of PSII, resulting in no tolerance to waterlogging. In a study with apple trees grown under long-term waterlogging conditions, the authors observed a significant reduction in F_v/F_m in Hongro when compared with that of the resistant variety Fuji (*M. pumila*) (Bhusal et al. 2020).

The light-saturated net photosynthesis CO_2 assimilation rate, stomatal conductance and transpiration were lower in waterlogged than non-waterlogged saplings for all species. This observation is corroborated by previous studies on trees of temperate ecosystems (Jaeger et al. 2009; Ferner et al. 2012; Lamba et al. 2018; Rawat et al. 2022). However, the extent of this

decrease varies with the ability of the species to tolerate soil oxygen limitation. A study with tree saplings of *Fraxinus angustifolia* and *Fraxinus excelsior* found that CO_2 assimilation of less tolerant or sensitive species strongly reduced rates of photosynthesis whereas highly tolerant trees sustain rates of photosynthesis at a high level or even not unaffected by the stress (Wagner 1996; Jaeger et al. 2009), that is, acclimation of species in the opposite direction to that found here. Similarly, experiments using water-tolerant species (*T. distichum and Fraxinus pennsylvanica*) show that they support photosynthesis throughout the period of waterlogging, (Kogawara et al. 2006). It is still unclear exactly what causes waterlogged trees to inhibit photosynthesis in response to photosynthesis as both non-stomatal and stomatal restrictions are involved (Pezeshki 2001), but here it appears that the decreased in stomatal conductance lead to lower *A* in waterlogged saplings, while it seemed that the photosynthetic apparatus remained unaffected. The stomatal closures of leaves observed during waterlogging in all saplings might be mediated by chemical signals as reported in earlier studies (Else et al. 1995; Kreuzwieser and Rennenberg 2014). Furthermore, stomatal closure triggered by root hypoxia typically reduces photosynthesis during waterlogging by limiting the availability of carbon dioxide, decreasing energy production (Tripepi & Mitchell, 1984) while it has been hypothesized that the decrease in root hydraulic conductance in saplings of *Quercus robur, Quercus petraea* and *Fagus sylvatica* is connected to the decrease in stomatal conductance (Schmull et al. 2000). Waterlogging resistant species may continue to use their stomata when subjected to waterlogging, as is typically the case with the temperate forest saplings investigated here (Kreuzwieser and Rennenberg 2014).

Waterlogging also decreased *E* rates in all saplings. This finding supports our second hypothesis that stomatal closure under waterlogged conditions lead to decreased *E* rates and could hinder CO_2 uptake. Numerous studies reported low transpiration rates in a range of plant

species including tree saplings within hours or days of waterlogging being imposed (Barrett-Lennard 2003;Zúñiga-Feest et al. 2017).

3.5.2 The impacts of waterlogging under elevated temperature on leaf greenness, chlorophyll fluorescence, gas exchange and water use efficiency

Combined stresses of elevated temperature and waterlogging decreased *A*, *gs* and *E* in all saplings. Generally, many saplings exhibit negative responses to elevated temperatures when they experience waterlogging. Prolonged exposure to elevated temperatures can lead to physiological stress, damage to cellular structures, and reduced photosynthetic efficiency (Ashraf and Harris 2013). Studies on the impact of waterlogging under elevated temperature on plant physiology have widely been reported in various terrestrial ecosystems (Bauweraerts et al. 2013; Jumrani and Bhatia 2019; Jiménez et al. 2020). However, no consistent patterns have been observed (Abo Gamar et al. 2021; Al-Deeb et al. 2023). Our findings in this study do not support our first hypothesis that waterlogging under elevated temperature increases transpiration and will result in reduced carbon assimilation and growth. We found negative effects of waterlogging on *A, gs* and *T* under elevated temperature that were observed in all species (Fig. 3.4). Under waterlogging, a reduction in leaf greenness was thought to be a kind of protection mechanism for photosynthetic structures in plants. This prevents photo-oxidation and reduces sunlight absorption (Du et al. 2012). The greater reduction in leaf greenness in *B. pendula*, and *S. aurita* signifies more injury in PSII following photosynthetic inhibition and subsequent reduction in ability to absorb and convert light energy to chemical energy; as a result, photosynthesis was more suppressed in *B. pendula, S. aurita* than in *A. glutinosa* and *B. pendula* (Bertolde et al. 2010). This finding may be primarily ascribed to impaired root function, nutrients imbalances and reduction in stomatal conductance both during waterlogging (Voesenek and Bailey-Serres 2015) and elevated temperature (Yamori et al. 2014).

3.5.3 The impact of waterlogging under elevated CO_2 on leaf greenness, chlorophyll fluorescence, gas exchange and water use efficiency

Leaf greenness in all studied species responded negatively to the effect of waterlogging under elevated CO_2, concurring with other studies on the impact of waterlogging under elevated CO_2 (Irfan et al. 2010; Shimono et al. 2012a; Lawson and Leishman 2017) on plants. The responses of the two closely related *Betula* species to waterlogging under elevated CO_2 showed a more significant reduction in F_v/F_m in *B. pendula* than in *B. pubescens* which is able to grow better in wetter areas. Furthermore, (F_v/F_m) was negatively affected by elevated CO_2 in all species under waterlogging in our study showing that elevated CO_2 enhance photoinhibition in stress conditions (Roden and Ball 1996).

Our findings on the responses of leaf gas exchange during increased waterlogging under eCO_2 do not support our third hypothesis that CO_2 enrichment would mitigate the negative impacts of waterlogging by enhancing photosynthetic rates and improving energy availability for stress recovery. Growth at eCO_2 resulted in a moderate negative effect of *A*, however, there was a significance heterogeneity among saplings in the magnitude of this effect. Waterlogged saplings exposed to eCO_2 showed a significant negative effect in all saplings (Fig. 3.5) but only *B. pubescens* and *S. aurita* showed strong negative effects. We anticipated that the photosynthetic response of saplings exposed to waterlogging under elevated CO_2 for 60 days would be detected in water-tolerant species only. Our results are only partially in agreement with our second hypothesis; we expected that water-tolerant species (*A. glutinosa*, *B. pubescens and S. aurita)* would better maintain photosynthesis and would more quickly acclimate to waterlogging than non-tolerant species (*B. pendula*). The photosynthesis rate in *B. pendula* was higher under waterlogging and elevated CO_2 than in *B. pubescens* and *S. aurita*. This has previously been reported for *B. pendula* in well drained conditions (Valanne et al., 1981). However, the reasons for inhibited photosynthesis of waterlogged species over non-water

tolerant species in our study could be associated with the combined effects of reduced oxygen availability and altered gas exchange (Crawford 1992).

The further decrease in *gs* by eCO_2 is less for woody than for herbaceous species (Wang et al., 2012) and our results are similar to the trend reported for trees showing a lower reduction in *gs* such as European beech (*Fagus sylvatica* L.) and pedunculate oak (*Quercus robur* L.) grown in elevated CO_2 (Heath et al. 1997). Elevated CO_2 reduced the *gs* level in *B. pubescens* saplings by 57%. Previous results for sweetgum trees have shown a 28-44% reduction in leaf level *gs* under elevated CO_2 conditions (Herrick et al. 2004; Norby et al. 2006). The reduction in transpiration during waterlogging under eCO_2 in this study was primarily dependent on reduced *gs* for these species.

All flooded saplings displayed some form of tolerance to waterlogging by development of hypertrophic lenticels, adventitious roots or enhanced stem growth and formation of aerenchyma (*A. glutinosa* and *S. aurita*) (Abdulrazq Iliya personal observation). The increased stem diameter of the flooded saplings is linked to development of intercellular spaces and increased in bark thickness (Tang and Kozlowski 1982) or as result of an increase in the number of wood fibres in submerged parts of the stem (Yamamoto et al. 1995).

Total dry root biomass was significantly higher under eCO_2 of waterlogged *S. aurita* and *A. glutinosa* saplings. This may be caused by the requirement for structural support of air spaces in aerenchymous root tissue which has been linked to a higher dry matter content in the roots (Ryser et al. 2011). Further, conversion of cell wall into root hypodermal tissues often takes place under waterlogging as a means of reducing radial oxygen loss (Colmer and Voesenek 2009a) and result in increased dry root matter. In contrast, *B. pendula* and *B. pubescens* had lower dry matter content under waterlogging, which may be attributed to these species

proliferating lower density roots and lower carbon investment in root tissue (Wright et al. 2004; Reich et al. 2014).

3.6 Conclusion

Examining the leaf gas exchange, biomass accumulation and how temperate trees responded to waterlogging in the presence of elevated temperature and elevated CO_2 provides an opportunity to assess whether these responses persisted or temporary. We found that the physiological responses were lower in waterlogged than non-waterlogged saplings in all species, although the extent of this decrease varies on the ability of the species to tolerate soil oxygen limitation. However, the interactive effects of the combined stresses of elevated temperature and waterlogging decreased net photosynthesis rate, stomatal conductance, and transpiration in all saplings. Furthermore, the interactive effect of elevated temperature and waterlogging response on chlorophyll content and chlorophyll fluorescence affected *Betula pendula* and *Salix pentandra* saplings negatively while elevated CO_2 and waterlogging had negative effects on *Betula pendula* and *Salix aurita* saplings.

Finally, plant data presented from controlled environment are invaluable in allowing researchers to determine effects of specific biotic abiotic parameters on plants. However, it has been shown that although they are highly controlled, they are not uniform which can result in variation termed chamber effect i.e. variability in the data due to growing plants in different chambers. Infrastructural limitation prevented treatment from being replicated in our experiments, therefore the results should be treated as such.

Chapter 4: Exploring the influence of root anatomical traits on leaf-level physiology and their responses to climate change in woody temperate trees saplings

4.1 Abstract

Plant anatomical and physiological adaptation moderate adaptation responses to anatomical changes. To examine the effects of climate change on root anatomical and physiological traits, we measured adaptive root traits and leaf physiological traits of five woody temperate tree species- *Alnus glutinosa, Betula pendula, Betula pubescens, Salix pentandra and Salix aurita* and observed their responses to elevated temperature and elevated CO_2 with waterlogging in a growth room experiment. We found that woody temperate tree saplings differed in their root anatomical traits and water-leaf physiological traits regardless of the severity of waterlogging periods (i.e., 30 or 60 days). Higher transpiration rates and intrinsic water use efficiency were seen in species with larger root cortical aerenchyma, total stele area and total cortex area but lower stomatal conductance. Increased temperature enhanced aerenchyma area, cortical cell file number and total stele area in *Salix pentandra* as well as total cortical area in *Betula pubescens*. Temperature enhanced transpiration, photosynthesis, and stomatal conductance rates in *Betula pubescens*. Waterlogging enhanced root cortical aerenchyma, cortical cell file number, aerenchyma number, total stele number, total cortical area, and cortical cell size in all species. Increased CO_2 enhanced aerenchyma area and total stele area in *Betula pendula* as well as photosynthesis, stomatal conductance, and transpiration rates, but lower intrinsic water use efficiency. Overall, we found that the district variation in root anatomy among woody temperate species has resulted in variations in leaf physiological traits and their responses to global change. These results demonstrate the critical roles that root anatomical traits play in regulating physiological processes at the leaf level in temperate forest and response to climate change.

4.2 Introduction

Climate change has been predicted to impact on plant growth and development adversely (Bailey-Serres and Voesenek 2008). Plant tissue responses to the effect of climate change mediated by water stress, depends on the physiological properties of the cell components and the anatomic characteristics that regulate the transmission of the water stress to the cells (Steudle and Peterson 1998). Plants employ various root-based strategies to compensate the negative effects of floods and heatwaves (George et al. 2024) such as changes in root architecture, anatomy and physiology (Schuldt et al. 2013; Hazman and Brown 2018). Therefore, the effects of climate change on the environment will be observed belowground and the root and rhizosphere are involved in adaptation and mitigation of these changes (Calleja-Cabrera et al. 2020).

Roots are expected to present the most significant barrier to water movement in the soil-plant-atmosphere system due to their primary roles in water absorption and transportation (Daly et al. 2015). Notably, living cells within roots, such as those in the cortex and endodermis, contribute substantial resistance to water uptake (Kramer and Jackson 1954; Rieger and Litvin 1999). Under optimal soil moisture conditions, root hydraulic conductivity may account for approximately two-thirds of water transport resistance in the soil-plant system (Huang and Eissenstat 2000). As a result, the ecophysiological processes of photosynthesis and water use efficiency during transpiration are influenced by the close relationship between root traits and hydraulic conductivity (Rieger and Litvin 1999; Rodríguez-Gamir et al. 2010).

Root anatomical traits such as cross-section area, cortex area and the proportion of root cortical aerenchyma, as well as the root cortical cell file number have been reported to be dependent on how easily water can move through these tissues (Schuldt et al. 2013; Chimungu et al. 2014; Wang et al. 2015b; Yamauchi et al. 2019). In addition, previous research has shown evidence

of a correlation between root anatomical traits and leaf physiological traits (photosynthesis, stomatal conductance, and transpiration) as well as water use efficiency (Zhou et al. 2021). The first- to second/third order roots or absorptive fine root are responsible for water transportation and for determining hydraulic conductance (Guo et al. 2008). Further, plant roots are a crucial feature in linking above- and belowground C processes (Hoyos-Santillan et al. 2016; Ma et al. 2017), and play an important role in shaping the whole-plant functions, biotic interactions and biogeochemical cycles (Soana and Bartoli 2013; Plante et al. 2014). Changes to anatomical characterises of absorptive roots due to global climate change reported an uncertainty largely because root attributes are more difficult to measure than root biomass (Norby et al. 2004; Iversen et al. 2017; Mueller et al. 2018). Characterizing the response of anatomical traits of absorptive fine roots as well as their influence on leaf-level physiology is crucial for understanding the resource utilisation strategies and plant performance of species in trees under future climate change.

Several studies have explored the anatomical characteristics of absorptive roots and their role in hydraulic conductivity of plants (i.e. radial and axial water movement) (Tyree and Ewers 1991; Steudle and Peterson 1998; Huang and Eissenstat 2000; Schuldt et al. 2013). Water travels through a sequence of root cells and enters the root xylem from the soil solution. This process is known as radial water flow. Roots with thinner cortex impose less radial resistance for water transport and have higher hydraulic conductance because they may have a shorter radial path for water movement from the root surface into the xylem than large-diameter roots in the radial water flow (Passioura 1988; Rieger and Litvin 1999). Water then moved axially in the xylem vessels after flowing radially from the root surface to the xylem. Increases in the efficiency of water transportation have been attributed to higher stele/root area (Kong et al. 2017). The development of a suberized exodermis correlates with the development of aerenchyma in plants (Parent et al. 2008) and is linked with a decline in radial loss of root

oxygen (Jackson and Armstrong 1999a). Further, vessels with larger areas have been associated with water exploitation strategies (Pineda-García et al. 2015). Therefore, the number or size of stele, the proportion of cortex as well as the proportion of aerenchyma are positively correlated with the axial conductance capacity (Guo et al. 2008; Voesenek and Bailey-Serres 2015; Zhou et al. 2021). Further research is vital to understand the ecological significance of absorptive roots in terms of water-related leaf physiology and water use strategy, given that the anatomical traits of these roots are important for water uptake and transportation. This is particularly relevant for temperate species where the relationship between absorptive root anatomy and leaf-level physiology is unclear (Warren et al. 2015).

The root anatomical architecture in woody plants includes secondary growth with abundant xylem that might aid our understanding of how they regulate water-related leaf physiology (McElrone et al. 2004). Superficial lateral roots of *Banksia prionotes* have been reported to exhibit large-area xylem conduits, greater length, and higher-area-specific conductivity than lateral roots of the same species (Pate et al. 1995). Differences in xylem characteristics can radially disrupt the functions of the different portion of the conducting system as stated in the fourth-power relationship between radius and flow through a capillary tube (Tyree and Ewers 1991). Therefore, even a small increase in mean conduit area has exponential impacts on specific hydraulic conductivity for the same pressure differential over a segment. However, due to the dearth of experimental data that compare the variations between root anatomical traits between different woody species and the rarity of observations that determine whether anatomical traits can result in differentiation of leaf physiological traits (photosynthesis rates, transpiration rates and stomatal conductance rates) between woody species in such experiments, the potential effects of such interactive effects of plant-water relations needs further investigation.

Anthropogenically driven increases in CO_2, temperature and precipitation patterns are affecting the growth and survival of woody species in temperate and boreal forest (IPCC 2022; Rawat et al. 2022). While warming has resulted in an increase in GHG emission in high northern latitudes (Bloom et al. 2010), increase in atmospheric CO_2 and interannual variation in precipitations in woody plants resulted in an increase in photosynthesis and increment in biomass (Arenque et al. 2014; Lawson and Leishman 2017). Considering the variations in root characteristics and absorption strategies among the herbaceous species in temperate steppe (Zhou 2019), it is possible that various woody plants have developed unique water-use strategies to adapt to situations with fluctuating water availability or increased temperature and CO_2. The anatomical architecture of the xylem in different plant species can be linked to the variations in their water use strategies (Schuldt et al. 2013). However, most experimental studies to date have focused on root responses to elevated CO_2, warming and increased precipitation in semi-arid grassland (Mueller et al. 2018) or how root anatomical traits drive the responses of leaf physiological traits associated with water use efficiency in herbaceous species (Zhou 2021). Therefore, a better understanding of whether and how anatomical root trait respond to interactive effects of global change is needed to give insights into the potential impacts of climate change on root anatomy in specific ecosystems and to generate observations of how leaf-level physiological responses to interactive effects of climate change. However, in Chapter 3, we found that the physiological responses were reduced by waterlogging in ambient and elevated temperatures and the different species inhibit different parts of a similar response curve.

Here, we examined the anatomical root traits, and the leaf physiological traits associated with water use efficiency of five temperate tree species in a two-year growth room experiment, manipulating temperature, CO_2 and precipitation change. The 2–3-year-old saplings include *Alnus glutinosa*, *Betula pendula*, *Betula pubescens*, *Salix pentandra* and *Salix aurita*.

Anatomical traits investigated include aerenchyma-related traits (i.e. root cortical aerenchyma and aerenchyma area) and diameter/area related traits (i.e. total stele area, total cortical area, and cortical cell file number and cortical cell size). Leaf physiological traits include the photosynthesis rates, transpiration rates and stomatal conductance. Water use efficiency refers to the intrinsic water use efficiency. The specific research questions were:

i. Do temperate woody species differ in their root anatomical traits, physiological traits and water use efficiency?
ii. How are root anatomical traits, leaf physiological traits and intrinsic water use efficiency related in temperate woody species?
iii. How do root anatomical traits and leaf physiological traits as well as intrinsic water use efficiency respond to global change in temperate woody species?
iv. How do root anatomical traits influence how leaf physiological traits and water use efficiency react to global change?

4.3 Materials and Methods

4.3.1 Study sites

This growth room experiments that simulated the anticipated rise in temperature, CO_2 and waterlogging is fully described in Chapter 2 (section 2.2)

4.3.2 Experimental design

Detailed information on waterlogging, elevated temperature and elevated CO_2 experiment is fully described in Chapter 2 (section 2.3).

4.3.3 Root samples collection

In each experiment, roots were collected from soil at the depth of 5 cm. Six replicate plants were collected for each treatment, with four roots collected from each plant. For the temperature experiment, the roots were sampled in October 2021, while for the CO_2 experiment

in late November 2022. The root samples were carefully dug up and gently rinsed in water, following the procedure of (Atkinson and Wells 2017). All root samples collected were ~4 cm in length. Each root sample was immediately stored in a 50 mL falcon tubes containing 70% v/v ethanol and stored in a 4°C cold room for later anatomical measurements. Around 3 root segments of the first two orders of each species in each treatment were randomly selected for anatomical measurement.

4.3.4 Anatomical sampling and image analysis

To date, optical sectioning and 3D imaging often requires either sample fixation and storage, and the use of traditional light microscopy which can blur details in thick specimens because it collects light from all depth simultaneously (Verhertbruggen et al. 2017). However, to some extent, advances in technology such as the CLSM (Confocal laser scanning microscope) are suited to overcome these limitations while providing high throughput (Atkinson and Wells 2017). Confocal scanning microscopy also offers superior resolution, contrast, and depth imaging, allowing for clear distinction between tissues based on their chemical composition. Its ability to use fluorescence for precise labelling and quantification, alongside its multi-channel imaging capabilities, makes CLSM a powerful tool for distinguishing chemically distinct tissues, far beyond the capabilities of traditional light microscopy (Atkinson and Wells 2017).

Root anatomical traits were investigated following the new updated protocols described by Atkinson and Wells (2017). Briefly, root samples were placed and embedded into a custom designed, 3D printed polylactic acid (PLA) mold (Fig. 4.1E). Prior to placing samples in the molds, 5% (w/v) agarose (Sigma–Aldrich, Co. Ltd) was prepared using a microwave. The molds were then filled with agarose and sealed with pressure sensitive tape and left to solidify. The roots were then cut into sections of between 150 and 250 µm using a vibrating microtome (7000smz-2, Campden Instruments Ltd). The sectioned roots were incubated in calcofluor

white (Sigma–Aldrich, Co. Ltd) solution for 60 s before being rinsed in deionised water. The stained roots were photographed using an Eclipse Ti CLSM confocal laser scanning microscope (Nikon Instrument). Root cortical aerenchyma, total cortical area, total stale area, cortical cell file number and cortical cell size were measured using IMAGEJ (Fig 4.2) and RootScan software (Fig 4.4). The cortex thickness was defined as the one-sided distance from the stele to the epidermis. The number of aerenchyma were counted manually. The cortical area, stele area, cell size and cell file number were calculated. The measured root traits were list in Table 4.1.

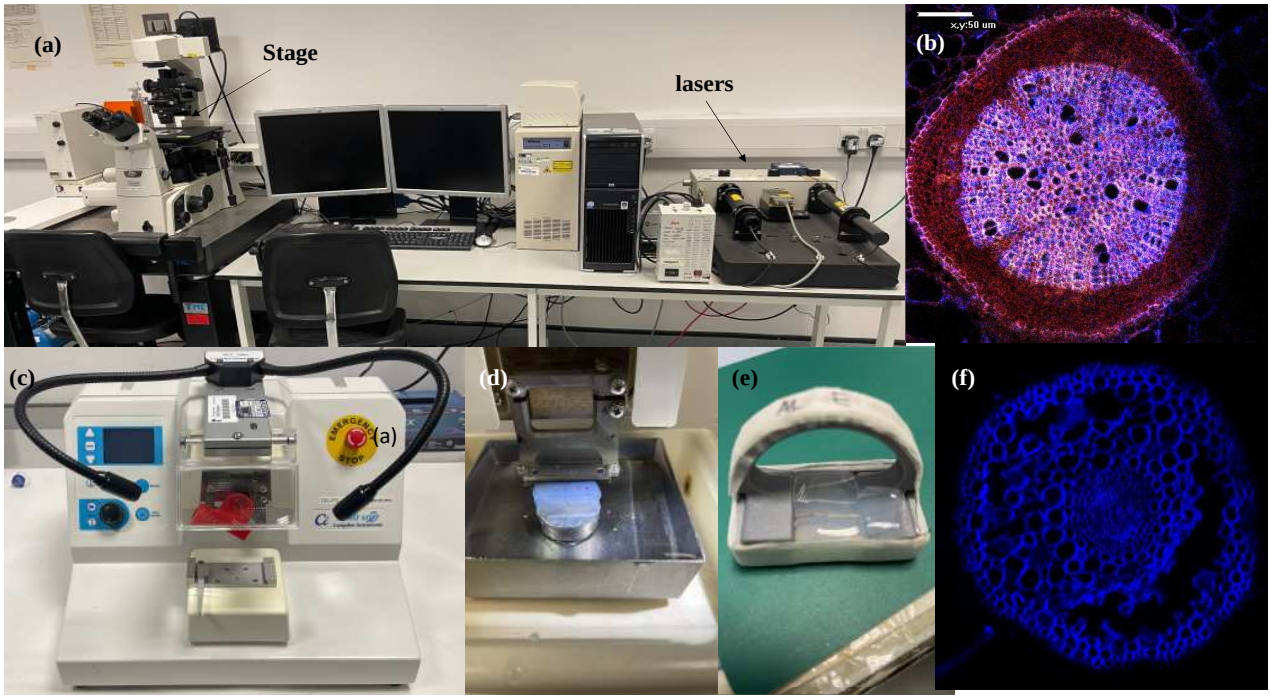

Figure 4:1: (a) confocal laser scanning microscope (b) root cross-section under no waterlogging condition obtained from vibratome and confocal microscope, (c) vibrating microtome, (d) mold mounted in vibratome ready for sectioning, (e) roots are fixed into place and the mold is sealed with a pressure-sensitive tape ready for embedding and (f) cross-section of roots under waterlogging conditions obtained using vibratome and confocal scanning microscope.

4.3.5 Measurements of leaf physiological traits

The light-saturated net photosynthetic rates (A_{max}), transpiration rates (E) and stomatal conductance (g_s) were measured using an open gas exchange system with a 2 × 3 cm cuvette and a red and blue LEDs LICOR Li6800 (Li-cor Biosciences, Lincoln, NE, USA). Measurements were at one light intensity (Qin) in the Multi Control Loops, where the measure

to be obtained with Qin= 2000 µmol m^{-2} $s^{-}1$ and temperature was held at 30°C, growth (CO_2) (400 µmol m^{-2} s^{-1}), leaf-to-air vapour pressure deficit (VPD) and RH of 0.2 kPa and of 60% respectively. All measurements were conducted from 08:30 h to 15:00 h (local time) during the sampling months. One fully expanded leaf on healthy individual plants (three plants for each species in each treatment combination) was randomly selected for measurement. Before measurements, leaves chosen for sampling were acclimated in the cuvette under setting conditions for 5-10 min, when parameters were stable, values were recorded.

4.3.6 Water-use efficiency estimation

The intrinsic water-use efficiency (iWUE) was calculated as measure of photosynthesis rate (*A*) divided by the transpiration rate (*E*) (Farquhar et al. 1989). iWUE was calculated as:

$$WUEi = \frac{A}{T}$$

Where WUEi is the intrinsic water use efficiency expressed in µmol CO_2 mmol H_2O; *A* represent the photosynthesis rate expressed in $\mu mol^{-2}s^{-1}$ and *E* represent the transpiration rate expressed in $\mu mol^{-2}s^{-1}$.

Table 4-1: Root anatomical and leaf physiological traits measured.

Traits	Abbreviation	Units
Root anatomical traits		
Root cortical aerenchyma	RCA	%
Total cortical area	TCA	mm^2
Total stele area	TSA	mm^2
Aerenchyma area	AA	AA^2
Cortical cell file number	CCFN	-
Cortical cell size	CCS	mm^2
Leaf physiological traits		
Saturated net photosynthesis rate	A_{max}	µ mol $m^{-2}s^{-1}$·
Stomatal conductance rate	g_s	m mol $m^{-2}s^{-1}$·
Transpiration rate	*E*	m mol $m^{-2}s^{-1}$·
Water-use efficiency		
Intrinsic water-use efficiency	iWUE	µ mol m mol^{-1}

4.3.7 Statistical analysis

GENSTAT (21st edition) was used to run a mixed linear model using residual maximum likelihood (REML) method to test the impact for the main effects of and interactions between species, elevated temperature or elevated CO_2 and high-water level on anatomical traits, physiology (photosynthesis assimilation (A_{max}), stomatal conductance (g_s), transpiration (E)), and intrinsic water-used efficiency. The model has species (*Alnus glutinosa*, *Betula pendula, Betula pubescens, Salix pentandra and Salix aurita*), waterlogging and treatment (temperature or CO2 level) as fixed effects and block as the random effect. All anatomical data were log-transformed to comply with the assumption of normality of the REML. Level of significance of the differences between the fixed effects was estimated by Wald test using F distribution. Significance was attributed to $P < 0.05$. Standard error of the differences was predicted from the mixed linear model and used to assess which specific differences were significant. In order to compare tissue characteristics across roots of varying dimensions, we normalized tissue areas in relation to different root sizes to account for the differences in root size using the formula:

$$Normalized\ Tissue\ Area = \frac{Tisue\ Area}{Total\ Root\ \ Area}$$

Where the Total root area is the cross-sectional area of each root and Tissue area is the specific tissues or anatomical regions

Similarities in the root anatomical and leaf physiological traits of the species from different temperature or CO_2 treatment were explored by Principal Component Analysis (PCA), based on correlation matrices. The % variance accounted (adjusted R^2) by regression statistical models is referred to as R^2 in text and figures. Results throughout the text, figures and tables are presented as mean ±SE. Full ANOVA tables are reported in Appendix B.

4.4 Results

4.4.1 Variations in root anatomical traits among the four species in response to 30 days waterlogging

There were significant differences in root anatomical traits between species in controls (Table 4.2). The highest mean root cortical aerenchyma was found in *A. glutinosa* (29.75%, Fig. 4.3A) while the lowest values were found in *S. pentandra* (9.9 %, Fig. 4.3A).

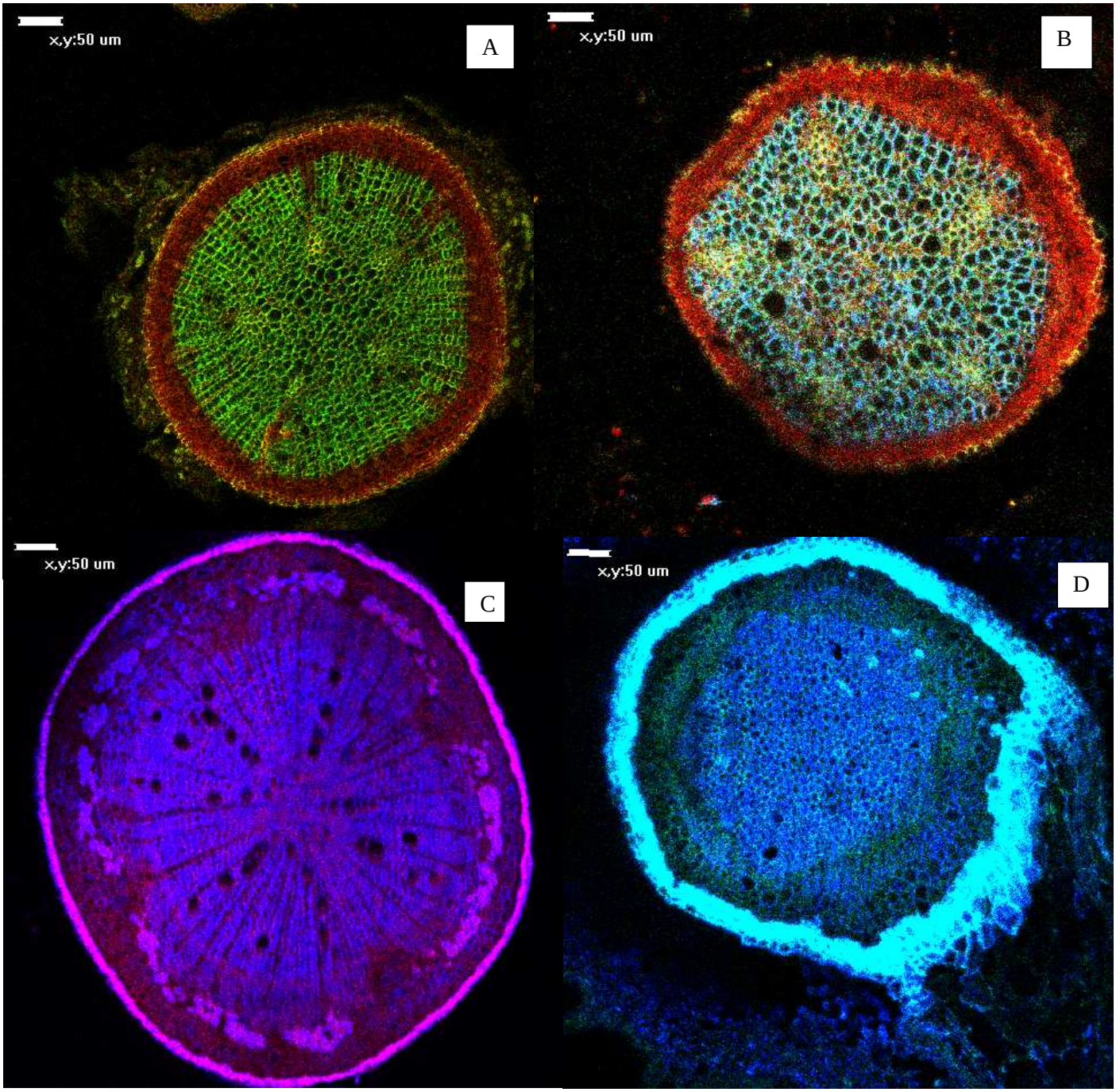

Figure 4:2: Cross-sections of root highlighting the anatomical changes in flooded plants (B, D) and some comparisons with non-flooded plants (A, C). (A & B) Non-flooded and flooded plant of *Alnus glutinosa*. Detail of the cortex with the presence of well-developed porous xylem tissue in the cortex of flooded plant. Xylem and phloem are less developed in contrast to small pith in the flooded plant. (C&D) Non-flooded and flooded *Betula pubescens*. Non-flooded plant showing many small piths. Root of flooded plants showing well-developed phloem composed of many cells.

Table 4-2: The summary results of Mixed models (REML) analysis.

Temperature experiment														
Anatomical traits	Species (S)		Temperature (eT)		Waterlogging (W)		S × eT		S × W		eT × W		S × eT ×W	
	F	*P*	*F*	*P*	*F*	*P*	*F*	*P*	*F*	*P*	*P*	*F*	*F*	*P*
RCA	10.89	**0.005**	2.02	0.198	85.87	**<0.001**	1.14	0.398	6.53	**0.019**	1.42	0.445	0.36	0.785
TSA	0.82	0.522	0.04	0.849	0	0.978	0.59	0.638	0.09	0.963	1.58	0.428	2.17	0.18
TCA	-	-	-	-	-	-	-	-	-	-	-	-	-	-
Aerenchyma area	2.22	0.174	2.27	0.176	0.01	0.925	0.82	0.524	0.28	0.84	5.87	0.249	0.79	0.536
CCFN	0.4	0.756	0.6	0.462	0.68	0.437	0.46	0.719	0.15	0.925	1.97	0.394	0.34	0.795
CCS	0.71	0.575	1.41	0.273	0.32	0.588	0.19	0.9	0.2	0.892	4.9	0.27	0.07	0.976
Leaf physiological traits														
A_{MAX}	1.75	0.244	8.56	0.022	12.71	**0.009**	0.18	0.908	1.11	0.408	20.1	0.14	0.97	0.461
E	3.19	0.093	7.38	**0.03**	24.12	**0.002**	0.35	0.788	2.82	0.117	3.61	0.308	1.11	0.407
g_s	2.57	0.137	3.75	0.094	6.76	0.035	0.34	0.795	2.72	0.125	9.92	0.196	1.01	0.443
Water use efficiency														
iWUE	3.03	0.103	0.48	0.512	1.61	0.245	2.71	0.126	2.61	0.133	0.83	0.53	1.91	0.216
CO_2 experiment														
	Species (S)		Treatment (eCO_2)		Waterlogging (W)		S × eCO_2		S × W		eCO_2 × W		S × eCO_2 × W	
	F	*P*	*F*	*P*	*F*	*P*	*F*	*P*	*F*	*P*	*P*	*F*	*F*	*P*
RCA	11.56	**0.004**	14.77	**0.006**	37.94	**<0.001**	0.95	0.467	1.32	0.342	0.38	0.648	0.42	0.744
TCA	12.7	**0.003**	0.34	0.576	15.32	**0.006**	1.26	0.358	1.36	0.331	0.39	0.646	0.91	0.484
TSA	3.99	**0.06**	0.08	0.783	5.74	0.048	3.96	0.061	4.27	0.052	0	0.998	3.28	0.089
Aerenchyma area	3.97	0.061	15.14	**0.006**	23.88	**0.002**	1.06	0.425	0.64	0.613	0.04	0.869	1.91	0.216
CCFN	1.08	0.409	0	1	3.23	0.11	1.28	0.345	0.63	0.614	2.93	0.125	2.11	0.177
CCS	15.02	**0.002**	2.78	0.139	7.62	0.028	0.92	0.477	0.05	0.984	0.01	0.928	0.97	0.459
Leaf physiological traits														
A_{MAX}	2.62	0.133	3.19	0.117	16.8	**0.005**	0.38	0.768	7.05	**0.016**	0.41	0.636	7.98	**0.012**
E	0.66	0.603	3.38	0.109	0	0.997	0.65	0.608	4.56	0.045	0.07	0.833	8.58	**0.01**
g_s	5.66	**0.028**	0.01	0.919	5.91	0.045	1.42	0.315	10.65	**0.005**	0.04	0.875	4.3	0.051
Water use efficiency														
iWUE	1.72	0.25	16.97	**0.004**	16.73	**0.005**	0.07	0.975	0.41	0.751	38.87	0.101	5.26	0.033

A_{max}, saturated net photosynthesis rate; *E*, transpiration rate; *gs*, stomatal conductance; *iWUE*, intrinsic water efficiency use. Indicating the effect of species and increased waterlogging and elevated temperature of CO_2 on root anatomical, leaf physiology and water-use efficiency. The bold numbers indicate the significant effects.

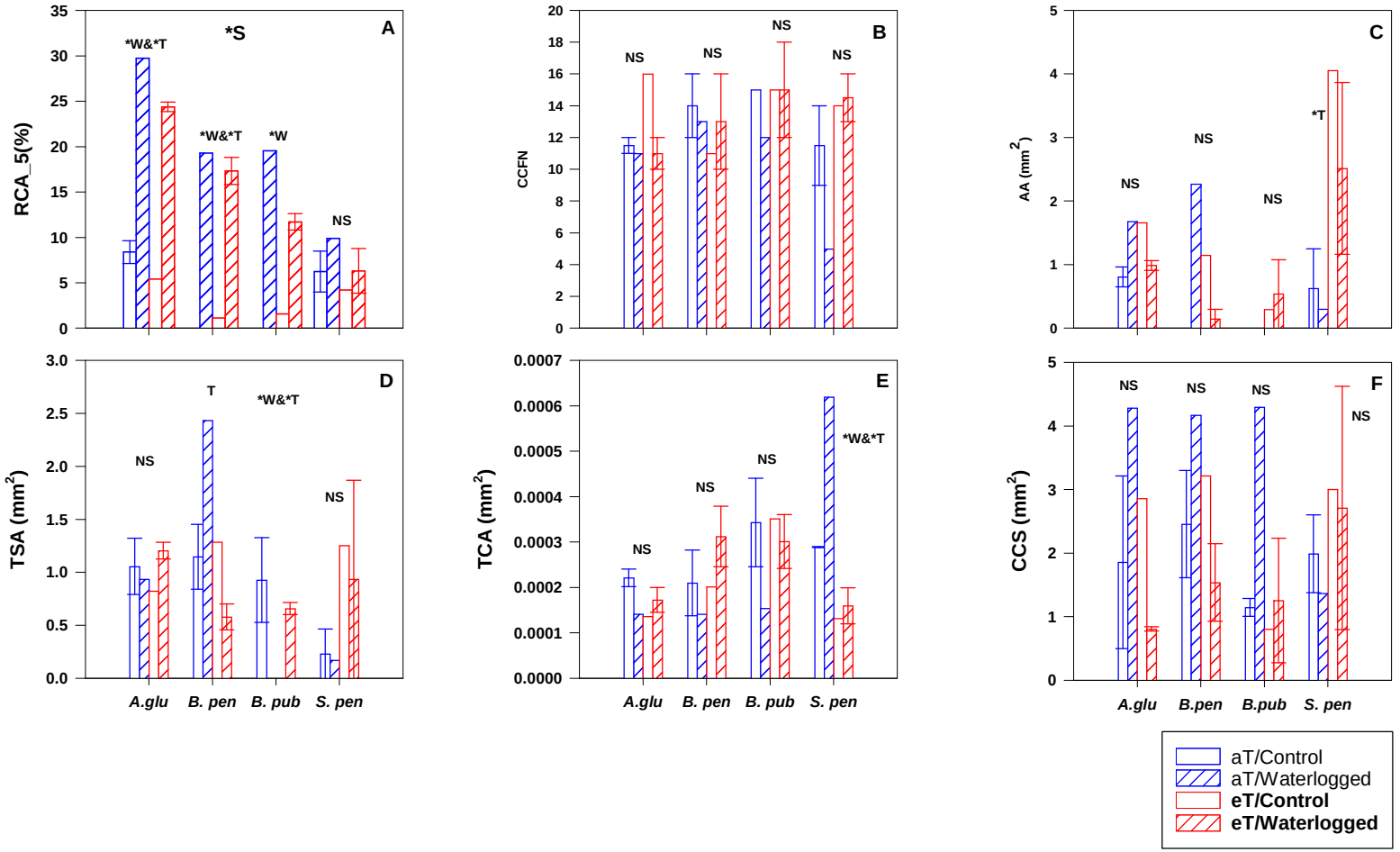

Figure 4:3: Differences in root anatomical traits among temperate species after interactive effect of 30 days waterlogging and elevated temperature. Mean +/- SEM. *-letters denoted statistical significance of difference between treatment condition at $P < 0.05$ levels (S = significant difference between temperate species; T = significant difference between temperature level treatments; W = significant difference between waterlogging treatments; NS = no significant difference). Note: No data for some species.

Substantial differences were found in anatomical traits across species (Fig 4.3). Although, *A. glutinosa* and *B. pendula* had similar cortical cell size in waterlogged plots (4.282 and 4.168 mm^2 respectively; Figure 4.3F), the anatomical traits were significantly different between the four species. For instance, *B. pendula* had a larger proportion of aerenchyma area, total stele area, and total cortical area (Fig. 4.3C, D and E, respectively), whereas *A. glutinosa* had a larger proportion of cortical cell (Fig 4.3F). For the cortical cell file number, *B. pendula* had the largest concentric layers of parenchyma cells (Fig. 4.3B). In general, waterlogged species had the largest root cortical aerenchyma in all species (Tab. 4.2, $P < 0.001$) compared with controlled species. Thirty-days waterlogging had no effects on total stele aerenchyma, total cortical area, total stele area, aerenchyma area, cortical cell file number and cortical cell size ($P>0.05$; Tab. 4.2) in any specie, however, we found significant effects of waterlogging on root cortical aerenchyma for *A. glutinosa, B. pendula* and *B. pubescens* ($P < 0.05$; Fig. 4.3A).

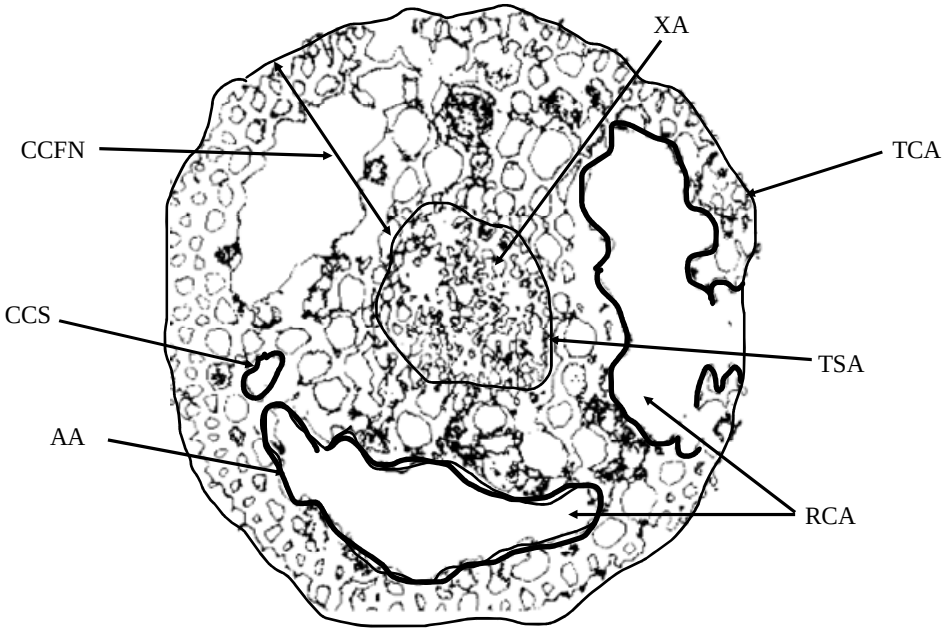

Figure 4:4: Root cross-section output from RootScan software showing TCA (total cortical area), TSA (total stele area), CCFN (cortical cell file number), RCA (root cortical aerenchyma), CCS (cortical cell size) and XA (metaxylem area) from *S. aurita* sapling.

4.4.2 Variations in root anatomical traits among the four species after 60 days waterlogging

For root anatomical traits, *S. aurita* had the largest root cortical aerenchyma (35.93 %, Figure 4.5A) and were distinguished by larger total cortical area (0.00060 mm^2, Figure 4.5E), bigger cortical cell size (1.447 mm^2, Figure 4.5F) and greater total stele area (5.415 mm^2, Figure 4.5D) while *B. pubescens* had the smallest root cortical area (24.22 %, Figure 4.5A) and were differentiated by their smaller aerenchyma area (0.545 mm^2, Figure 4.5C) and cortical cell size (0.315 mm^2, Figure 4.5F). However, the traits associated with root anatomy exhibited diverse patterns in response to waterlogging. For example, 60 days waterlogging had significant effects on root cortical aerenchyma, total cortical area, and cortical cell size for *A. glutinosa* and *S. aurita* saplings only ($P < 0.05$; Fig. 4.5A, E and F). In addition, waterlogging had a positive effect on aerenchyma area for *A. glutinosa* ($P < 0.05$; Fig. 4.5C) and there was no effect of waterlogging on any root anatomical traits for *B. pubescens* ($P > 0.05$; Fig.4.5A-F).

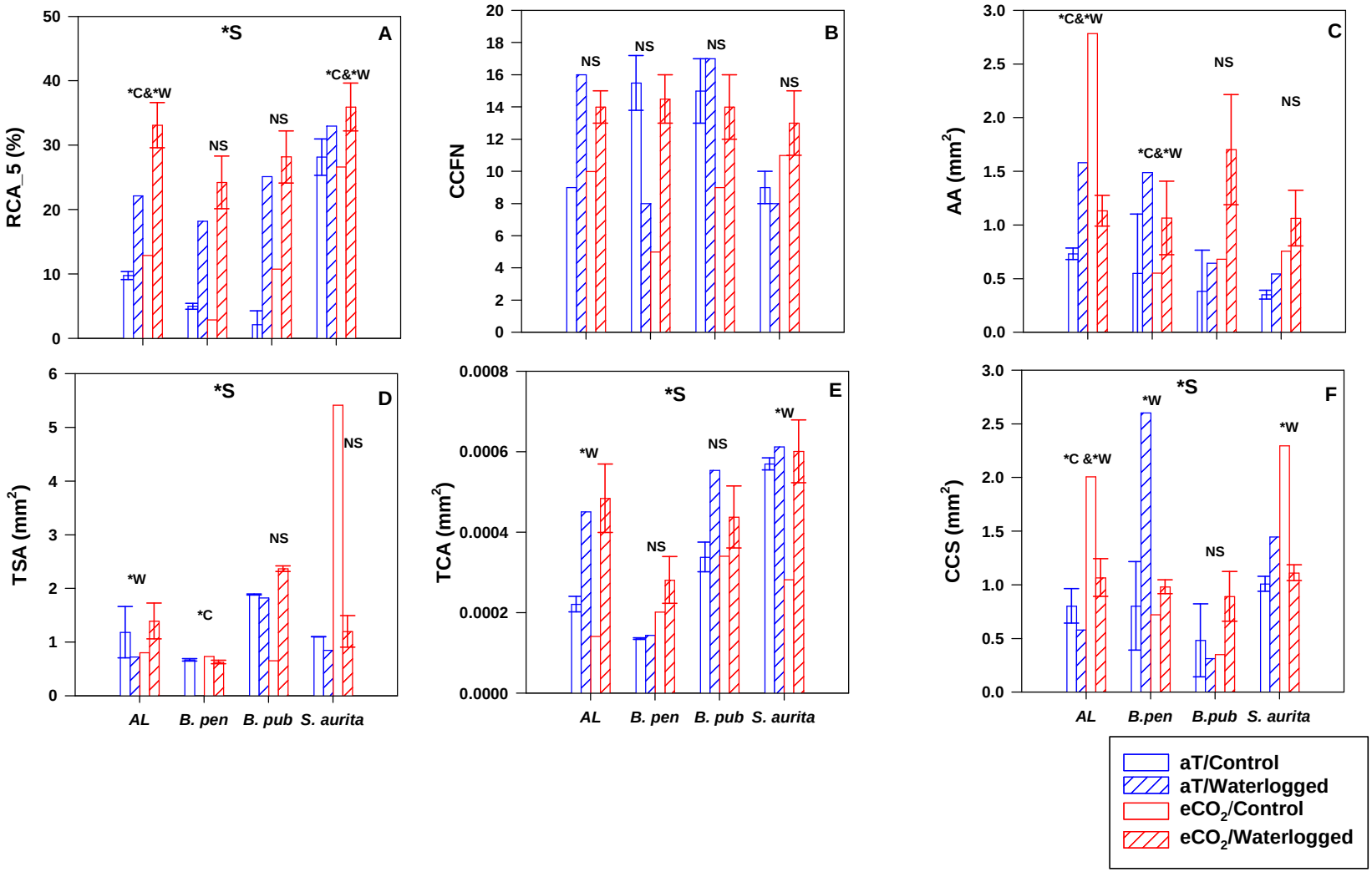

Figure 4:5: Differences in root anatomical traits among temperate species after interactive effect of 60 days waterlogging and elevated CO_2. Error bars represent the standard mean error. *-letters denoted statistical significance of difference between treatment condition at $P < 0.05$ levels (S = significant difference between temperate species; C = significant difference between CO_2 level treatments; W = significant difference between waterlogging treatments; NS = no significant differences).

4.4.3 Differences on leaf physiological traits and water efficiency and their associations with root anatomical traits after 30 days waterlogging

In order to correlate the multiple relationships underlying the different root anatomical traits, leaf physiological traits and water-use efficiency, a principal component analysis (PCA) was carried out. The result of the PCA revealed that the first two trait PCs accounted for 31.62% and 15.09% of total variation, respectively (Figure 4.6). Root anatomical traits (e.g., root cortical area, aerenchyma area, cortical cell file number and total stele area), leaf physiological traits (e.g., A_{max}, E and gs) exhibited high scoring on the PC-1, the total cortical area, cortical cell size and *iWUE* exhibited high scoring on PC-2 (Figure 4.6). These results suggests that the leaf physiological traits may be connected mainly to aerenchyma-related root anatomical traits. The species distribution in the trait space revealed that *A. glutinosa* and *S. pentandra* separated from *B. pubescens* and *B. pendula* primarily due to the differences in traits with high scoring in the first axis. The differences in trait syndromes that scored highly on the second axis separated *B. pubescens* from the other three species (Fig 4.6).

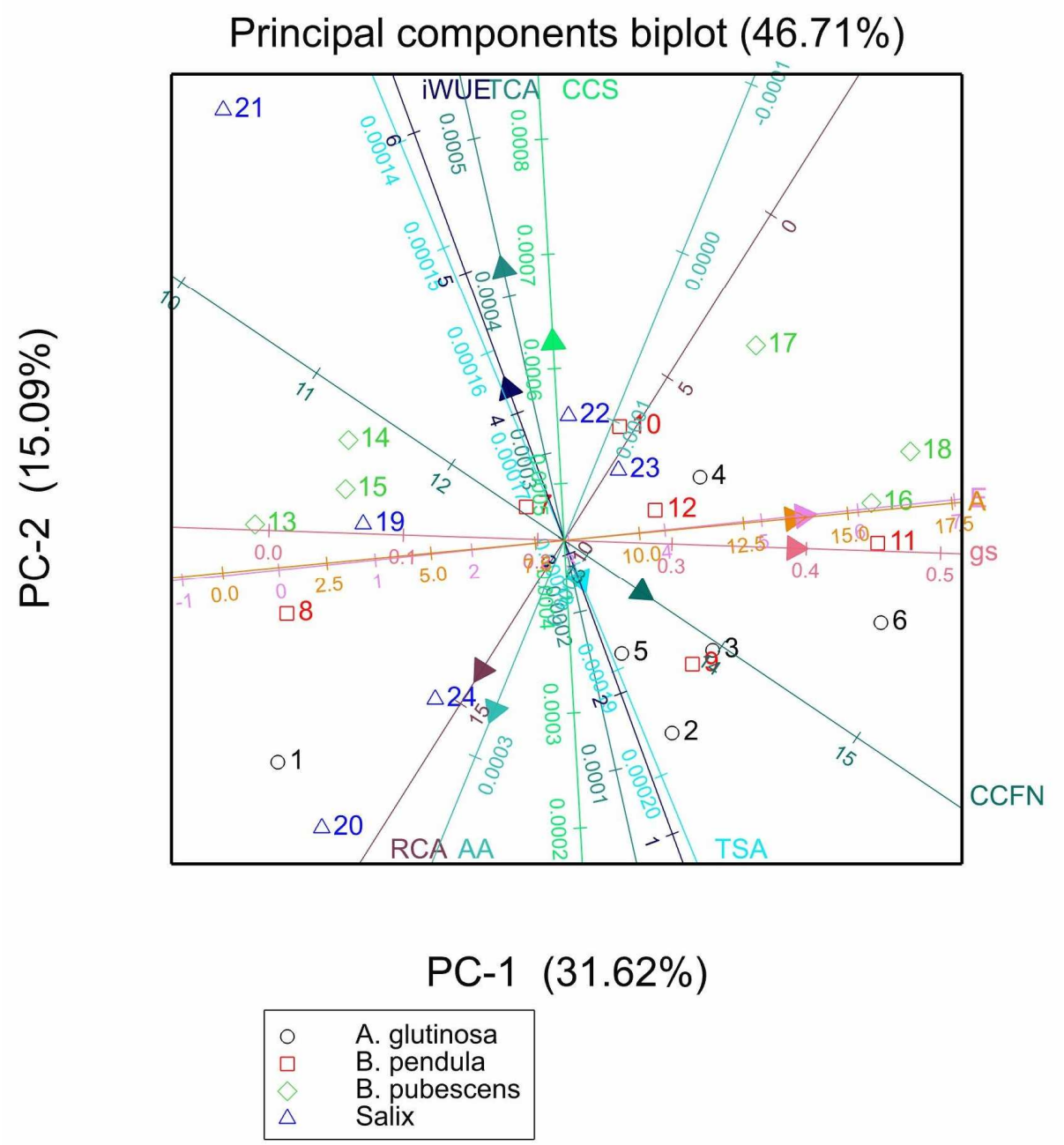

Figure 4:6: Principal component analysis for root anatomical and leaf physiological traits of the species. Trait loading biplot for interactive effect of 30 days waterlogging to elevated temperature. Species distribution in the trait space; RCA, root cortical aerenchyma; TCA, total cortical area; TSA, total stele area; AA aerenchyma area; CCFN, cortical cell file number; CCS, cortical cell size; A, photosynthesis; gs, stomatal conductance; E, transpiration; iWUE, intrinsic water use efficiency.

4.4.4 Differences on leaf physiological traits and water efficiency and their associations with root anatomical traits after 60 days waterlogging

PCA highlighted that leaf physiological, intrinsic water-use efficiency were correlated with different root anatomical traits (Figure 4.7). The results of the PCA showed that the first two PCs accounted for 38.52% and 25.9% of the total variation, respectively (Figure 4.7). Anatomical traits (e.g., cortical cell file number, aerenchyma area, total cortical area, root cortical aerenchyma, cortical cell size and total stele area), and physiological traits (*iWUE*) exhibited high scoring on the PC-1 while (*Amax, E* and *gs*) exhibited high scoring on the PC-2 (Figure 4.7). These findings imply that leaf physiological traits and iWUE may be connected to root anatomical traits. We observed that the species distribution in the trait space indicated *A. glutinosa* and *S. aurita* in the first and second axis separated from the other two species mostly due to the differences in traits with high scoring in the first axis like the root cortical aerenchyma area and cortical cell size as well as A_{max}, *E*, and *gs* in the second axis (Figure 4.7).

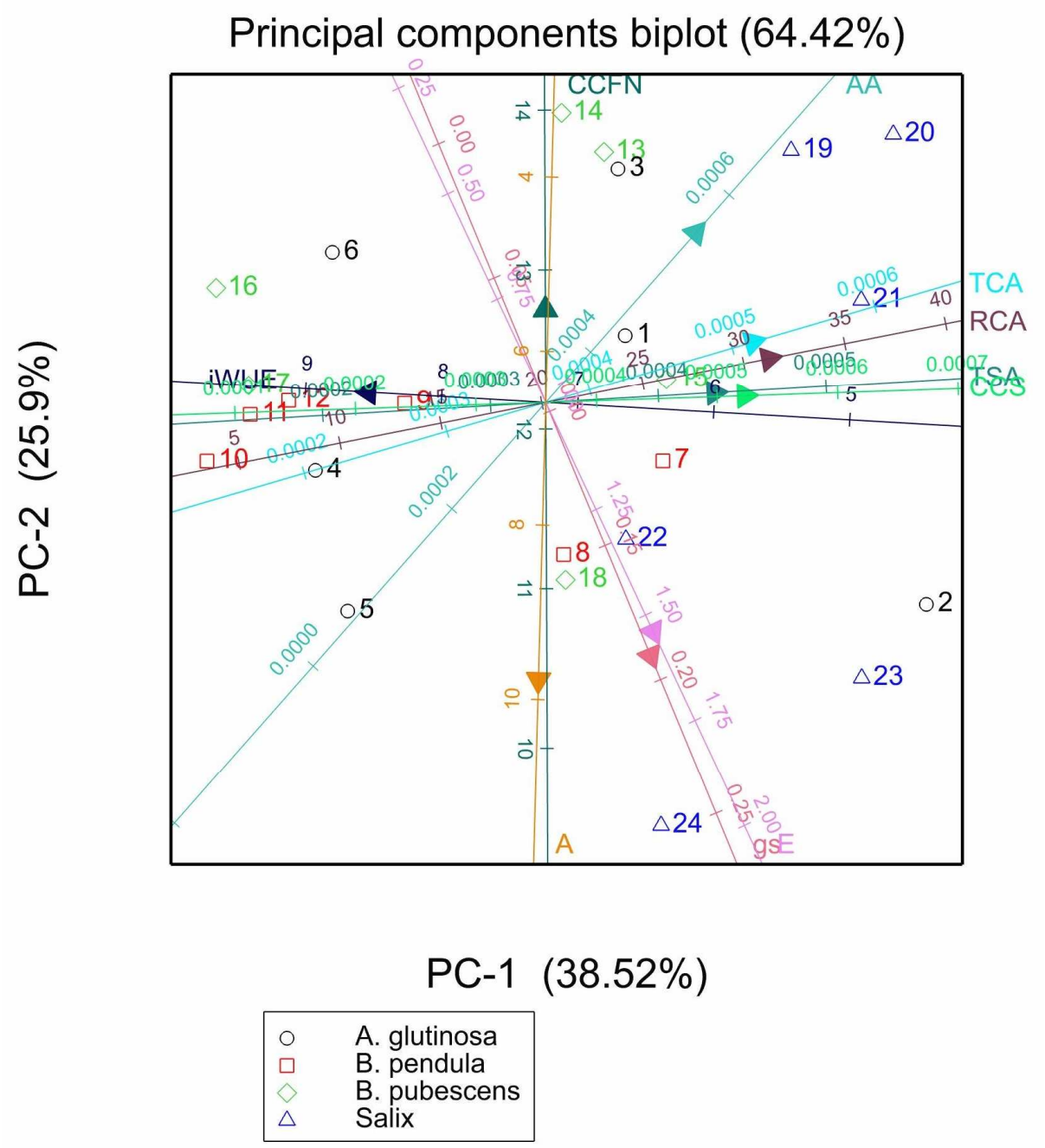

Figure 4:7: Principal component analysis for root anatomical and leaf physiological traits of the species. Trait loading biplot for interactive effect of 60 days waterlogging to elevated CO_2. Species distribution in the trait space; RCA, root cortical aerenchyma; TCA, total cortical area; TSA, total stele area; AA aerenchyma area; CCFN, cortical cell file number; CCS, cortical cell size; A, photosynthesis; gs, stomatal conductance; E, transpiration; iWUE, intrinsic water use efficiency.

4.4.5 Effects of 30 and 60 days waterlogging on root anatomiocal, leaf physiological traits, water -use efficiency

Root anatomical traits in the different species exhibited diverse patterns in response to 30 days waterlogging (Fig. 4.3). For instance, waterlogging had no significant effect on root cortical aerenchyma of *S. pentandra* ($P > 0.05$). However, waterlogging enhanced the root cortical aerenchyma of *A. glutinosa, B. pendula* and *B. pubescens* ($P < 0.05$). In addition, waterlogging only enhanced the total stele area of *B. pubescens* and total cortical area of *S. pentandra* ($P < 0.05$).

Similarly, leaf physiological trait parameters and water use efficiency presented a varied pattern in response to 30 days waterlogging. For instance, waterlogging had no significant effect on A_{max}, *gs*, *E* and *iWUE* of *A. glutinosa* and *B. pendula* ($P > 0.05$). By contrast, waterlogging improved A_{max}, *gs*, *E* and *iWUE* of *B. pubescens* and *S. pentandra* ($P < 0.05$), and waterlogging reduce *iWUE* of *S pentandra* ($P > 0.05$).

The root anatomical traits across the species showed a diverse pattern in in response to 60 days waterlogging. Root cortical aerenchyma for example had no effect on *A. glutinosa* and *B. pubescens* but we observed a P-value near the limit ($P <0.05$; Fig 4.5) for *B. pendula*. However, 60 days waterlogging improved the root cortical aerenchyma of *S. aurita* ($P < 0.05$; Fig. 4.5). Additionally, 60 days waterlogging enhanced the total cortical area, aerenchyma area, and cortical cell size of *A. glutinosa* and *S. aurita* ($P < 0.05$; Fig 4.5).

Leaf physiological traits and water use efficiency across the species varied in response to 60 days waterlogging. We observed an effect of waterlogging on the A_{max}, *gs*, *E* and *iWUE* of *B. pendula* and *S. aurita* ($P < 0.05$) and waterlogging reduced the A_{max} of *B. pendula* ($P > 0.05$). In addition, waterlogging enhanced the *iWUE* of *B. pubescens* ($P < 0.05$).

4.4.6 Effects of elevated temperature and elevated CO_2 on root anatomiocal, leaf physiological traits, water -use efficiency

Root anatomical traits did respond significantly to elevated temperature in diverse patterns. For example, elevated temperature changed the root cortical aerenchyma of *A. glutinosa* and *B. pendula* only ($P < 0.05$; Fig. 4.3).In addition, elevated temperature only enhanced the total stele area of *B. pendula* and reduced the total stele area of *B. pubescens* ($P < 0.05$; Fig. 4.3D). Furthermore, elevated temperature improved the aerenchyma area and total cortical area of *S. pentandra* ($P < 0.05$; Fig 4.3C and E). Similarly, the paramaters linked with leaf physiology and water-use efficiency in the different species did show diverse patterns in response to elevated temperature. Elevated temperature had no significant effect on $A_{max,}$ *E, gs* and *iWUE* of *A. glutinosa* and *B. pendula* ($P > 0.05$). By constrast, the A_{max}, *E,* and *gs* of *B. pubscens* were reduced by elevated temperature ($P < 0.05$) while the *iWUE* was enhanced by elevated temperature ($P < 0.05$). Similarly, the *gs* and *E* of *S. pentandra* were reduced by temperature increase ($P \leq 0.05$).

The parameters linked with root anatomical traits in the different species showed a diverse pattern in response to elevated CO_2. For example, elevated CO_2 enhanced root cortical area, aerenchyma area, and cortical cell size for *A. glutinosa* ($P < 0.05$; Fig 4.5A, C and F). In addition, elevated CO_2 improved the aerenchyma area, and total stele area for *B. pubescens* ($P < 0.05$; Fig. 4.5C and D). Similarly, root cortical aerenchyma for *S. aurita* was increased as a result of increased CO_2 ($P < 0.05$; Fig 4.5A). Leaf physiological traits across species showed varied pattern in response to elevated CO_2. Elevated CO_2 had significant effect on *E, gs* and *iWUE* for *B. pendula* only ($P < 0.05$). Increased elevated temperature enhanced *iWUE* for *B. pubescens* ($P < 0.05$) but the A_{max} and *iWUE* for *S. aurita* were reduced by elevated CO_2 ($P < 0.05$).

4.4.7 Relationship between root anatomical traits and the responses of leaf physiological traits and water use effieciency to 60 days waterlogging

To investigate the processes underlying the various response-patterns to waterlogging among the species, the linear regression analysis was conducted between root anatomical traits under ambient conditions and response values of leaf physiology and water use efficiency to 60 days waterlogging. The response values of *A, E* and *iWUE* were all negatively correlated with root cortical aerenchyma and cortocal cell size (Fig. 4.8A-D), whereas, the response values of *gs* was positively correlated with root cortical aerenchyma and cortical cell size (Fig. 4.8B and F) during sixty days waterlogging. These results indicate that species with larger root cortical aerenchyma and cortical cell size in the cortex will be able to regulate their gas exchange and water balance in response to sixty days waterlogging.

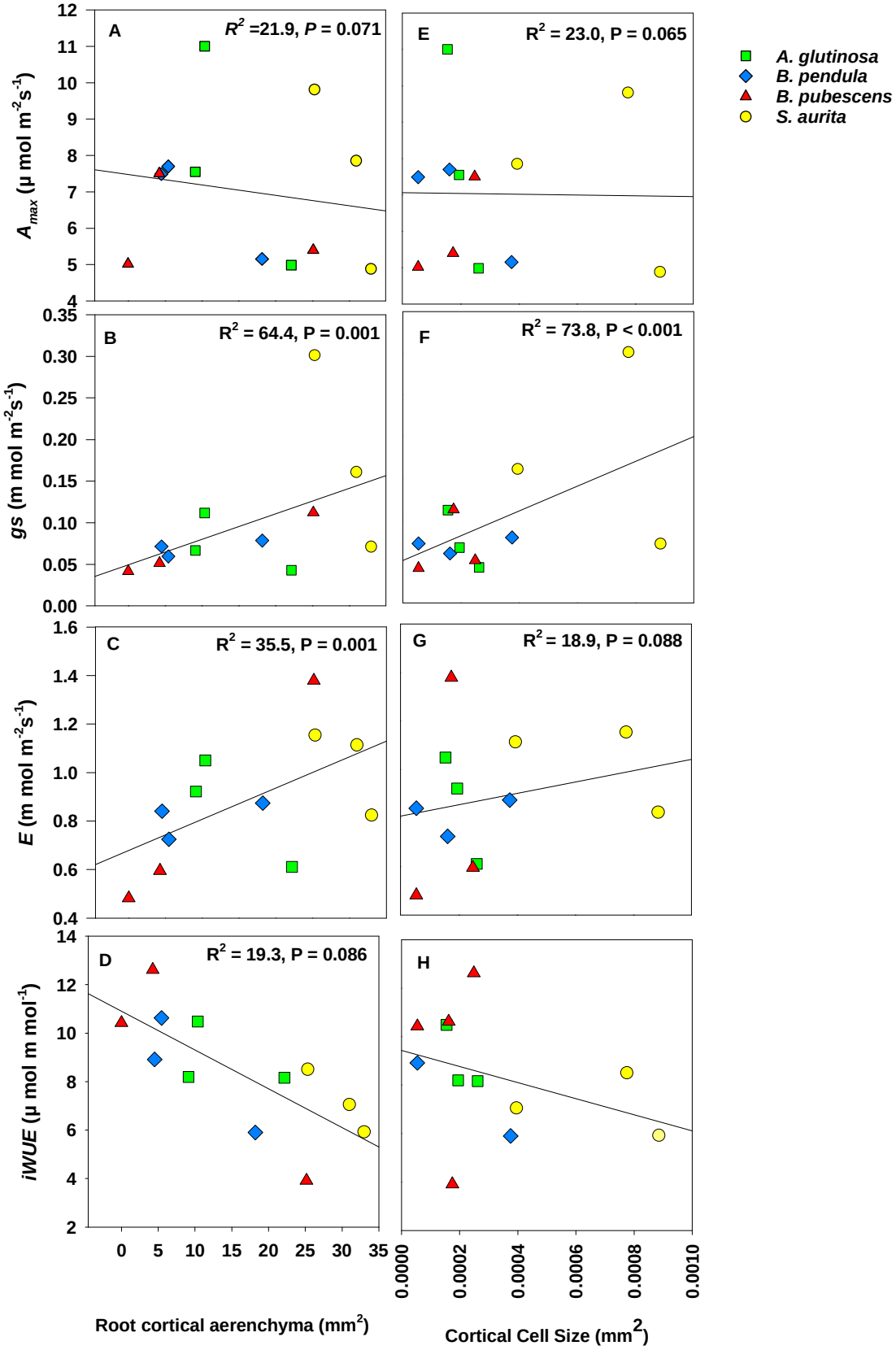

Figure 4:8: The linear regression relationship between response values of leaf physiological traits to 60 days waterlogging (vertical y-axis) and root anatomical traits in control plots (horizontal x-axis) among temperate species. Amax, net photosynthesis rate; gs, stomatal conductance; E, transpiration rate; iWUE, intrinsic water-use efficiency

4.5 Discussion

4.5.1 Anatomical, physiological traits and water-use efficiency of roots under different water conditions

Our first research question is to determine how woody species differ in their root anatomical traits, physiological traits, and water use efficiency. Interestingly, we found that woody temperate tree plants differed in their root anatomical traits and water-leaf physiological traits regardless of the severity of waterlogging periods (i.e., 30 or 60 days). We found *A. glutinosa* exhibited distinct root anatomical traits that differed from other studied species for 60 days waterlogging. These results indicate that anatomical root traits of woody temperate plants respond to waterlogging and that the adjustment of root traits occurs when the range of waterlogging duration exceeds a certain threshold.

Our findings showed an inconsistent relationship among aerenchyma-related root traits across the five woody temperate tree species during 30- and 60-days waterlogging (Fig. 4.3 and 4.5 respectively). In the 30 days waterlogging, *Alnus glutinosa* species had higher root cortical aerenchyma than any other species, but the cortical cell size was similar with *Betula pendula* and *Betula pubescens* (Fig. 4.3A and F). Moreover, there was little variance in total cortical area between *Alnus glutinosa*, *Betula pendula* and *Betula pubescens* (Fig. 4.3E) whereas the total stele area of *B. pubescens* was higher than any other species (Fig. 4.3D). While in the 60 days waterlogging, *Salix aurita* had a higher root cortical aerenchyma, aerenchyma area and cortical cell size than any other species (Fig. 4.5A, C and F). This asymmetric link among the root cortical aerenchyma, total stele area and total cortex area aligned with the literature theories regarding the formation of aerenchyma and its adaptive significance (Jackson and Armstrong 1999a; Drew et al. 2000b). It has been reported that, internal O_2 supply may increase via the formation of gas-filled aerenchyma in the root cortex because gas phase O_2 diffuses significantly faster than liquid phase O_2. In theory, aerenchyma is formed by the autolysis of

root cortical cells (lysigenous aerenchyma) (Yamauchi and Nakazono 2022). Certain wetland plants, like rice (*Oryza sativa*), develop constitutively (that is, even in drained soil) lysigenous aerenchyma, which is further stimulated by soil waterlogging. Thus, it is possible to differentiate between constitutive and inducible aerenchyma production (Colmer and Voesenek 2009a). Increase in total stele and cortex area has been reported to balanced nutrient transport and absorption (Kong et al. 2017). The relative increase in total size of cortex and stele area with root cortical aerenchyma would result in delay of nutrient absorption compared to nutrient transportation (Kong et al. 2017), whereas the increase in root cortical aerenchyma enhances gas exchange between belowground issues and atmosphere (Yamauchi and Nakazono 2022).

Trade-off between nutrient absorption and transportation as well as gas movement among the plants may be possible by the differential proportion of the root cortical aerenchyma, total cortical area and total stele area in the root cross-section area (Kong et al. 2017). This explanation is consistent with the variability patterns that have been reported for herbaceous species in a temperate steppe, except for root cortical aerenchyma (Zhou et al. 2021) and (Mano 2006) reporting that the degree of aerenchyma formed in the cortex of maize species increased when flooding is increased. In the present study, we also found differences in cortex of the roots which are composed of concentric layers of the parenchyma cells, the numbers of which is refer to as the cortical cell file number among the species. Despite the cortical cell file number not being significant in all the species, waterlogged species were characterized with having a lower cortical cell file number than non-waterlogged plants during the 30 days waterlogging, whereas the cortical cell file number in 60 days waterlogging varied substantially among the plants. This may imply that the aerenchyma related features in combination with the anatomical traits of the cortex can offer more broad knowledge on the variations in root anatomy among plants.

4.5.2 Correlation between anatomical, physiological traits and water-use efficiency of roots under different water conditions

The anatomical characteristics of roots and water-related leaf physiological traits were strongly connected in line with our second research question. We found multiple relationships among root anatomical and leaf physiological traits during the 30 days waterlogging such that leaf-level photosynthesis (A_{max}), transpiration rates (E) and stomatal conductance (gs) were negatively correlated with total cortical area and cortical cell size and positively correlated with root cortical aerenchyma, aerenchyma area, cortical cell file number and total stele area (Fig. 4.6A). During the 60 days waterlogging**,** root anatomical and leaf physiological traits, such as the intrinsic water use efficiency (*iWUE*) were negatively correlated with cortical cell file number, aerenchyma area, total cortical area, root cortical aerenchyma, cortical cell size and total stele area and positively correlated with A_{max}, E and gs (Fig. 4.7A). Several studies exploring the responses of root traits to climate change have revealed that the anatomy of transport root can strongly influence growth and survival due to their vital roles in gas and nutrient acquisition and transportation (Lambers et al. 2006; Warren et al. 2015; Iversen et al. 2017). Kong et al (2017) reported sufficient water transportation through the cortex to the vessels in species with thicker root cortex. Our results have shown that root cortical aerenchyma play an important role in plant gas exchange and water transpiration (Fig. 4.3A and 4.5A). Consistent with our observations, a positive relationship was reported between aerenchyma spaces and cortex thickness which are essential for high capacity oxygen transport along roots (Justin and Armstrong 1987; Yamauchi et al. 2019).

4.5.3 Response of anatomical, physiological traits and water-use efficiency under waterlogging, elevated temperature and elevated CO_2

Our third research question is to determine how anatomical traits and leaf physiological traits as well as intrinsic water use efficiency respond to climate change in temperate woody species.

For 30 days waterlogging, *Salix pentandra* plants had the highest intrinsic water use efficiency followed by *Betula pubescens*, *Betula pendula* and *Alnus glutinosa*, whereas for the 60 days waterlogging, *Alnus glutinosa* had the highest intrinsic water use efficiency followed by *Salix aurita, Betula pendula* and *Betula pubescens*. These results suggest that the intrinsic water use efficiency of temperate species is strongly determined by transpiration rather than photosynthetic assimilation. For *Salix pentandra*, the lower root cortical aerenchyma (Fig. 4.3A) may reduce the oxygen transport, and the higher proportion of total cortical area and cortical cell size (Fig. 4.3E and F) could facilitate the radial movement of water within the root. As a result, the lower root cortical aerenchyma can confer *Silax pentandra* with lower water transport, thus explaining their lower *E* and *gs* and the higher *iWUE* was as a result of the higher proportion of total cortical area and cortical cell size. After 60 days of waterlogging, *Alnus glutinosa* had a much higher aerenchyma area indicating a higher oxygen transport than other plants. Further, *Alnus glutinosa* species had a lower *gs* and higher *iWUE* compared to other species suggesting that a higher oxygen transport may be the reason for *Alnus glutinosa* plants to maintain relatively high photosynthetic rates. These findings imply that transport and movement of water and gases in *Salix pentandra* and *Alnus glutinosa* is determined by aerenchyma-related traits and the cortical region of plant roots. This support the theory on the functional attributes of aerenchyma in woody and herbaceous species (Jackson and Armstrong 1999b; McElrone et al. 2004; Parent et al. 2008; Kong et al. 2017).

Elevated temperature had significant effects on anatomical traits of roots and leaf physiological traits as well as water use efficiency of temperate trees. Root cortical aerenchyma, aerenchyma area, total stele area and total cortical area varied among the species as a result of increased temperature. *Alnus glutinosa* plants had a higher root cortical aerenchyma compared to the other species due to elevated temperature. The increased temperature enhanced the aerenchyma area in *Salix pentandra* plants only, but it did not affect the cortical cell file number in any

species. On the contrary, warming effects on root diameter decreased with warming magnitude in woody plants but increasing warming duration increased the root length (Zhao et al. 2023).

CO_2 level had significant effects on anatomical traits of roots of temperate trees. For example, *Alnus glutinosa* species had higher root cortical aerenchyma, aerenchyma area and cortical cell size due to increase in CO_2 (Fig. 4.5A, C and F). Moreover, increase CO_2 enhanced the aerenchyma area and total stele area of *Betula pendula*. This finding among anatomical traits and elevated CO_2 agrees with previous reports that atmospheric CO_2 enrichment increased the stele diameter and cortex of plants (Rogers et al. 1992; Madhu and Hatfeld 2013).

4.5.4 Influence of root anatomical traits on leaf physiological traits and water use efficiency under climate change

Our results on the different waterlogging response patterns of leaf physiology and water use efficiency among the species can be attributed to their inherent root anatomical trait characteristics. We found that the species with more root cortical aerenchyma and bigger cortical cell size are less sensitive to waterlogging (Fig. 4.8). An essential part of the root cortical aerenchyma development in wet soil, where low oxygen availability may prevent root respiration, is improved oxygen transfer. The limiting factor that may contribute to the correlation between the root cortical aerenchyma and the sensitivity of the response to waterlogging is the limitation of other edaphic stresses, including phosphorus, nitrogen and sulphur deficiency (Drew 1997). Species with more root cortical aerenchyma (*Alnus glutinosa* and *Salix aurita*) can also facilitates nutrient uptake. Adequate oxygen level enhances the activity of root-associated microorganisms and mycorrhizal fungi, promoting nutrient availability to the plant (Servais et al. 2019). However, these results may explain for example the increase in photosynthesis rates and water transportation in *Alnus glutinosa* by waterlogging. This adaptation to waterlogging conditions enables the transport of oxygen into the otherwise anoxic rhizosphere, enabling root growth deep into waterlogged soils (Evans

2003; Colmer and Voesenek 2009b) and explains why root anatomical traits of *Alnus glutinosa* and *Salix aurita* were not negatively affected by waterlogging. Thus, the observation that *Alnus glutinosa* and *Salix aurita* were more responsive to waterlogging may be attributed to having more root cortical aerenchyma with large aerenchyma area and cortical area.

4.6 Conclusion

We measured the unique root anatomical traits of temperate tree species and found significant differences in the five species. We also showed a strong relationship between the anatomical root and leaf physiological traits as well as the water use efficiency. We discovered that the root anatomical traits were less responsive to 30 days waterlogging for all species, however, we found that the root anatomical traits responded diversly to 60 days waterlogging among the species as well as their leaf physiological traits. Anatomical characteristics of roots and water-related leaf physiological traits were significantly related indicating a strong influence in growth and survival due to their vital roles in gas and nutrient acquisition and transportation. Among the plant species we examined, *Alnus glutinosa* and *Salix aurita* showed the best intrinsic water use efficiency for 60 days waterlogging, whereas *Betula pendula* and *Salix pentandra* exhibited the highest intrinsic water use efficiency for 30 days waterlogging. This observation is likely the effect from their low stomatal conductance due to larger cortical area and root cortical aerenchyma in *Alnus glutinosa* and *Salix species*. Similarly, Salix *pentandra* and *Alnus glutinosa* (both water-adaptive species) significantly increase aerenchyma area after 60 days waterlogging indicating higher oxygen transport thereby maintaining relatively high photosynthetic rates. Also, we observed that elevated temperature can significantly increase anatomical traits of roots (root cortical aerenchyma, aerenchyma area, total stele area and total cortical area) and leaf physiological traits as well as water use efficiency, but this variation depends on the species. Anatomical traits of roots of varies significantly among the species under elevated CO_2, with increased root cortical aerenchyma, aerenchym area and cortical cell

size in *Alnus glutinosa* under elevated CO_2 suggesting that *A. glutinosa* will be more resilient to flooding under elevated CO_2. Overall, our findings provide a novel and insights knowledge into how woody temperate tree saplings adapts to future climate change. This knowledge has implications for forestry and ecosystem management.

Chapter 5: Greenhouse Gas Emissions from temperate trees saplings: interplay between elevated temperature, CO_2, and waterlogging

5.1 Abstract

The effects of climate change, including elevated temperatures and increased atmospheric CO_2 levels, are expected to enhance methane (CH_4) and carbon dioxide (CO_2) emissions from temperate forests. However, the extent to which these emissions are influenced by temperature increases and CO_2 enrichment under flooding conditions, particularly in tree saplings, remains inadequately understood. To address this knowledge gap, we established a controlled environment mesocosm experiment using two-year-old saplings of common European tree species including common alder (*Alnus glutinosa*), silver birch (*Betula pendula*), downy birch (*Betula pubescens*), bay willow (*Salix pentandra*) and eared willow (*Salix aurita*). In this experiment, net ecosystem exchange (NEE) and soil CH_4 and CO_2 fluxes were determined in response to elevated temperature and CO_2. Waterlogging increased NEE of CH_4 emission from all species but the response varied among the species and in response to elevated temperature. Flooding increased NEE of CO_2 emissions under CO_2 enrichment whereas CH_4 emission did not respond to elevated CO_2. For the soil-only measurement, CH_4 emission was 75% higher under elevated CO_2 than in the control under waterlogging. Soil-CO_2 emissions varied significantly between the species, with the highest emission of 320.9 mg CO_2 m^{-2} hr^{-1} under *S. aurita* and the lowest 157.7 mg CO_2 m^{-2} hr^{-1} under *B. pendula*. From these results, we conclude that during flooding, CO_2 fluxes are expected to be more heavily impacted than CH_4 fluxes by CO_2 enrichment while CH_4 fluxes are expected to be more strongly impacted than CO_2 fluxes by higher temperatures, but that the magnitude responses may differ substantially among species. Such differences in temperature and CO_2 response among tree saplings need to be

considered when modelling ecosystem greenhouse gas responses and also during afforestation effort in flood prone areas to support effective carbon capture mitigation.

5.2 Introduction

Terrestrial biomes such as forest are generally net sinks of CO_2 and store large amounts of carbon in their soils (Roulet 2000; Gilliam 2016). Temperate forests contribute 0.72 ± 0.08 Pg C $year^{-1}$ to the forest C sink comprising 0.66 trillion trees (Hidalgo et al. 2007). However, forest soils also emit large amounts of CO_2 and may also be either a major source of CH_4 in wetlands or a sink in uplands reflecting the net CH_4 production and oxidation (Covey et al. 2012). However, despite the significance of trees in global GHG cycles, the responses to higher temperatures and elevated CO_2 of the impact of trees on CH_4 and CO_2 emissions in temperate areas remains poorly understood (Meier et al. 2016), limiting our ability to predict climate change responses of their CO_2 and CH_4 emissions.

The magnitude of greenhouse gas emissions from wetland plants have been investigated in herbaceous species (Bhullar et al. 2013) and woody plants (Pangala 2013). These fluxes may vary substantially due to differences in either microbial community or forest species composition (Li et al. 2019). Rice et al (2010), measured the CH_4 emissions from three woody riparian tree species grown in mesocosms: willow, ash, and poplar. They scaled these up globally using leaf area normalised mean emission rate for flooded forest regions and estimated the amount to be 60±20 Tg yr−1, or about 10% of the global CH_4 source. It is therefore important to determine the role of vegetation in the biogeochemical cycling of greenhouse gases as an important contribution to global greenhouse budget.

The roles of plants emission of greenhouse gases e.g. CH_4, and CO_2 have been established over the past few years (Rusch and Rennenberg 1998; Pangala 2014; Sjögersten et al. 2020b; Schindler et al. 2021). Plant-mediated greenhouse gas emission involves release of gases via the stem and/or leaf surfaces. Previous studies by Rusch and Rennenberg (1998) of wetland adapted saplings (*Alnus glutinosa*) showed significant CH_4 emissions via stem surfaces. A

number of subsequent studies of other tree species have consistently reported the presence of tree-mediated emissions (Machacova et al. 2016; Maier et al. 2018; Schindler et al. 2021). Emissions may be as a result of either plant physiological gas production or microbial production within the stem where elevated concentrations of CO_2, and CH_4 can be found (Covey et al. 2012). In addition, gas may also be produced within the soil and transported via roots into above-ground plant tissues.

Climatic change with impacts on CO_2 and CH_4 emissions include an increase in mean annual temperature, more episodic and intense precipitation events and extreme hot days (IPCC 2007). Although these climate change trends will persist in the future, the exact magnitude of changes is quite unclear (IPCC 2022). For instance, the estimated increase in the global mean temperature by 2100 is between 1.4 and 3.2 °C, depending on the magnitude of greenhouse gas emissions in the future (IPCC 2022). To date, precipitation changes in the temperate region have been linked with wetter wet seasons and drier dry season but no change in mean precipitation despite the change in seasonality for the region (IPCC 2022). Daily precipitation intensities have increased in winter over recent decades (Osborn et al. 2000) and are predicted to continue to do so in the future (IPCC 2022). Precipitation in the temperate regions is predicted to increase by 10-40% under the Intergovernmental Panel on Climate Change (IPCC) scenarios, increasing the risk of flooding (IPCC 2022). Together these changes in precipitation are expected to increase microbial decomposition rates (Ceulemans et al. 1999), while increased precipitation could result in decreased soil CO_2 emissions and increased in CH_4 emissions (Dolman et al. 2018a).

Numerous experiments and observational studies have been carried out to gain a better understanding of the possible impacts of increasing temperatures, rising CO_2 and changing precipitation on forest ecosystems. For instance, CO_2-enrichment studies in forests indicate that net primary productivity will rise in the presence of increased CO_2, although this response

may eventually decline due to nutrient or water scarcity (Norby et al. 2006; Warren et al. 2011; Servais et al. 2019; Gardner et al. 2022). Under elevated CO_2, there is also evidence of reduced stomatal conductance to water vapour and little sign of acclimatisation (Medlyn et al. 1999; Gardner et al. 2023). Further, experiments on the role of plants in the emission of greenhouse gas show a range of ecosystem response, but for temperate ecosystems, anticipated warming often increases process rates (Gunderson et al. 2000; Aerts et al. 2006; Hyvönen et al. 2006). Further, it is important to consider climate change responses of tree saplings in the context of water-level status in the temperate region arising from wetter wet seasons and there is a strong relationship between water table level and GHG emissions (Evans et al. 2021).

In this study, controlled environment experiments were used to investigate the effects of future temperature and atmospheric CO_2 scenarios on ecosystem function in temperate forest under flooded and non-flooded conditions. We assessed the effect of increasing temperature and CO_2 levels, combined with periods of waterlogging stress, on greenhouse gas emissions from temperate tree saplings. The aim is to understand how these environmental factors influence the release of greenhouse gases, such as CO_2 and CH_4, from the soil-plant-atmosphere continuum. We focus on the interactive effect of waterlogging between elevated temperature and CO_2 enrichment respectively, and the impacts on CO_2 and CH_4 emission from plant-soil mesocosm planted with temperate tree saplings. We explored net GHG exchange, soil and stem emissions.

5.3 Material and methods

The study was conducted using 192 mesocosms, each containing a single *Alnus glutinosa*, *Betula pendula*, *Betula pubescens*, *Salix pentandra* and *Salix aurita* sapling. The mesocosms were divided into two treatments (n= 96) based upon elevated temperature and water-table

position or elevated CO_2 and water-table position. Further details on the mesocosms can be found in Chapter 2 (section 2.5).

5.3.1 Study Site

Details of the growth rooms can be found in 2.2.

5.3.2 Mesocosm experiment

The mesocosms consisted of 10-L containers constructed of durable polyvinyl chloride. Wetland soil from Jubilee woods and commercial topsoil were mixed and added into each of the mesocosms. Two-year-old *Alnus glutinosa*, *Betula pendula*, *Betula pubescens*, *Salix pentandra* and *Salix aurita* saplings purchased from a nursery in the UK were planted in the mixture in 2021 for the temperature experiment and 2022 for the CO_2 experiment. We investigated four treatments in each experimental year. For the first experiment, we investigated control + ambient temperature (control + aT), waterlogging + ambient temperature WL + aT, control + elevated temperature (control + eT) and waterlogging + elevated temperature (WL + eT), while for the second experiment, we investigated control + ambient CO_2 (control+aCO_2), waterlogging + aCO_2 (WL+aCO_2), control + eCO_2 (control+eCO_2) and waterlogging + eCO_2 (WL+eCO_2). The 24 replicates of each treatment were randomly allocated to four blocks in each of the rooms (Fig. 5.1). Following the emergence of leaves, waterlogging was then initiated in late August 2021 (hottest month) for 30 days and for the CO_2 experiment, saplings were transferred into the growth room in May 2022 and CO_2 treatment was initiated on the same day. Thirty days after, when leaves have emerged, saplings were subjected to 60 days of waterlogging in July 2022.

Figure 5:1: The mesocosm setup consisting of 2-year-old saplings planted in peat and soil mixture.

5.3.3 Greenhouse gas measurements

5.3.3.1 NEE mesocosm static chambers

To measure the net ecosystem exchange (NEE), samples were collected from the soil plus plants in the mesocosms (i.e. plant-soil system; Fig 5.2) using the static transparent chambers method (Alskaf et al. 2021). in the growing period (29-31st of August 2021 for temperature and 15-17th July of 2022 for CO_2). Static chambers were constructed from transparent polycarbonate with an internal diameter of 24 mm and a height of 105 cm. Initially, ground tubes of 10 cm height with an internal diameter 24 mm were inserted down into the soil surface of each mesocosm leaving 5 cm above the soil surface to fix the transparent chambers on. Gases were collected from headspaces fitted with Suba seal® rubber septa (Fisherbrand, Loughborough, UK) between 10 am and 4 pm on each sampling day, with samples collected 0, 3, 20 60 minutes following chamber installation (Alskaf et al. 2021). The plastic cylinders were moved from one plot to another after collecting the samples. Each of these cylinders was provided with two computer fans to stir the gas inside before collecting the samples. The

samples were taken from the top of the chamber through sealed rubber septum fixed to the chamber for this purpose. Headspace gases were mixed using a 20 ml syringe (20 Gx1", TERUMO, UK) and needle and injected into pre-evacuated 12 mL glass exetainers sealed with a screw cap septum, resulting in a slight over-pressurisation (Exetainer; LABCO, UK). The gas samples were kept at a constant temperature of 24 °C until they are analysed using a gas chromatograph (GC) (GC-2014; Shimadzu, Milton Keynes, UK). CO_2, and CH_4 concentrations were measured using a single injection system with a 1 mL sample loop using N_2 as a carrier gas through a non-polar methyl silicone capillary column (CBP1-W12-100, 0.53 mm I.D., 12 m, 5 mm) and porous polymer packed column (HayeSep Q 80/100). A thermal conductivity detector and flame ionization detector were used to measure CO_2 and CH_4, respectively.

Figure 5:2: Static chambers used to measure NEE mesocosm greenhouse gas emissions.

5.3.3.2 Soil emission of CO_2 and CH_4

The soil emission was done for the CO_2 experiment only. Static chambers used to measure greenhouse gases from the soil in each mesocosm were constructed using a transparent

polycarbonate collar (30 cm height × 7 cm diameter) inserted 5 cm into the soil surface securely in order to ensure no disturbance during measurement (Fig 5.3). Static chambers are fitted with Suba seal® rubber septa (Fisherbrand, Loughborough, UK) and gases where collected (20 mL) through the sampling ports using hypodermic needles and plastic syringes at 0, 3, 20 60 minutes after chamber was placed into the soil (Sjögersten et al. 2011). Samples were analysed in the same way as described previously.

5.3.3.3 Flux calculations

Flux calculations were based on Eq. s (1) and (2). Time series data was used for obtaining a linear response used for calculations and gas samples that did not follow a linear accumulation trend were discarded. The gas data was converted from volume per volume (ppm) to mass per weight using the molecular weight of each gas and the ideal gas equation (Denef et al. 2007).

$N = PV/RT$ (1)

N: Number of moles of CO_2 or CH_4

P: atmospheric pressure

V: the volume of headspace dm^3

R: The ideal gas constant (0.082057462 atm^1 k^{-1} mol^{-1})

T: the temperature of sampling (273.15 + room temperature in 8C).

$E= (NM/AT)\ 1000$ (2)

E: is the flux of each gas in mg m^{-2} h^{-1}

N: Number of moles of CO_2 or CH_4

M: the molar weight of CO_2 (44.01) or CH_4 (16.04)

A: an area of the soil used

T: time in hours (h).

The transparent chambers measured NEE (Eq.3) by definition negative fluxes implied net uptake of CO_2 or CH_4 from the atmosphere while positive fluxes equate net source of CO_2 or CH_4.

NEE - CO_2 = -photosynthesis + plant respiration + soil - CO_2 (negative fluxes),

Here the equation describes the NEE is related to the different CO_2 fluxes in the ecosystem. Plants absorb CO_2 from the atmosphere during photosynthesis. This is a negative flux because CO_2 is being removed from the atmosphere (absorbed by plants). Plants also release CO_2 through respiration (the process by which they convert sugars into energy), which is a positive flux because CO_2 is being emitted into the atmosphere. Similarly, microbes and other organisms in the soil release CO_2 during decomposition of organic matter, which is another positive flux. For NEE of CO_2 means the ecosystem is a net sink of CO_2 when this value is negative, meaning more CO_2 is absorbed through photosynthesis than is released through respiration.

NEE + CO_2 = photosynthesis + plant respiration + soil + CO_2 (positive fluxes) (3)

Here, equation restates the concept but in terms of positive fluxes, indicating the amount of CO_2 being sequestered by plants, and it is balanced against the positive fluxes of plant respiration and soil respiration, which add CO_2 to the atmosphere. NEE + CO_2 indicates that the ecosystem might be a net source of CO_2 when positive, meaning more CO_2 is being released than absorbed (i.e., respiration exceeds photosynthesis).

Figure 5:3: Static chambers used to measure soil greenhouse gases from the mesocosms.

5.3.4 Data Analysis

Data analyses were carried out in GenStat (v23.1, VSN International Ltd, UK). Differences in CO_2 and CH_4 fluxes were assessed using linear mixed effects model fitted using Residual Maximum Likelihood (REML) to account for variable dependence between mesocosms. During the analysis of the gas fluxes, species, timepoints (during waterlogging), treatment (ambient or elevated) and waterlogging were the fixed model and block as a random effect. The residuals were checked for normality and homogeneity of variance by visual inspection of residual plots. Rates of CO_2 and CH_4 production were log-transformed, and significance was assessed at $p \leq 0.05$. Relationships between gas fluxes and environmental factors (water table, temperature and CO_2) were explored using regression analyses. The % of variance accounted for (adjusted R^2) by regression statistical models is referred to as r^2 in text and figures. Results through text and graphs are presented as mean ± SE.

5.4 Results

5.4.1 Elevated temperature and GHG fluxes

5.4.1.1 Mesocosm CH_4 and CO_2 emissions

Mean fluxes from mesocosms with *S. pentandra* and *B. pubescens* were higher (537.3 and 522.5 µg CH_4 m^{-2} hr^{-1}) compared to *B. pendula* and *A. glutinosa* (297.9 and 293.6 µg CH_4 m^{-2} hr^{-1}) (Figure 5.4A). CH_4 fluxes were significantly higher during the waterlogging treatment for all species (Figure 5.4B).

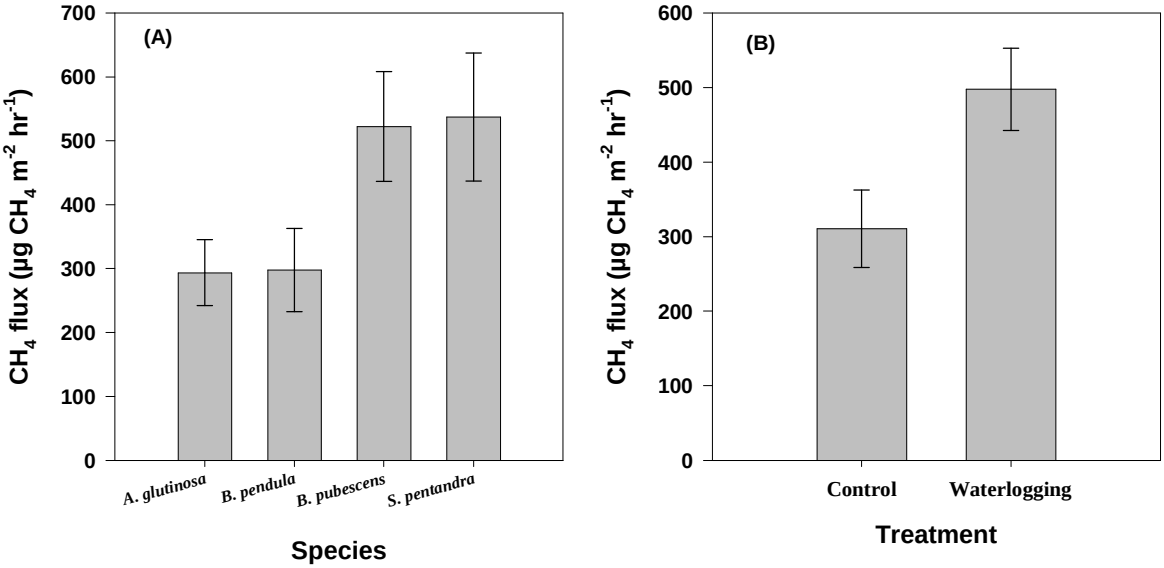

Figure 5:4: (A) NEE of CH_4 during waterlogging from *A. glutinosa, B. pendula, B. pubescens* and *S. pentandra* sampling (B) NEE of CH_4 under control and waterlogging treatment.

In contrast, CO_2 fluxes was not significantly different among species during the waterlogging treatment. However, there was a significant difference between species ($p = 0.05$) after waterlogging. The highest NEE of CO_2 was observed from *S. pentandra* (478.8 mg CO_2 m^{-2} hr^{-1}) while the lowest from *B. pendula* (264.2 mg CO_2 m^{-2} hr^{-1}) (Figure 5.5A). CO_2 fluxes also varied significantly between species × CO_2 ($P = 0.042$). Elevated temperatures reduced the CO_2 emission of *B. pendula* and *S. pentandra* while CO_2 fluxes from *A. glutinosa* and *B. pubescens* remained similar to those under ambient conditions (Figure 5.5B).

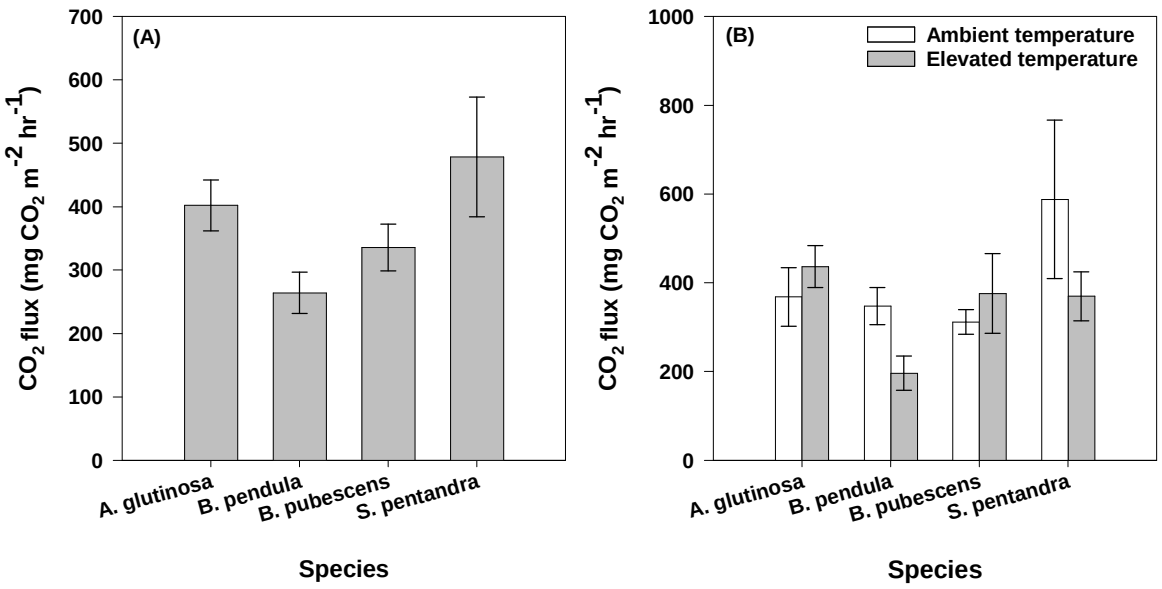

Figure 5:5: NEE CO_2 fluxes after waterlogging treatment from *A. glutinosa*, *B. pendula*, *B. pubescens* and *S. pentandra* (B) CO_2 fluxes after waterlogging from the different species in ambient and elevated temperature conditions

5.4.2 Elevated CO_2 and greenhouse gases

5.4.2.1 Mesocosm CH_4 and CO_2 emissions

During waterlogging, CO_2 fluxes were significantly different between species (*P = 0.033*). Mean fluxes were lowest under *A. glutinosa* (251.2 mg CO_2 m^{-2} hr^{-1}) and highest under *B. pendula* (406.8 mg CO_2 m^{-2} hr^{-1}) (Figure 5.5A) during the sampling period. CO_2 fluxes also varied significantly between ambient and elevated CO_2 treatments (*P = 0.018*) with greater CO_2 losses under elevated CO_2 during waterlogging. No effects of were found on mesocosm CH4 emission (P > 0.05).

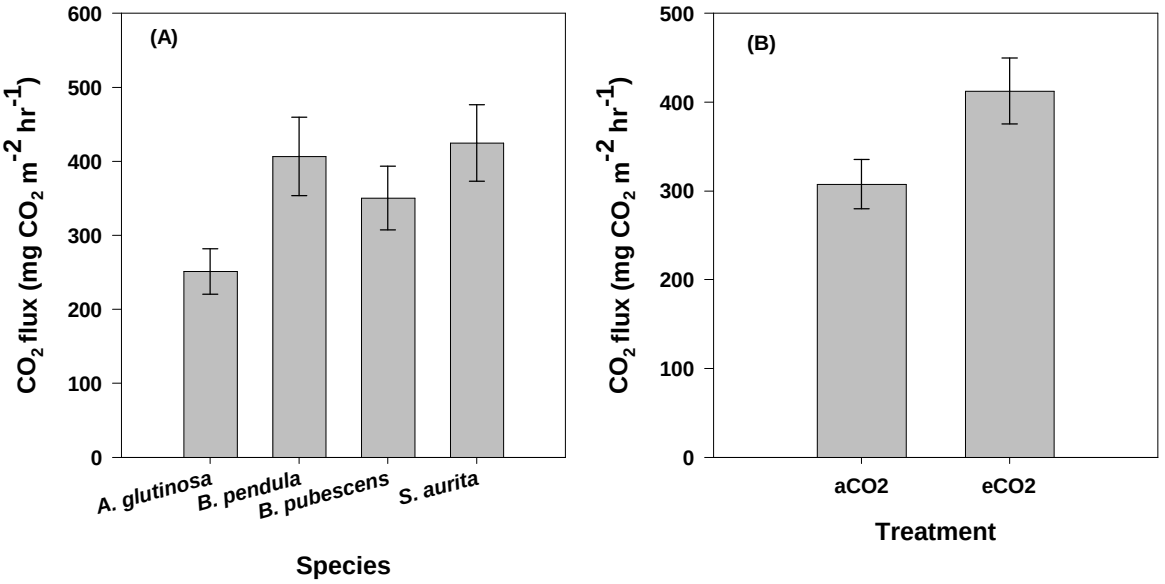

Figure 5:6: (A) NEE mesocosm CO_2 fluxes during waterlogging from *A. glutinosa, B. pendula, B. pubescens* and *S. aurita* saplings (B) CO_2 fluxes during waterlogging treatment under ambient and elevated CO_2 conditions

5.4.2.2 Shoot CH_4 and CO_2 emissions

Shoot-CH_4 emissions varied significantly between the species (*P = 0.026*). The highest stem CH4 emission was observed from *S. aurita* and *B. pubescens* (449.6 and 441.4 µg CH_4 m^{-2} hr^{-1} respectively) while the lowest from *A. glutinosa* and *B. pendula* (166.7 and 257.3 µg CH_4 m^{-2} hr^{-1} respectively) (Figure 5-8A). Shoot-CH_4 emissions also varied significantly between species and timepoints (*P = 0.041*). The highest averaged shoot-CH_4 emissions was observed during waterlogging (469 µg CH_4 m^{-2} hr^{-1}) and the lowest (325.3 µg CH_4 m^{-2} hr^{-1}) after waterlogging (Figure 5-7B).

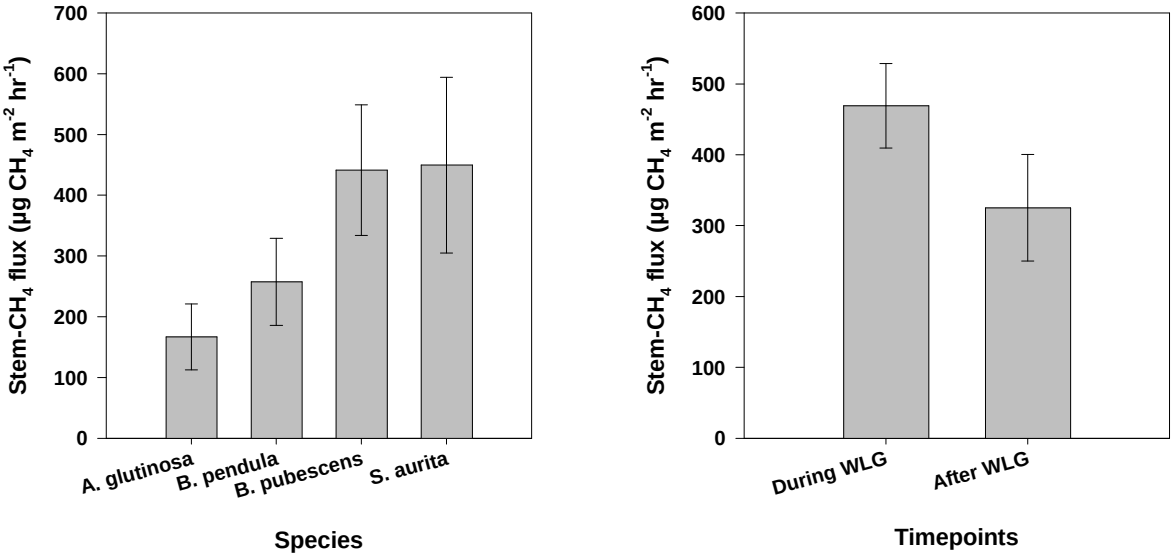

Figure 5:7: (A) Shoot-CH_4 flux during waterlogging from *A. glutinosa, B. pendula, B. pubescens* and *S. aurita* saplings (B) Shoot-CH_4 fluxes during the waterlogging treatment

Shoot emissions (NEE mesocosm chamber fluxes minus soil chamber fluxes) varied with timepoint, with lowest levels measured during waterlogging -10.18 mg CO_2 m^{-2} hr^{-1} and highest after waterlogging respectively 57.72 mg CO_2 m^{-2} hr^{-1} (Figure 5-8). Similarly, shoot emissions responded positively to the interactive effects of species, treatments and timepoint (*P = 0.003*).

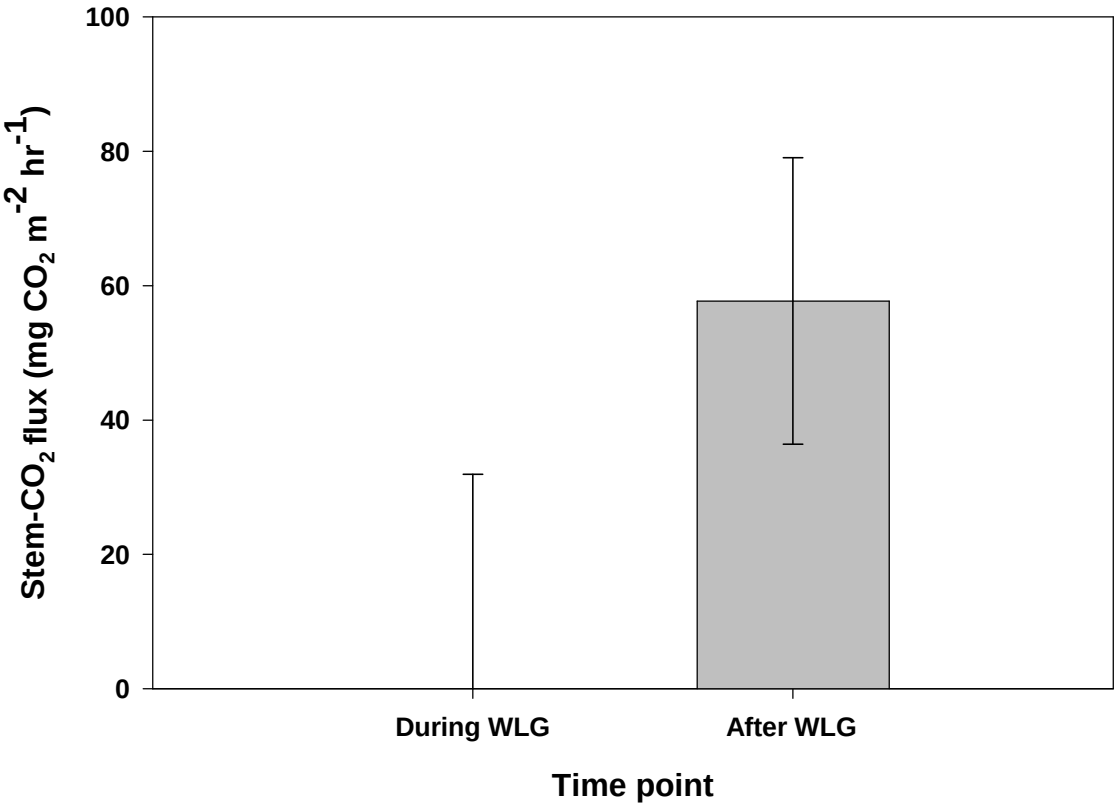

Figure 5:8: Shoot-CO_2 flux during the waterlogging treatment averaged from all species

5.4.2.3 Soil CH_4 and CO_2 emissions

Mean CH_4 fluxes were higher under the elevated CO_2 treatment from *A. glutinosa* (205.2 µg CH_4 m^{-2} hr^{-1}) decreasing (35 µg CH_4 m^{-2} hr^{-1}) under *S. aurita* before the waterlogging treatment (Figure 5.9), and there was a statistically significant interaction between species × CO_2 ($P = 0.015$). However, there was no significant effect of waterlogging on CH_4 ($P > 0.05$).

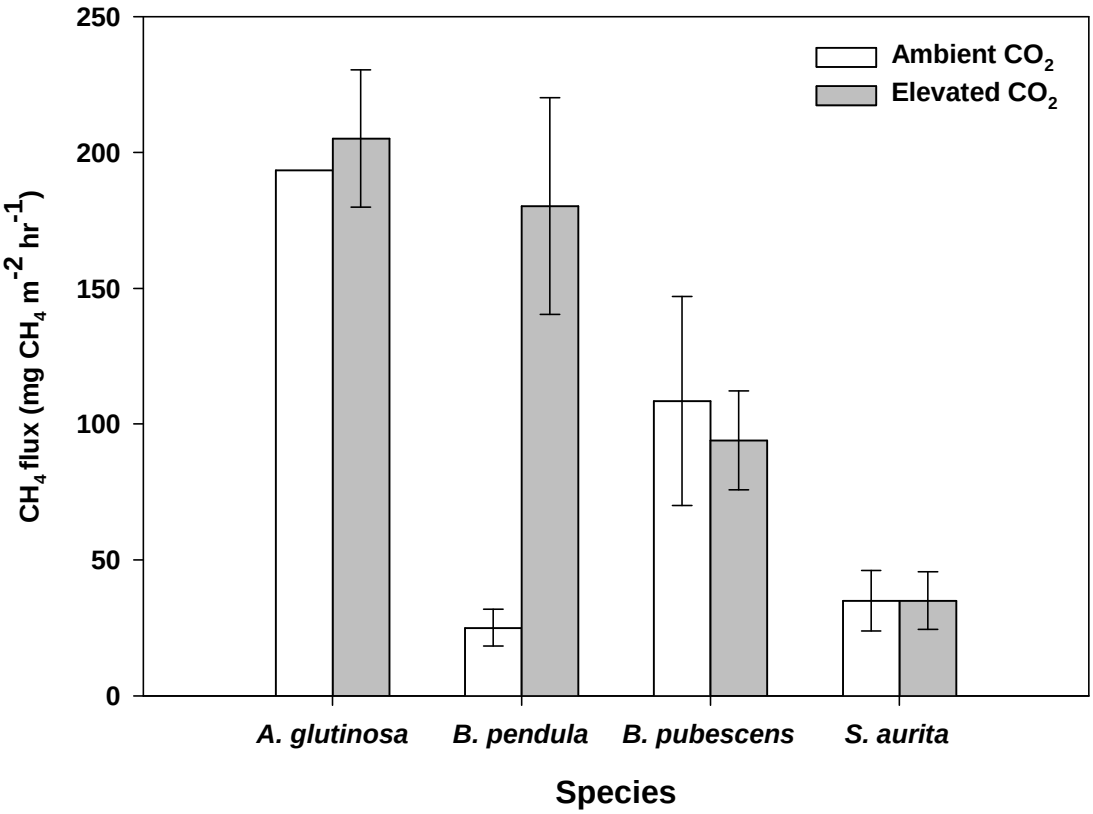

Figure 5:7: Soil-CH_4 fluxes before waterlogging from *A. glutinosa*, *B. pendula*, *B. pubescens* and *S. aurita* saplings under ambient and elevated CO_2 conditions

CO_2 fluxes were significantly different between species before waterlogging (*P = 0.032*). Mean fluxes were higher under *S. aurita* (320.9 mg CO_2 m^{-2} hr^{-1}) and lower under *B. pendula* saplings (157.7 mg CO_2 m^{-2} hr^{-1}) (Figure 5.10A). During waterlogging, CO_2 fluxes were not significantly different between ambient and elevated CO_2 treatments (*P = 0.07*). After waterlogging, there was a significant interactive effect of waterlogging × CO_2 treatment (*P = 0.034*). Mean fluxes under the elevated CO_2 condition were lower in controlled waterlogging treatment (193.9 mg CO_2 m^{-2} hr^{-1}), increasing to (238.3 mg CO_2 m^{-2} hr^{-1}) in waterlogging treatment (Figure 5.8).

Oxygen concentrations decreased significantly under all species (*P = 0.006*). Decreases were generally most pronounced under elevated CO_2 treatment (Figure 5.10B). Oxygen concentrations were significantly higher under *A. glutinosa* (53.75%). In *B. pubescens* and *S.*

aurita elevated CO_2 plots, concentrations decline by 2%, compared to a 4% decline in *A. glutinosa* and *B. pendula* plots.

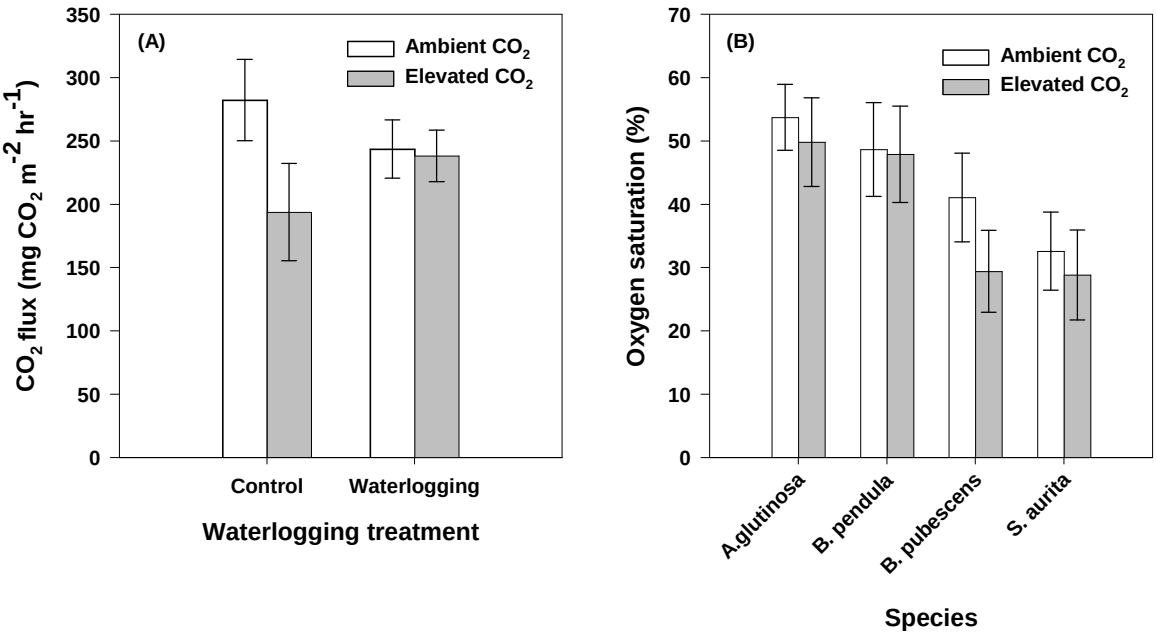

Figure 5:8: (A) CO_2 fluxes from waterlogging treatment under ambient and elevated CO_2 treatment (B) Oxygen percentage from *A. glutinosa, B. pendula, B. pubescens* and *S. aurita* under ambient and elevated temperature and elevated CO_2 conditions

5.5 Discussion

5.5.1 The role of plant species in greenhouse gas emissions

Results show that species impacted CO_2 and CH_4 emission differently. *Salix aurita and Salix pentandra* – two wet tolerant species were the strongest sources of CO_2 and CH_4. Significant differences in greenhouse emission concentrations between plants during waterlogging are likely associated with species differences in tree species, height and stem diameter (refer to chapter 3) (Pangala et al. 2014). Further, differences in CH_4 and CO_2 emissions among wetland species, with rates determined by the morphological adaptations (refer to chapter 4) such as the enlarged aerenchyma which enhance gas exchange between the atmosphere and the rhizosphere (Tsukahara and Kozlowski 1986; Weiss et al. 2005). These findings collectively

suggest the importance of aerenchyma development in the exchange of gases and the importance of vegetation competition in determining greenhouse emissions.

The egress of CH_4 during waterlogging and the absence of CH_4 emission after waterlogging in our experiment further indicate that water-table was a dominant control on CH_4 production and release. This finding is consistent with previously reported studies that water-table position strongly regulates soil CH_4 production and consumption in wetlands. However, the variations in CO_2 emissions after waterlogging were largely dependent on the soil and air temperature.

Waterlogging increased NEE of CH_4 markedly from the species. Significant quantities of CH_4 were released from the whole mesocosms, but the magnitude and pattern of the emissions differed between the species (Fig. 5.4A). Differences in magnitude and pattern of CH_4 emissions between *A. glutinosa* and *B. pubescens* have previously been reported in wetland vegetation (Pangala et al. 2015). It has long been known that waterlogging affects CH_4 emissions by influencing its production, consumption and transport (Whiting and Chanton 1996; Joabsson et al. 1999).

5.5.2 The role of elevated temperature and waterlogging in greenhouse gas emissions

CH_4 fluxes were detected from all saplings from stem surfaces, consistent with previous studies by (Kankaala et al. 2005; Pangala et al. 2015). These findings not only suggest that stem surfaces are major pathways of methane egress but also temperature plays an important role in methane emission rates.

Various studies have shown that CO_2 emissions resulting from respiration in soil and vegetation are the sources from which this gas enters the atmosphere (Blodau et al. 2007; Saunders et al. 2014; Maier et al. 2018). We found CO_2 fluxes to vary between ambient and elevated CO_2. (Fig. 5.10A), as well as waterlogging. We found waterlogging to reduce the CO_2 emission from ambient and elevated CO_2 conditions. Our observations of CO_2 fluxes under waterlogging and

CO_2 enrichment are consistent with other studies that have reported that rising levels of CO_2 will reduce CO_2 sensitivity in *Betula alleghaniensis*. Our data suggests that *elevated* CO_2 will stimulate CH_4 emissions more than methane CH_4 sinks in waterlogged soils.

5.5.3 The role of elevated CO_2 and waterlogging in greenhouse gas emissions in soils

Unlike previous elevated CO_2 and waterlogging studies on CH_4 emissions in different species (Vann and Megonigal 2003; Dolman et al. 2018b), we could not observe a significant difference within our studied periods. However, slight changes in waterlogging treatment were detected ($P = 0.071$). Even the observed impact of elevated CO_2 on the species showed no significant effects before waterlogging.

In contrast to CH_4 emissions, we found CO_2 fluxes to vary between species and the interaction CO_2 enrichment in our study (Fig. 5.6A and B). These differences in CO_2 emissions among vegetation/soil types have been previously reported for in temperate wetlands (Medlyn et al. 1999) and have been linked to microbial adaptation and processes. Indeed, varying responses of species to CO_2 in temperate microbial communities have been linked to the influence of CO_2 on microbial and plant metabolisms as well as plant phenology (Creed et al. 2013; Hanson and Wullschleger 2018). The interaction between waterlogging and increased CO_2 emission during waterlogging (Fig. 5.6B) suggest that oxygen inputs from roots (Armstrong et al. 2009) and water as well water table drawdown maybe important catalysts for aerobic breakdown processes below the water table. For instance, the increase in soil CO_2 emissions under elevated CO_2 conditions in our study could have the potential to alter nutrient availability and soil carbon storage as reported under a free-air CO_2 enrichment (FACE) experiment from a deciduous forest system (Norby et al. 2006). The presence of oxygen in the soil profile controls aerobic and anaerobic decomposition pathways. We observed a decrease in oxygen concentration

under elevated CO_2 conditions suggesting that decay will occur more slowly under increased CO_2 presence.

5.6 Conclusion

Waterlogging increased CH_4 emission from all species and we also found waterlogging to increased CO_2 emission under elevated CO_2 treatment, but the magnitude and pattern of the emissions differed between the species. The soil was a significant emitter of CH_4 and CO_2 into the atmosphere and the quantity of these fluxes varied between the species. The observed impact of elevated CO_2 on the species showed no significant effects before waterlogging, however, we found significantly more CH_4 emissions than CO_2 emission in the waterlogged soils in our study Waterlogging enhanced anaerobic conditions in the soil thereby promoting the production of CH_4 fluxes from NEE mesocosms, however, the dynamics of CH_4 fluxes is species specific. The responses to temperature, CO_2 and waterlogging stress vary between the saplings resulting in significant differences in GHG emissions.

Chapter 6: General discussion

6.1 Introduction

This study assesses the physiological, morphological, and anatomical impacts of climate change as well as greenhouse gas (GHG) fluxes in a temperate tree sapling. Globally, temperate forests absorb and store significant amount of carbon dioxide and methane but are subject to increasing pressure from anthropogenic activities and human activities (Schulze et al. 2010; IPCC 2022), and therefore a better understanding of temperate trees responses to climate change will facilitate the projections of the responses and promote resilience and sustainability in temperate forest systems.

This study, together with previous studies, confirms that the effect of any stress on photosynthesis could be triggered by stomatal, nonstomatal or both responses and that the stress regulation depends on the species (Leverenz et al. 1999; Saibo et al. 2009; Jiménez et al. 2020). Previous studies of the impact of climate change on tree saplings in temperate ecosystems have assessed the physiological, morphological and anatomical responses of saplings to flooding (Yamamoto et al. 1995; Tanaka et al. 2011; Du et al. 2012), elevated temperature and waterlogging (Luo et al. 2008; Wang et al. 2012; Jumrani and Bhatia 2019) and elevated CO_2 (Wang and Taub 2010; Shimono et al. 2012a; Lawson et al. 2017). Studies that have assessed the physiological, morphological, and anatomical changes of tree saplings in response to climate change have predominately focussed on measuring the main effects of single factors (i.e. differences in observed variable between treatment levels and control of the factor) with few studies addressing interactive effects (i.e. depression or amplification of one factor's effects by the other factors (Luo et al. 2008; Bai et al. 2010; Duan et al. 2019).

The research presented here addresses a series of significant knowledge gaps regarding the impact of climate change on temperate tree saplings. In chapter three, I have shown that the

anticipated increases in future temperature and CO_2 levels, along with waterlogging, exert control over the growth and physiology in 2–3-year-old saplings, and these controls can vary substantially between four temperate tree species. For one species, *Alnus glutinosa* elevated temperature decreased photosynthesis, stomatal conductance and transpirations rates but increased following recovery after waterlogging. In chapter four, I demonstrated that woody temperate tree species differed in their root anatomical traits and water-leaf physiological traits regardless of the severity of waterlogging periods (i.e., 30 or 60 days) and greater transpiration rates and intrinsic water use efficiency were seen in species with larger root cortical aerenchyma, total stele area and total cortex area but lower stomatal conductance. In addition to differences in root anatomical traits due to waterlogging, aerenchyma area and total stele area were increased by elevated temperature, and elevated CO_2. In chapter 5, I demonstrated how waterlogging enhanced anaerobic conditions in the soil thereby promoting the production of CH_4 from the NEE mesocosm, even though the dynamic of CH_4 fluxes is species-specific. This chapter presents a synthesis of key findings, and context as well as recommendations for further work.

6.2 Key findings

- The light-saturated net photosynthesis CO_2 assimilation rate, stomatal conductance, and transpiration were lower in waterlogged than non-waterlogged saplings in all species, although the extent of this decrease varies on the ability of the species to tolerate soil oxygen inundation (Chapter 3).
- Waterlogging increased the WUE in all the saplings in elevated temperature conditions (Chapter 3), indicating photosynthetic increase in carbon gained as a result of elevated CO_2. (Chapter 3).

- Interactive effects of the combined stresses of elevated temperature and waterlogging decreased net photosynthesis CO_2 assimilation rate, stomatal conductance, and transpiration in all saplings (Chapter 3).
- CO_2 enrichment did not mitigate the negative impacts of waterlogging on saplings under waterlogging, and growth under elevated CO_2 resulted in a moderate negative effect on net photosynthetic assimilation, however, there was a significance heterogeneity among saplings of different species in the magnitude of this effect (Chapter 3).
- Flooded saplings displayed some form of tolerance to waterlogging by development of hypertrophic lenticels, adventitious roots or enhanced stem growth and formation of aerenchyma (*A. glutinosa* and *S. aurita*) with increase in total dry root biomass specifically under waterlogging in both species under elevated CO_2. (Chapter 3).
- Root anatomical traits significantly differ in root cortical aerenchyma and cortical area among the species during 30- and 60-days waterlogging (Chapter 4).
- Anatomical characteristics of roots and water-related leaf physiological traits were significantly related indicating a strong influence in growth and survival due to their vital roles in gas and nutrient acquisition and transportation (Chapter 4).
- *Salix pentandra* and *Alnus glutinosa* (both water-adaptive species) significantly increase aerenchyma area after 60 days waterlogging indicating higher oxygen transport thereby maintaining relatively high photosynthetic rates (Chapter 4).
- Elevated temperature can significantly increase anatomical traits of roots (root cortical aerenchyma, aerenchyma area, total stele area and total cortical area) and leaf physiological traits as well as water use efficiency, but this variation depends on the species (Chapter 4).

- Anatomical traits of roots of varies significantly among the species under elevated CO_2, with increased root cortical aerenchyma, aerenchym area and cortical cell size in *Alnus glutinosa* under elevated CO_2 suggesting that *A. glutinosa* will be more resilient to flooding under elevated CO_2.
- Waterlogging increased markedly the tree mediated CH_4 emissions from the species, but the magnitude and pattern of the emissions differed between the species.
- The observed impact of elevated CO_2 on the species showed no significant effects before waterlogging, however, we found significantly more CH_4 emissions than CO_2 emission in the waterlogged soils in our study.

6.3 Physiological response of temperate trees to climate change

Leaf gas exchange results indicated that the impact of climate change on temperate tree saplings inhibit different parts of a similar response curve under both elevated temperature, elevated CO_2 and increase flooding scenarios. Additional stress indicators include leaf greenness and chlorophyll fluorescence as well as water use efficiency which has been associated with strong photosynthetic inhibition in species under stress conditions (Kreuzwieser et al. 2002; Bhusal et al. 2020). Results from chapter 3 indicate that the single effect of waterlogging can be significant in driving physiological responses of temperate trees saplings (Figure 3.3 and 3.6), providing a possible mechanism for this finding.

Interactive effects of the impact of climate change in both elevated temperature × waterlogging or elevated CO_2 × waterlogging indicate corresponding inclinations in leaf gas exchange between the species (Figure 3.3 and 3.6), likely as a result of a combination of similarities ascribed to impaired root function, similarity in reduction stomatal conduction, increased water demand, and similar nutrient imbalances. Measurement of root biomass indicate that under

elevated temperature or CO_2 × waterlogging provides structural supports in form of air spaces comprising aerenchymous tissues (Ryser et al. 2011), and that this trait is species-specific (Figure 3.5 and 3.8). These results highlight significant changes in root functioning among the different species. It is therefore possible that plant communities in temperate forests under flooding conditions will also have a significant species-specific physiological imbalances that strongly impact the growth, development and survival of flooded species (Wang et al. 2013; Dolman et al. 2018b). Overall, water and temperature stress- two stress factors among the abiotic factors on plant saplings have been linked to irreversibly stimulate plant growth and development. Additionally, both stresses can reduce plant biomass by decreasing photosynthesis, and increasing stomatal conductance and transpiration (Al-Deeb et al. 2023), where there are visible symptoms, such as a decrease in stem elongation and leaf expansion (Pires et al. 2018), although elevated temperature might alleviate the damage caused by waterlogging in *Alnus glutinosa* (Figure 3.3) (Kramer and Jackson 1954) and by enhancing the photosynthetic supplies of carbohydrates to roots, permitting more efficient production of adenosine triphosphate (ATP).

6.4 Morphological and anatomical response of temperate trees to climate change

Prior research has indicated that root anatomy, for instance aerenchyma, cortex area and total stele area plays an important role in the control of leaf water relations (Huang and Eissenstat 2000; Zhou et al. 2021) and contribute two thirds of the resistance to water transport within the soil-plant system under optimal soil moisture conditions (Passioura 1988; Huang and Eissenstat 2000) but have never completely investigated. In chapter 4, I provide evidence that woody temperate tree species differ in their root anatomical traits and to precipitation change and that the changes in root traits occurs when the range of waterlogging duration exceeds a certain threshold (Figure 4.3 and 4.5). Moreover, root cortical aerenchyma (RCA) was found

to differ significantly between species at 30- and 60-days waterlogging, with *Alnus glutinosa* having 8.4% RCA after 30 days compared to 9.76% after 60 days. At elevated temperature conditions, RCA was 5.4% in 30 days and 12.9% after 60 days. A similar trend was observed in root traits in the other species and may be associated with induction of RCA by stress in oxygenated roots by reducing root respiration and converting living cortical tissues to air spaces (Figure 4.3a and 4.5a) (Lynch et al. 2014). In addition, the differences in root anatomical traits may partially explain the differences found in chapter 3 regarding species-specific differences in physiological responses of temperate trees to climate change. *Alnus glutinosa* and *Salix aurita*- two species with higher root cortical aerenchyma, total stele area and total cortical area exhibited higher transpiration rate and intrinsic water use efficiency but lower stomatal conductance. Trees saplings adaptation to elevated temperature, CO_2 and waterlogging modifies root anatomical traits to maximize nutrient acquisition (Figure 4.3 and 4.5).

6.5 Greenhouse gas emissions from temperate trees mesocosms in response to climate change

The results of the greenhouse gas emissions under climate change scenarios demonstrate that saplings can serve as conduits for soil-derived trace gases into the atmosphere, whether before, during and after waterlogging and that the quantity of gases may be specie-specific. These differences may be associated species-specific differences in vegetation height and biomass (Joabsson et al. 1999), carbon allocation (Ström et al. 2012), assimilation (Whiting and Chanton 1996), plant-root-microbial consortium (Huang et al. 2014) and CH_4 oxidation capacity (King 1994). Our results of chapter 3 and 4 demonstrate that vegetation height and biomass and well as root anatomy may be critical due to the differences in size and composition which may be linked to significant increases in greenhouse gas production and emissions.

Additionally, the varying changes in greenhouse gas emission rates in response to waterlogging (Figure 5.4B, 5.5B and 5.10), agree with findings from previous studies which showed that such differences can be attributed to distinct microbial communities (McElrone et al. 2004; Larson and Funk 2016; Girkin et al. 2018; Zhou et al. 2019). For instance, the transport of O_2 via a wetland vegetation has shown to enrich O_2 in the rhizosphere, thereby stimulating below-ground CH_4 oxidation and suppressing methanogenesis in the process (Whiting and Chanton 1996). Similarly, the decrease in CH_4 emissions after wetland vegetation removal has been reported in numerous studies and the emission response is overall consistent between studies; reports of a reduction in CH_4 emissions in the presence of wetland vegetation have also been made, and in both cases, the magnitude varied both within and between studies (Dinsmore et al. 2009; van Winden et al. 2012).

Moreover, significant changes in CH_4 emission from species and waterlogging treatment were observed (Figure 5.4A and B), mostly likely driven by water-table depths which affect the degree of anaerobic conditions and the depth of aerobic layer, thus the ratio of CH_4 production and oxidation (Joabsson et al. 1999). In chapter 5, I provide evidence that waterlogging enhancing and promoting the production of CH_4 is species-specific which is as a result of different trees ability to alter assimilation, growth and root distribution, and consequently affect methanogenesis and CH_4 transport (Vann and Megonigal 2003).

6.6 Implications for future research

This study sheds light on the physiological, morphological, and anatomical adaptations as well as the greenhouse gas production of temperate trees to climate change. Chapter 3, which showed how increased in temperature, CO_2 and waterlogging in combination or alone can modify tree adaptation, has implications for future studies investigating physiological, morphological, and anatomical changes under different tree types, as it highlights significant

species-specific effects. Additionally, results from chapter 4 adopted a new technique by (Atkinson and Wells 2017) which presented an updated method to provide rapid and high-quality cross-sections of plant tissues which were often time consuming and difficult to conduct. To my knowledge, this study was the first to adopt this technique on tree sapling roots. The technique for quantification of tissue and cellular structure of plant material therefore has the possibility to be more extensively used in assessing morphological and anatomical changes in stems and leaves, with potential applications including investigating changes in leaves and stems under climate change scenarios, investigating more specie-specific differences from different tree species and assessing the impacts of establishment, distribution, and survival of trees species.

Chapter 4 showed that increased temperature, CO_2, and waterlogging can significantly enhance root anatomical traits of tree saplings, but the effects were species-specific, further studies on anatomical traits should investigate these changes across various ecosystems and how these vary with tree development stage. Moreover, much remains to be known about the species-specific differences in stem structure (e.g., aerenchyma content) and stem tissue composition and their effect on water-related leaf physiological traits.

Chapter 5 demonstrated that under future CO_2 conditions, CO_2 fluxes are expected to be impacted more than CH_4 under flooding while CH_4 fluxes are expected to be more strongly impacted than CO_2 fluxes under higher temperatures, but that responses may differ substantially among species. Having demonstrated this important observation, further assessment is needed, however, to explore the interactions between the flux magnitudes and soil structure, redox potential in the rooting zone, stem diameter and wood specific density (Maier et al. 2018).

Finally, as growth rooms generally provide more consistent plant growth and development future studies should assess the extent to which elevated temperature, CO_2 and waterlogging have on these species on field experiment with longer term studies and matured trees.

Appendix A

Table A 1: Statistical analysis summary of the main effects and interactions of species, temperature, CO_2, and waterlogging

	Temperature (Experiment 1)			**CO_2 (Experiment 2)**		
Parameters	**Treatment effects *(P)***			**Treatment effects *(P)***		
	Temperature	**Waterlogging**	**T × W**	**CO_2**	**Waterlogging**	**CO_2 × W**
Alnus glutinosa						
SPAD	0.905	0.818	0.868	0.26	**<0.001**	0.941
Chlorophyll fluorescence	0.717	0.281	0.31	0.463	**<0.001**	0.964
Stem height (cm)	**<0.001**	**0.009**	0.524	**<0.001**	**<0.001**	**<0.001**
Stem diameter (mm)	-	-	-	0.224	**<0.001**	0.86
Dry root biomass (g)	**<0.001**	0.551	0.138	0.714	0.416	0.085
Transpiration *E* (mol $m^{-2}s^{-1}$)	**0.006**	**<0.001**	0.126	0.069	0.904	0.42
Photosynthesis CO_2 assimilation *A* ($\mu mol^{-2}s^{-1}$)	**0.002**	**<0.001**	0.129	0.096	0.012	0.89
Stomatal conductance *gs* (m mol $m^{-2}s^{-1}$)	**<0.001**	0.033	0.167	0.125	0.532	0.474
Water use efficiency (*A/E*)	0.375	0.301	0.33	0.357	**0.018**	0.9
Betula pendula						
SPAD	0.351	**<0.001**	0.963	**0.003**	0.419	0.239
Chlorophyll fluorescence	0.634	**<0.001**	0.944	0.518	0.018	0.302
Stem height (cm)	0.128	0.038	0.175	0.653	**<0.001**	0.366
Stem diameter (mm)	-	-	-	0.124	**<0.001**	0.138
Dry root biomass (g)	0.06	0.192	0.634	**<0.001**	0.331	0.226
Transpiration *E* (mol $m^{-2}s^{-1}$)	**0.001**	**<0.001**	0.433	0.825	0.276	0.861
Photosynthesis CO_2 assimilation *A* ($\mu mol^{-2}s^{-1}$)	0.046	**<0.001**	0.620	0.915	**<0.001**	0.442
Stomatal conductance *gs* (m mol $m^{-2}s^{-1}$)	0.148	**<0.001**	0.956	0.537	**0.05**	0.857
Water use efficiency (*A/E*)	0.283	0.249	0.3	0.877	**<0.001**	0.474
Betula pubescens						
SPAD	0.586	**0.006**	0.531	**<0.001**	**<0.001**	0.535

Chlorophyll fluorescence	0.546	**0.003**	0.798	0.167	**0.002**	0.254
Stem height (cm)	0.569	0.099	0.027	0.647	**<0.001**	0.633
Stem diameter	-	-	-	0.553	**<0.001**	0.181
Dry root biomass (g)	0.781	0.197	0.35	**0.008**	0.615	0.764
Transpiration *E* (mol $m^{-2}s^{-1}$)	0.191	**<0.001**	0.39	0.276	0.013	0.22
Photosynthesis CO_2 assimilation *A* ($\mu mol^{-2}s^{-1}$)	0.513	**<0.001**	0.506	0.178	**<0.001**	0.075
Stomatal conductance *gs* (m mol $m^{-2}s^{-1}$)	0.365	**<0.001**	0.836	0.256	0.005	0.149
Water use efficiency (*A/E*)	0.712	**<0.001**	0.364	0.557	**<0.001**	0.427
Salix pentandra/ Salix aurita						
SPAD	0.168	**<0.001**	0.162	**<0.001**	0.09	**<0.001**
Chlorophyll fluorescence	0.259	**<0.001**	0.81	**0.003**	**<0.001**	0.018
Stem height (cm)	**0.001**	0.71	0.437	**0.002**	**<0.001**	**<0.001**
Stem diameter	-	-	-	0.331	**<0.001**	0.763
Dry root biomass (g)	**<0.001**	0.695	0.373	0.665	0.329	0.557
Transpiration *E* (mol $m^{-2}s^{-1}$)	0.087	**<0.001**	**0.004**	0.261	**<0.001**	0.495
Photosynthesis CO_2 assimilation *A* ($\mu mol^{-2}s^{-1}$)	0.012	**<0.001**	0.397	0.52	**<0.001**	0.187
Stomatal conductance *gs* (m mol $m^{-2}s^{-1}$)	0.791	**<0.001**	0.153	0.295	**<0.001**	0.583
Water use efficiency (*A/E*)	0.276	**0.013**	0.22	0.256	**0.005**	0.149

Table A 2: Mean and standard error of means (in parentheses) of measured SPAD, chlorophyll fluorescens, stem height and diameter, root biomass and leaf gas exchange for each combination of ambient or elevated temperature and ambient or elevated CO_2 and waterlogging treatments

	Temperature (Experiment 1)						CO2 (Experiment 2)							
	Control		Waterlogging		After waterlogging		Control		Waterlogging		After waterlogging		Significant effect	
	aT	**eT**	**aT**	**eT**	**aT**	**eT**	**aCO_2**	**eCO_2**	**aCO_2**	**eCO_2**	**aCo_2**	**eCO_2**	**Temperature**	**CO_2**
Alnus glutinosa														
SPAD	55.94 (2.044)	55.24 (2.324)	55.24 (2.324)	55.08 (3.032)	-	-	32.26 (0.847)	30.65 (0.654)	41.43 (1.853)	39.55 (2.918)	-	-	NS	W
Chlorophyll fluorescence	0.78 (0.004)	0.74 (0.16)	0.72 (0.05)	0.73 (0.015)	-	-	0.715 (0.008)	0.73 (0.009)	0.65 (0.02)	0.68 (0.028)	-	-	NS	W
Stem height (cm)	35.35 (2.429)	42.03 (2.745)	42.67 (2.981)	54.11 (5.284)	-	-	18.54 (0.824)	16.47 (0.653)	-	-	40.86 (2.608)	63.31 (5.21)	T & W	C & W
Stem diameter (mm)	-	-	-	-	-	-	3.836 (0.18)	3.432 (0.0791)	-	-	7.769 (0.4012)	7.266 (0.388)	-	W
Dry root biomass (g)	82.83 (3.1)	103.29 (4.0)	93.24 (5.08)	96.54 (3.9)	-	-	20.65 (3.2)	-	-	25.22 (5.1)	26.04 (4.8)	15.85 (3.2)	T	NS
Transpiration E (mol $m^{-2}s^{-1}$)	4.808 (0.19)	4.102 (0.62)	3.34 (0.6)	1.207 (0.5)	2.618 (0.432)	2.694 (0.454)	0.4766 (0.21)	2.618 (0.4328)	2.694 (0.4545)	1.1245 (0.31)	0.6874 (0.23)	0.9685 (0.15)	T & W	NS
Photosynthesis A (µmol$^{-2}s^{-1}$)	14.47 (1.026)	12.54 (1.44)	10.35 (1.32)	4.32 (1.51)	7.485 (0.742)	8.142 (1.245)	2.1 (1.02)	7.485 (0.7422)	8.142 (1.24)	4.477 (1.29)	4.78 (0.90)	6.90 (1.02)	T & W	NS
Stomatal conductance gs (m mol $m^{-2}s^{-1}$)	0.37 (0.038)	0.27 (0.05)	0.339 (0.051)	0.115 (0.047)	0.2536 (0.045)	0.2552 (0.5035)	0.036 (0.017)	0.2536 (0.046)	0.2552 (0.501)	0.085 (0.023)	0.062 (0.03)	0.084 (0.015)	T & W	W
Betula pendula														
SPAD	47.97 (2.15)	49.81 (1.10)	35.27 (2.11)	37.3 (2.39)	-	-	29.81 (1.06)	25.86 (0.82)	32.89 (1.44)	25.28 (2.55)	-	-	W	C
Chlorophyll fluorescence	0.77 (0.003)	0.744 (0.0093)	0.52 (0.078)	0.48 (0.074)	-	-	0.70 (0.008)	0.72 (0.011)	0.64 (0.041)	0.59 (0.061)	-	-	W	W
Stem height (cm)	56.32 (2.847)	58.08 (4.186)	58.87 (3.498)	70.18 (3.872)			29.98 (2.257)	28.56 (2.135)			52.42 (4.255)	57.38 (4.871)	W	W
Stem diameter (mm)	-	-	-	-	-	-	2.957 (0.1991)	2.923 (0.2038)	-	-	7.91 (0.676)	6.646 (0.3922)	-	W

Dry root biomass (g)	87.81 (1.85)	106.96 (5.52)	93.98 (5.45)	117.98 (16.95)	-	-	27.76 (1.34)	-	-	14.8 (3.12)	16.25 (3.28)	12.28 (4.27)	NS	C
Transpiration E (mol $m^{-2}s^{-1}$)	3.308 (0.498)	4.284 (0.516)	0.887 (0.265)	1.16 (0.362)	0.214 (0.074)	0.728 (0.315)	0.5972 (0.182)	0.214 (0.0074)	0.728 (0.3155)	0.4998 (0.162)	0.7779 (0.118)	0.7647 (0.049)	T & W	NS
Photosynthesis A (µmol$^{-2}s^{-1}$)	8.272 (1.27)	10.555 (0.93)	2.992 (0.80)	4.181 (1.21)	0.775 (0.304)	2.457 (0.724)	3.594 (0.85)	0.775 (0.3046)	2.457 (0.724)	3.124 (0.88)	6.344 (0.67)	6.987 (0.46)	T & W	W
Stomatal conductance gs (m mol $m^{-2}s^{-1}$)	0.2454 (0.044)	0.2808 (0.036)	0.0801 (0.025)	0.1112 (0.038)	0.0177 (0.006)	0.0675 (0.032)	0.05152 (0.012)	0.0177 (0.006)	0.0675 (0.032)	0.0415 (0.013)	0.0696 (0.010)	0.0632 (0.004)	T & W	W
Betula pubescens														
SPAD	45.65 (1.87)	48.11 (1.41)	41.23 (1.44)	41.1 (3.090)	-	-	35.5 (1.65)	30.67 (1.01)	45.95 (2.41)	38.68 (2.09)	-	-	W	C & W
Chlorophyll fluorescence	0.7683 (0.003)	0.7483 (0.008)	0.6725 (0.038)	0.6675 (0.040)	-	-	0.7367 (0.008)	0.7317 (0.0090)	0.7033 (0.022)	0.6608 (0.021)	-	-	W	W
Stem height (cm)	48.28 (4.248)	59.66 (3.449)	61.58 (4.963)	57.73 (3.219)	-	-	28.23 (1.534)	28.59 (1.077)	-	-	66.72 (3.207)	63.84 (5.462)	NS	W
Stem diameter	-	-	-	-	-	-	3.056 (0.1262)	2.923 (0.2038)	-	-	5.965 (0.5175)	6.69 (0.405)	-	W
Dry root biomass (g)	81.22 (5.808)	89.2 (8.809)	79.24 (2.91)	78.21 (2.963)	-	-	19.97 (2.41)	-	-	12.76 (2.75)	17.7 (2.95)	11.67 (0.93)	NS	C
Transpiration E (mol $m^{-2}s^{-1}$)	4.211 (0.448)	1.214 (0.332)	5.463 (0.50)	1.674 (0.54)	0.67 (0.164)	0.849 (0.358)	0.7241 (0.112)	0.67 (0.1641)	0.849 (0.3584)	0.4866 (0.174)	1.2007 (0.285)	0.4998 (0.162)	W	W
Photosynthesis A (µmol$^{-2}s^{-1}$)	11.891 (1.178)	4.141 (0.88)	12.193 (0.87)	5.713 (1.151)	2.176 (0.5022)	2.996 (1.146)	5.661 (0.644)	2.176 (0.5022)	2.996 (1.147)	2.55 (0.767)	7.953 (0.957)	2.029 (0.690)	W	W
Stomatal conductance gs (m mol $m^{-2}s^{-1}$)	0.3314 (0.039)	0.1061 (0.030)	0.3735 (0.0454)	0.166 (0.059)	0.0584 (0.014)	0.0804 (0.035)	0.05946 (0.0099)	0.0584 (0.014)	0.0804 (0.0354)	0.03697 (0.0132)	0.10665 (0.0270)	0.0364 (0.012)	T & W	W
Salix pentandra/ Salix aurita														
SPAD	51.43 (2.392)	50.66 (1.475)	43.83 (2.26)	35.13 (4.596)	-	-	33.66 (1.313)	39.49 (1.678)	32.43 (1.12)	17.68 (4.554)	-	-	W	C
Chlorophyll fluorescence	0.7417 (0.010)	0.6433 (0.0366)	0.7233 (0.0134)	0.6117 (0.035)	-	-	0.7242 (0.0033)	0.6617 (0.0312)	0.7558 (0.0075)	0.4175 (0.1067)	-	-	W	C & W
Stem height (cm)	43.49 (1.314)	54.82 (2.377)	42.63 (1.73)	57.26 (3.761)	-	-	43.48 (2.107)	40.98 (1.706)	-	-	43 (1.343)	59.46 (3.186)	T	C & W
Stem diameter	-	-	-	-			3.366 (0.181)	3.163 (0.1279)	-	-	6.927 (0.2995)	6.583 (0.307)	-	W

Dry root biomass (g)	71.02 (2.266)	78.1 (0.984)	70.06 (0.901)	79.36 (1.939)			45.98 (5.233)	-	-	47.11 (15)	41.9 (13.965)	29.71 (6.722)	T	NS
Transpiration E (mol $m^{-2}s^{-1}$)	2.24 (0.239)	1.537 (0.3815)	3.874 (0.512)	0.947 (0.296)	0.743 (0.254)	0.663 (0.311)	1.5965 (0.176)	0.743 (0.2545)	0.663 (0.3117)	0.2968 (0.103)	1.717 (0.376)	0.775 (0.303)	W	W
Photosynthesis A (µmol$^{-2}s^{-1}$)	8.251 (0.619)	2.6 (1.514)	11.098 (0.914)	3.556 (1.049)	1.001 (0.444)	2.062 (1.724)	9.373 (0.695)	1.001 (2.062)	0.4443 (1.725)	1.506 (0.546)	8.713 (1.450)	3.488 (1.069)	T & W	W
Stomatal conductance gs (m mol $m^{-2}s^{-1}$)	0.2119 (0.028)	0.1413 (0.0356)	0.2521 (0.0365)	0.0868 (0.028)	0.0674 (0.024)	0.056 (0.0262)	0.14166 (0.0155)	0.0674 (0.024)	0.056 (0.026)	0.01745 (0.0070	0.15506 (0.0356)	0.0556 (0.022)	T & W	W

Table A 3: Monthly temperatures for growthrooms during the span of the experiment. Temperatures were obtained and calculated from the daily weather report database recorded by the Sutton Bonington Meteorological station.

Month	Ambient temperature (°C)	Elevated temperature (°C)
March	Day: 9.4 Night: 5.0	Day: 11.3 Night: 5.8
April	Day: 14.7 Night: 10.0	Day: 18.2 Night: 10.0
May	Day: 17.2 Night: 10.0	Day: 22.0 Night: 11.2
June	Day: 18.3 Night: 12.1	Day: 19.8 Night: 15.2
July	Day: 18.8 Night: 13.2	Day: 19.8 Night:15.2
August	Day: 20.6 Night: 14.8	Day: 22.7 Night: 17.0

Appendix B

Table B 1: The summary results of Mixed models (REML) analysis.

Temperature experiment

Anatomical traits	Species (S)		Temperature (eT)		Waterlogging (W)		S × eT		S × W		eT × W		S × eT ×W	
	F	*P*	*F*	*P*	*F*	*P*	*F*	*P*	*F*	*P*	*P*	*F*	*F*	*P*
RCA	10.89	**0.005**	2.02	0.198	85.87	**<0.001**	1.14	0.398	6.53	**0.019**	1.42	0.445	0.36	0.785
TSA	0.82	0.522	0.04	0.849	0	0.978	0.59	0.638	0.09	0.963	1.58	0.428	2.17	0.18
TCA	-	-	-	-	-	-	-	-	-	-	-	-	-	-
Aerenchyma area	2.22	0.174	2.27	0.176	0.01	0.925	0.82	0.524	0.28	0.84	5.87	0.249	0.79	0.536
CCFN	0.4	0.756	0.6	0.462	0.68	0.437	0.46	0.719	0.15	0.925	1.97	0.394	0.34	0.795
CCS	0.71	0.575	1.41	0.273	0.32	0.588	0.19	0.9	0.2	0.892	4.9	0.27	0.07	0.976
Leaf physiological traits														
A_{MAX}	1.75	0.244	8.56	0.022	12.71	**0.009**	0.18	0.908	1.11	0.408	20.1	0.14	0.97	0.461
E	3.19	0.093	7.38	**0.03**	24.12	**0.002**	0.35	0.788	2.82	0.117	3.61	0.308	1.11	0.407
g_s	2.57	0.137	3.75	0.094	6.76	0.035	0.34	0.795	2.72	0.125	9.92	0.196	1.01	0.443
Water use efficiency														
iWUE	3.03	0.103	0.48	0.512	1.61	0.245	2.71	0.126	2.61	0.133	0.83	0.53	1.91	0.216

CO_2 experiment

	Species (S)		Treatment (eCO_2)		Waterlogging (W)		S × eCO_2		S × W		eCO_2 × W		S × eCO_2 × W	
	F	*P*	*F*	*P*	*F*	*P*	*F*	*P*	*F*	*P*	*P*	*F*	*F*	*P*
RCA	11.56	**0.004**	14.77	**0.006**	37.94	**<0.001**	0.95	0.467	1.32	0.342	0.38	0.648	0.42	0.744
TCA	12.7	**0.003**	0.34	0.576	15.32	**0.006**	1.26	0.358	1.36	0.331	0.39	0.646	0.91	0.484
TSA	3.99	**0.06**	0.08	0.783	5.74	0.048	3.96	0.061	4.27	0.052	0	0.998	3.28	0.089
Aerenchyma area	3.97	0.061	15.14	**0.006**	23.88	**0.002**	1.06	0.425	0.64	0.613	0.04	0.869	1.91	0.216
CCFN	1.08	0.409	0	1	3.23	0.11	1.28	0.345	0.63	0.614	2.93	0.125	2.11	0.177
CCS	15.02	**0.002**	2.78	0.139	7.62	0.028	0.92	0.477	0.05	0.984	0.01	0.928	0.97	0.459
Leaf physiological traits														
A_{MAX}	2.62	0.133	3.19	0.117	16.8	**0.005**	0.38	0.768	7.05	**0.016**	0.41	0.636	7.98	**0.012**
E	0.66	0.603	3.38	0.109	0	0.997	0.65	0.608	4.56	0.045	0.07	0.833	8.58	**0.01**
g_s	5.66	**0.028**	0.01	0.919	5.91	0.045	1.42	0.315	10.65	**0.005**	0.04	0.875	4.3	0.051
Water use efficiency														
iWUE	1.72	0.25	16.97	**0.004**	16.73	**0.005**	0.07	0.975	0.41	0.751	38.87	0.101	5.26	0.033

Table B 2: Mean and standard error of means (in parentheses) of measured root anatomical and leaf physiological values of temperate saplings in control and waterlogging plots during temperature and CO_2 experiment. Abbreviations: RCA, root cortical aerenchyma; TCA, total cortical area; TSA, total stele area; AA, aerenchyma area; CCFN, cortical cell file number; CCS, cortical cell size; Amax, saturated net photosynthesis rate; E, Transpiration rate; gs, Stomatal conductance rate; iWUE, intrinsic water-use efficiency

	Temperature (Experiment 1)				**CO2 (Experiment 2)**			
	Control		Waterlogging		Control		Waterlogging	
	aT	**eT**	**aT**	**eT**	**aCO_2**	**eCO_2**	**aCO_2**	**eCO_2**
Alnus glutinosa								
RCA (%)	8.4 1.255	5.43 -	29.75 -	24.39 0.527	9.76 0.637)	12.9 -	22.17 -	33.1 (3.509)
TCA (mm^2)	0.0002212 (0.00001945)	0.000141 -	0.0001365 -	0.0001724 (0.00002719)	0.0002212 (0.00001945)	0.0001412 -	0.0004511 -	0.0004841 (0.00008499)
TSA (mm^2)	1.0551 (0.2653)	0.8226 -	0.9348 -	1.2039 (0.0796)	1.184 0.4787	0.806 -	0.726 -	1.391 0.3331
AA (mm^2)	0.808 (0.1573)	1.659 -	1.676 -	0.806 (0.0346)	0.732 (0.0536)	2.783 -	1.58 -	1.134 (0.1444)
CCFN	11.5 (0.5)	16 -	11 -	11 (1)	9 (0)	10 -	16 -	14 (1)
CCS (mm^2)	1.856 1.3591	2.86 -	4.282 -	4.168 -	0.804 (0.161)	2.007 -	0.581 -	1.068 (0.1747)
A_{max} (µ mol $m^{-2}s^{-1}$)	12.038 (1.555)	16.328 -	14.44 -	4.985 (1.929)	9.276 (1.7249)	4.159 -	4.987 -	8.078 (1.0771)
E (m mol $m^{-2}s^{-1}$)	4.096 (0.2117)	6.188 -	4.596 -	2.16 (0.123)	0.985 (0.0641)	0.461 -	0.611 -	1.614 (0.06038)
gs (m mol $m^{-2}s^{-1}$)	0.2591 (0.03649)	0.4373 -	0.4486 -	0.2117 (0.020839)	0.08917 (0.02248)	0.0384 -	0.0428 -	0.12072 (0.05242)
iWUE (µ mol m mol^{-1})	2.927 (0.2284)	2.638 -	3.142 -	1.92 (0.3948)	9.339 (1.1428)	9.014 -	8.161 -	5.528 (1.4006)
Betula pendula								
RCA (%)	0 0	1.15 -	19.31 -	17.33 (1.507)	4.99 (0.462)	2.89 -	18.21 -	24.22 (4.073)
TCA (mm^2)	0.0002099	0.0002018	0.0001415	0.0003119	0.0001353	0.0002018	0.0001441	0.000281

	(0.00007244	-	-	(0.00006666)	(0.00000213)	-	-	(0.00005791)
TSA (mm^2)	1.1465 (0.3064)	1.2855 -	2.4345 -	0.5788 (0.1232)	0.668 0.021	0.736 -	- -	0.626 (0.0324)
AA (mm^2)	0 0	1.147 -	2.27 -	0.148 (0.1484)	0.551 (0.5507)	0.552 -	1.488 -	1.067 (0.3436)
CCFN	14 (2)	11 -	13 -	13 (3)	15.5 (1.7)	5 -	8 -	14.5 (1.5)
CCS (mm^2)	2.455 (0.8443)	3.215 -	4.168 -	1.536 (0.6096)	0.803 (0.4131)	0.724 -	2.604 -	0.981 (0.0648)
A_{max} (µ mol $m^{-2}s^{-1}$)	11.238 (3.037)	10.145 -	12.915 -	3.289 (1.323)	7.595 0.1038	5.339 -	5.156 -	7.507 (0.211)
E (m mol $m^{-2}s^{-1}$)	4.716 (0.3772)	4.048 -	3.71 -	0.995 (0.1829)	0.783 (0.0578)	0.672 -	0.874 -	1.541 (0.2502)
gs (m mol $m^{-2}s^{-1}$)	0.2964 (0.06333)	0.2724 -	0.4159 -	0.0929 (0.00919)	0.06546 (0.00601)	0.04905 -	0.07865 -	0.11595 (0.0146)
iWUE (µ mol m mol^{-1})	2.35 (0.1568)	2.506 -	3.482 -	0.246 (0.0966)	9.769 (0.8542)	7.945 -	5.9 -	4.982 (0.67230
Betula pubescens								
RCA (%)	0 0	1.59 -	19.55 -	11.72 (0.921)	2.13 (2.129)	10.77 -	25.14 -	28.18 (4.053)
TCA (mm^2)	0.000343 (0.00009729	0.0003512 -	0.0001541 -	0.0003011 (0.00005927)	0.0003383 (0.0000365)	0.0003407 -	0.0005541 -	0.0004375 (0.00007718)
TSA (mm^2)	0.9266 (0.4005)	0 -	0 -	0.6579 (0.0577)	1.885 (0.0086)	0.658 -	1.827 -	2.367 (0.0515)
AA (mm^2)	0 0	0.296 -	0 -	0.54 (0.5398)	0.383 (0.3833)	0.682 -	0.644 -	1.703 (0.5135)
CCFN	15 0	15 -	12 -	15 3	15 (2)	9 -	17 -	14 (2)
CCS (mm^2)	1.146 (0.1422)	0.806 -	4.295 -	1.254 (0.98)	0.483 (0.3404)	0.351 -	0.315 -	0.893 (0.2321)
A_{max} (µ mol $m^{-2}s^{-1}$)	12.767 (1.555)	14.5 -	2.881 -	1.982 (0.995)	6.263 (1.2395)	7.284 -	5.399 -	3.765 (0.8536)
E (m mol $m^{-2}s^{-1}$)	5.553 (0.3411)	7.193 -	0.577 -	0.247 (0.1153)	0.538 (0.0565)	1.576 -	1.379 -	0.517 (0.1237)
gs (m mol $m^{-2}s^{-1}$)	0.379 (0.03455)	0.5222 -	0.0467 -	0.0208 (0.00956)	0.0465 (0.00479)	0.14714 -	0.11222 -	0.03651 (0.006990
iWUE (µ mol m mol^{-1})	2.291 (0.1393)	2.016 -	4.993 -	7.877 (0.3504)	11.521 (1.0944)	4.621 -	3.914 -	7.307 (0.0973)

Salix pentandra/ Salix aurita								
RCA (%)	6.25 (2.245)	4.22 -	9.9 -	6.32 (2.458)	28.16 (2.833)	26.61 -	32.98 -	35.93 (3.694)
TCA (mm^2)	0.000289 (0.00000072)	0.000132 -	0.0006197 -	0.0001594 (0.00003967)	0.0005697 (0.00014848)	0.0002824 -	0.0006122 -	0.0006008 (0.00007795)
TSA (mm^2)	0.232 (0.232)	1.253 -	0.1713 -	0.9335 (0.9335)	1.1 (0.0001)	5.415 -	0.849 -	1.197 (0.2927_
AA (mm^2)	0.625 (0.6245)	4.055 -	0.299 -	2.515 (1.3506)	0.351 (0.0414)	0.757 -	0.545 -	1.065 (0.2592)
CCFN	11.5 (2.5)	14 -	5 -	14.5 (1.5)	9 (1)	11 -	8 -	13 (2)
CCS (mm^2)	1.989 (0.6131)	3.005 -	1.365 -	2.711 (1.9156)	1.009 (0.0708)	2.297 -	1.447 -	1.112 (0.0744)
A_{max} (µ mol $m^{-2}s^{-1}$)	11.112 (1.956)	6.425 -	3.044 -	0.578 (0.572)	8.833 (0.9806)	11.511 -	4.882 -	3.427 (1.1403)
E (m mol $m^{-2}s^{-1}$)	3.305 (0.5035)	1.49 -	0.472 -	0.268 (0.1454)	1.133 (0.0203)	1.897 -	0.824 -	0.691 (0.1297)
gs (m mol $m^{-2}s^{-1}$)	0.2171 (0.05623)	0.089 -	0.0396 _	0.0236 (0.014120	0.23115 (0.01029)	0.27331 -	0.07111 -	0.04783 (0.00861)
iWUE (µ mol m mol^{-1})	3.342 (0.0819)	4.312 -	6.448 -	1.414 (0.3659)	7.78 (0.7259)	6.067 -	5.926 -	4.817 (0.7458)

Table B 3: The results of linear regression showing the regression relationship between response values of leaf physiological traits to the interactive effect of waterlogging and temperature or CO_2 with root anatomical traits in control plots among temperate tree species. The bolds and italics indicating a significant and marginally significant regression relationship between the response values of leaf physiological traits to interactive effect of waterlogging and temperature or CO_2 with root anatomical traits in control plots, respectively.

Temperate experiment

Response value	RCA		TSA		TCA		AA		CCFN		CCS	
	R^2	*P*	R^2	*P*	R^2	*P*	R^2	*P*	R^2	*P*	R^2	*P*
A	-	0.501	-	0.782	-	0.872	-	0.525	2.6	0.282	-	0.769
gs	-	0.501	-	0.721	-	0.499	9.5	0.173	9.6	0.172	-	0.681
E	-	0.601	-	0.904	-	0.502	13.3	0.132	11.2	0.153	-	0.604
iWUE	13.2	0.134	-	0.533	13.2	0.132	49.6	***0.006***	-	0.579	-	0.428
CO_2 experiment												
A	21.6	***0.071***	-	0.612	0.6	0.326	-	0.869	-	0.598	23.0	***0.065***
gs	64.4	***0.001***	15.5	0.113	45.4	***0.010***	0.6	0.326	-	0.408	73.8	***<0.001***
E	35.5	***0.024***	-	0.458	-	0.346	-	0.551	-	0.443	18.9	***0.088***
iWUE	19.3	***0.086***	-	0.346	-	0.609	-	0.479	-	0.349	-	0.402

Table B 4: The results of REML variance analysis showing specie-specific effect of elevated temperature or elevated CO_2 on root anatomical traits, leaf physiological traits and water use efficiency among the four temperate tree species. The bold numbers indicate a significant difference among the four species.

Temperature experiment

Response value	*A. glutinosa* eT		*B. pendula* eT		*B. pubescens* eT		*S. pentandra* eT		*S. aurita*	
	F	*P*	*F*	*P*	*F*	*P*	*F*	*P*	*F*	*P*
RCA	18.45	***<0.001***	19.97	***<0.001***	5.89	***0.015***	0.07	0.796		
TSA			14.72	***<0.001***	48.04	***<0.001***	0.23	0.632		
TCA							57.01	***<0.001***		
AA			0.03	0.871	1.07	0.301	18.13	***<0.001***		
CCFN					0.04	0.838				
CCS	1.34	0.246	0.02	0.898	1.66	0.197				
Amax	0.59	0.442			52.58	***<0.001***	4.19	***0.041***		
gs					52.21	***<0.001***	3.84	***0.05***		
E	0.16	0.69			15.49	***<0.001***	4.73	***0.03***		
iWUE					251.14	***<0.001***	2.86	***0.091***		
CO_2 experiment										
	eCO_2		eCO_2		eCO_2				eCO_2	
RCA	8.00	***<0.001***	1.2	0.273					18.91	***<0.001***
TSA	1.74	0.187	15.39	***<0.001***						
TCA	1.81	0.179	5.63	***0.018***					2.4	0.122
AA	53.79	***<0.001***	9.28	***0.002***					3.89	***0.049***
CCFN	2.67	0.102	1.04	0.307	4.17	0.041			1.26	0.262
CCS	111.35	***<0.001***	4.99	***0.025***	1.48	0.223			0.17	0.679
Amax	4.13	***0.042***							114.37	***<0.001***
gs	0.64	0.424	11.51	***<0.001***					1.18	0.276
E	0.7	0.402	7.77	***0.005***					0.5	0.48
iWUE			285.48	***<0.001***	10	***0.002***			13976.33	***<0.001***

Table B 5: The results of REML variance analysis showing specie-specific effect of waterlogging on root anatomical traits, leaf physiological traits and water use efficiency among the four temperate tree species. The bold numbers indicate a significant difference among the four species

Temperature experiment

Response value	*A. glutinosa* W		*B. pendula* W		*B. pubescens* W		*S. pentandra* W		*S. aurita*	
	F	*P*	*F*	*P*	*F*	*P*	*F*	*P*	*F*	*P*
RCA	1022.74	***<0.001***	184.82	***<0.001***	345.65	***<0.001***	0.15	0.703		
TSA			1.42	0.233	24.02	***<0.001***	0.02	0.892		
TCA							26.2	***<0.001***		
AA			2.25	0.133	0.07	0.788	2.63	0.105		
CCFN					0.08	0.733				
CCS	0.01	0.941	0.24	0.622	1.36	0.244				
Amax	0.63	0.426			533.12	***<0.001***	5.18	***0.023***		
gs					371.06	***<0.001***	3.97	***0.046***		
E	0.76	0.383			929.24	***<0.001***	6.09	***0.014***		
iWUE					548.46	***<0.001***	0.01	0.934		
CO_2 experiment										
	W		W		W				W	
RCA	63.28	***<0.001***	5.37	***0.021***					90.1	***<0.001***
TSA	64.14	***<0.001***	0.05	0.819						
TCA	25.47	***<0.001***	0.72	0.397					8.73	***0.003***
AA	278.41	***<0.001***	18.81	***<0.001***					4.13	***0.042***
CCFN	40.33	***<0.001***	0.33	0.564	4.08	0.043			0.02	0.885
CCS	45.56	***<0.001***	123.85	***<0.001***	1.5	0.22			10.26	***0.001***
Amax	0.11	*0.742*							1893.39	***<0.001***
gs	0.48	0.488	28.96	***<0.001***					13.02	***<0.001***
E	0.69	0.405	8.29	***0.004***					63.98	***<0.001***
iWUE			470.38	***<0.001***	8.12	***0.004***			8051.91	***<0.001***

Appendix C

Table C 1: Linear mixed effects models assessing differences CH_4 and CO_2

CO_2 experiment (NEE-tree static chamber)									
	Control			**Waterlogging**			**After waterlogging**		
LogCH_4	**F- statistic**	**d.f.**	**P**	**F- statistic**	**d.f.**	**P**	**F- statistic**	**d.f.**	**P**
Species	0.99	48	0.404	2.46	59.2	0.071	1.86	15.4	0.188
Treatment	1.64	48	0.206	1.61	5.6	0.255	2.78	2.9	0.196
Waterlogging treatment				2	59.7	0.163	3.03	16.8	0.1
Species*Treatment	0.53	48	0.665	1.18	59.4	0.327	0.62	15.5	0.549
Species*Waterlogging treatment				1.14	60.4	0.34	0.49	15.5	0.622
Treatment*Waterlogging treatment				0.08	59.4	0.779	0.53	16	0.478
Species*Treatment*Waterlogging treatment				0.6	60.6	0.615	0	15.2	0.952
LogCO_2									
Species	0.11	52.2	0.956	3.09	66	0.033	0.42	61.9	0.74
Treatment	0.44	7.1	0.528	17.61	3.5	0.018	0.31	6	0.6
Waterlogging treatment	0.58	52.8	0.628	0.37	16.6	0.553	2.85	60.9	0.096
Species*Treatment				0.87	52	0.465	0.38	62.4	0.767
Species*Waterlogging treatment				1.4	46	0.254	1.36	64	0.263
Treatment*Waterlogging treatment				2.13	68	0.149	2.81	61.2	0.099
Species*Treatment*Waterlogging treatment				1.27	46.2	0.297	0.39	63.5	0.758
CO_2 experiment (Soil-flux static chamber)									
LogCH_4									
Species	1.55	15.5	0.24	0.12	33	0.948	0.09	39.9	0.966
Treatment	0.05	4.2	0.834	0.11	32.7	0.747	0.09	40.4	0.767

Waterlogging treatment	4.69	16.7	0.015	0.06	4.1	0.821	1.81	5.2	0.234
Species*Treatment				2.12	33.8	0.116	0.58	41	0.63
Species*Waterlogging treatment				0.55	33.4	0.651	0.52	40.4	0.674
Treatment*Waterlogging treatment				0.88	30.3	0.355	0.36	40.4	0.551
Species*Treatment*Waterlogging treatment				1.29	33.6	0.263	0.58	41.5	0.633
LogCO_2									
Species	3.15	55	0.032	0.65	50.4	0.588	1.53	64.1	0.214
Treatment	1.31	5.6	0.299	1.69	52.6	0.199	0.88	64.8	0.352
Waterlogging treatment	0.22	55.4	0.883	5	5.5	0.07	1.49	5.8	0.269
Species*Treatment				0.38	51.9	0.77	1.8	65.3	0.156
Species*Waterlogging treatment				2.21	50.4	0.098	2.17	64.2	0.1
Treatment*Waterlogging treatment				0.65	53.1	0.424	4.69	64.8	0.034
Species*Treatment*Waterlogging treatment				0.5	52.2	0.681	0.74	65.5	0.53
Temperature experiment (NEE-tree static chamber)									
LogCH_4									
Species	0.66	52.1	0.578	4.63	61.6	0.005	1.5	18.8	0.249
Treatment	0.07	5	0.801	0.04	6	0.84	0.15	4.1	0.718
Waterlogging treatment	0.89	52.2	0.45	4.62	61.6	0.036	1.5	17.5	0.237
Species*Treatment				0.29	61.6	0.831	0.65	18.8	0.532
Species*Waterlogging treatment				0.91	62.4	0.439	0.34	20.4	0.714
Treatment*Waterlogging treatment				0.49	61.6	0.489	0.51	17.6	0.483
Species*Treatment*Waterlogging treatment				1.04	62.4	0.383	0.69	20.8	0.514
LogCO_2									
Species	1.24	65.5	0.301	0.91	63.1	0.443	4.74	57.3	0.005
Treatment	2.23	5.8	0.188	0.57	5.5	0.479	1.66	5.8	0.247
Waterlogging treatment	0.85	65.7	0.473	0.03	63.2	0.86	0.04	58.6	0.841

Species*Treatment	1.2	63.1	0.315	2.91	57.4	0.042
Species*Waterlogging treatment	0.33	64.6	0.801	0.32	58.8	0.813
Treatment*Waterlogging treatment	0	63.2	0.999	0.01	58.8	0.923
Species*Treatment*Waterlogging treatment	0.24	64.6	0.87	0.4	58.9	0.757

References

Abo Gamar MI, Dixon SL, Qaderi MM (2021) Single and interactive effects of temperature, carbon dioxide and watering regime on plant growth and reproductive yield of two genotypes of Arabidopsis thaliana. Acta Physiol Plant 43:1–16. https://doi.org/10.1007/s11738-021-03299-x

Addo-Danso SD, Prescott CE, Smith AR (2016) Methods for estimating root biomass and production in forest and woodland ecosystem carbon studies: A review. For Ecol Manage 359:332–351. https://doi.org/10.1016/j.foreco.2015.08.015

Aerts R, Cornelissen JHC, Dorrepaal E (2006) Plant performance in a warmer world: General responses of plants from cold, northern biomes and the importance of winter and spring events. Plant Ecol 182:65–77. https://doi.org/10.1007/s11258-005-9031-1

Ainsworth EA, Rogers A (2007) The response of photosynthesis and stomatal conductance to rising [CO 2]: Mechanisms and environmental interactions. Plant, Cell Environ 30:258–270. https://doi.org/10.1111/j.1365-3040.2007.01641.x

Al-Deeb T, Abo Gamar M, Khaleel S, et al (2023) Individual and Interactive Ecophysiological Effect of Temperature, Watering Regime and Abscisic Acid on the Growth and Development of Tomato Seedlings. Agronomy 13:. https://doi.org/10.3390/agronomy13030930

Alskaf K, Mooney SJ, Sparkes DL, et al (2021) Short-term impacts of different tillage practices and plant residue retention on soil physical properties and greenhouse gas emissions. Soil Tillage Res 206:. https://doi.org/10.1016/j.still.2020.104803

Arenque BC, Grandis A, Pocius O, et al (2014) Responses of senna reticulata, a legume tree from the amazonian floodplains, to elevated atmospheric co2 concentration and waterlogging. Trees - Struct Funct 28:1021–1034. https://doi.org/10.1007/s00468-014-1015-0

Armstrong W, Webb T (1985) A critical oxygen pressure for root extension in rice. J Exp Bot 36:1573–1582. https://doi.org/10.1093/jxb/36.10.1573

Armstrong W, Webb T, Darwent M, Beckett PM (2009) Measuring and interpreting respiratory critical oxygen pressures in roots. Ann Bot 103:281–293. https://doi.org/10.1093/aob/mcn177

Ashraf M, Harris PJC (2013) Photosynthesis under stressful environments: An overview. Photosynthetica 51:163–190. https://doi.org/10.1007/s11099-013-0021-6

Atkinson JA, Wells DM (2017) An updated protocol for high throughput plant tissue sectioning. Front Plant Sci 8:1–8. https://doi.org/10.3389/fpls.2017.01721

Aubrey DP, Teskey RO (2009) Root-derived CO2 efflux via xylem stream rivals soil CO 2 efflux. New Phytol 184:35–40. https://doi.org/10.1111/j.1469-8137.2009.02971.x

Bader MKF, Siegwolf R, Körner C (2010) Sustained enhancement of photosynthesis in mature deciduous forest trees after 8 years of free air CO2 enrichment. Planta 232:1115–1125. https://doi.org/10.1007/s00425-010-1240-8

Bai W, Wan S, Niu S, et al (2010) Increased temperature and precipitation interact to affect

root production, mortality, and turnover in a temperate steppe: Implications for ecosystem C cycling. Glob Chang Biol 16:1306–1316. https://doi.org/10.1111/j.1365-2486.2009.02019.x

Bailey-Serres J, Fukao T, Gibbs DJ, et al (2012) Making sense of low oxygen sensing. Trends Plant Sci 17:129–138. https://doi.org/10.1016/j.tplants.2011.12.004

Bailey-Serres J, Voesenek LACJ (2008) Flooding stress: Acclimations and genetic diversity. Annu Rev Plant Biol 59:313–339. https://doi.org/10.1146/annurev.arplant.59.032607.092752

Barba J, Bradford MA, Brewer PE, et al (2019) Methane emissions from tree stems: a new frontier in the global carbon cycle. New Phytol 222:18–28. https://doi.org/10.1111/nph.15582

Barros C, Thuiller W, Münkemüller T (2018) Drought effects on the stability of forest-grassland ecotones under gradual climate change. PLoS One 13:1–18. https://doi.org/10.1371/journal.pone.0206138

Bauweraerts I, Wertin TM, Ameye M, et al (2013) The effect of heat waves, elevated [CO2] and low soil water availability on northern red oak (Quercus rubra L.) seedlings. Glob Chang Biol 19:517–528. https://doi.org/10.1111/gcb.12044

Bertolde FZ, Almeida AAF De, Correa RX, et al (2010) Molecular, physiological and morphological analysis of waterlogging tolerance in clonal genotypes of Theobroma cacao L. Tree Physiol 30:56–67. https://doi.org/10.1093/treephys/tpp101

Bhullar GS, Edwards PJ, Olde Venterink H (2013) Variation in the plant-mediated methane transport and its importance for methane emission from intact wetland peat mesocosms. J Plant Ecol 6:298–304. https://doi.org/10.1093/jpe/rts045

Bhusal N, Kim HS, Han SG, Yoon TM (2020) Photosynthetic traits and plant–water relations of two apple cultivars grown as bi-leader trees under long-term waterlogging conditions. Environ Exp Bot 176:104111. https://doi.org/10.1016/j.envexpbot.2020.104111

Blodau C, Roulet NT, Heitmann T, et al (2007) Belowground carbon turnover in a temperate ombrotrophic bog. Global Biogeochem Cycles 21:1–12. https://doi.org/10.1029/2005GB002659

Bloom AA, Lee-Taylor J, Madronich S, et al (2010) Global methane emission estimates from ultraviolet irradiation of terrestrial plant foliage. New Phytol 187:417–425. https://doi.org/10.1111/j.1469-8137.2010.03259.x

Bokhorst S, Bjerke JW, Street LE, et al (2011) Impacts of multiple extreme winter warming events on sub-Arctic heathland: Phenology, reproduction, growth, and CO2 flux responses. Glob Chang Biol 17:2817–2830. https://doi.org/10.1111/j.1365-2486.2011.02424.x

Boulanger Y, Taylor AR, Price DT, et al (2017) Climate change impacts on forest landscapes along the Canadian southern boreal forest transition zone. Landsc Ecol 32:1415–1431. https://doi.org/10.1007/s10980-016-0421-7

Bowles AMC, Bechtold U, Paps J (2020) The Origin of Land Plants Is Rooted in Two Bursts of Genomic Novelty. Curr Biol 30:530–536. https://doi.org/10.1007/s13280-010-0083-7

Brady MA (1997) Effects of Vegetation Changes on Organic Matter Dynamics in Three

Coastal Peat Deposits in Sumatra, Indonesia. Trop Peatlands 113–134

Brix H, Sorrell BK, Orr PT (1992) Internal pressurization and convective gas flow in some emergent freshwater macrophytes. Limnol Oceanogr 37:1420–1433. https://doi.org/10.4319/lo.1992.37.7.1420

Buchel HB, Grosse W (1990) Localization of the porous partition responsible for pressurized gas transport in Alnus glutinosa (L.) Gaertn. Tree Physiol 6:247–256. https://doi.org/10.1093/treephys/6.3.247

Calleja-Cabrera J, Boter M, Oñate-Sánchez L, Pernas M (2020) Root Growth Adaptation to Climate Change in Crops. Front Plant Sci 11:. https://doi.org/10.3389/fpls.2020.00544

Carmichael MJ, Bernhardt ES, Bräuer SL, Smith WK (2014) The role of vegetation in methane flux to the atmosphere: Should vegetation be included as a distinct category in the global methane budget? Biogeochemistry 119:1–24. https://doi.org/10.1007/s10533-014-9974-1

Carmichael MJ, Smith WK (2016) Standing Dead Trees: a Conduit for the Atmospheric Flux of Greenhouse Gases from Wetlands? Wetlands 36:1183–1188. https://doi.org/10.1007/s13157-016-0845-5

Ceulemans R, Janssens IA, Jach ME (1999) Effects of CO2 enrichment on trees and forests: Lessons to be learned in view of future ecosystem studies. Ann Bot 84:577–590. https://doi.org/10.1006/anbo.1999.0945

Chanton JP, Bauer JE, Glaser PA, et al (1995) Radiocarbon evidence for the substrates supporting methane formation within northern Minnesota peatlands. Geochim Cosmochim Acta 59:3663–3668. https://doi.org/10.1016/0016-7037(95)00240-Z

Chimungu JG, Brown KM, Lynch JP (2014) Reduced root cortical cell file number improves drought tolerance in maize. Plant Physiol 166:1943–1955. https://doi.org/10.1104/pp.114.249037

Christensen JH, Christensen OB (2003) Severe summertime flooding in Europe. Nature 421:805–806. https://doi.org/10.1038/421805a

Colmer TD (2003) Aerenchyma and an inducible barrier to radial oxygen loss facilitate root aeration in upland, paddy and deep-water rice (Oryza sativa L.). Ann Bot 91:301–309. https://doi.org/10.1093/aob/mcf114

Colmer TD, Voesenek LACJ (2009a) Flooding tolerance: Suites of plant traits in variable environments. Funct Plant Biol 36:665–681. https://doi.org/10.1071/FP09144

Colmer TD, Voesenek LACJ (2009b) Flooding tolerance : suites of plant traits in variable environments. 665–681

Conrad R (2009) The global methane cycle: Recent advances in understanding the microbial processes involved. Environ Microbiol Rep 1:285–292. https://doi.org/10.1111/j.1758-2229.2009.00038.x

Covey KR, Wood SA, Warren RJ, et al (2012) Elevated methane concentrations in trees of an upland forest. Geophys Res Lett 39:1–6. https://doi.org/10.1029/2012GL052361

Crawford RMM (1992) Oxygen Availability as an Ecological Limit to Plant Distribution. Adv Ecol Res 23:93–185. https://doi.org/10.1016/S0065-2504(08)60147-6

Creed IF, Webster KL, Braun GL, et al (2013) Topographically regulated traps of dissolved organic carbon create hotspots of soil carbon dioxide efflux in forests. Biogeochemistry 112:149–164. https://doi.org/10.1007/s10533-012-9713-4

Curtis PS, Wang X (1998) A meta-analysis of elevated CO2 effects on woody plant mass, form, and physiology. Oecologia 113:299–313. https://doi.org/10.1007/s004420050381

Daly KR, Mooney SJ, Bennett MJ, et al (2015) Assessing the influence of the rhizosphere on soil hydraulic properties using X-ray computed tomography and numerical modelling. J Exp Bot 66:2305–2314. https://doi.org/10.1093/jxb/eru509

Delatorre J, Pinto M, Cardemil L (2008) Effects of water stress and high temperature on photosynthetic rates of two species of Prosopis. J Photochem Photobiol B Biol 92:67–76. https://doi.org/10.1016/j.jphotobiol.2008.04.004

Denef K, Zotarelli L, Boddey RM, Six J (2007) Microaggregate-associated carbon as a diagnostic fraction for management-induced changes in soil organic carbon in two Oxisols. Soil Biol Biochem 39:1165–1172. https://doi.org/10.1016/j.soilbio.2006.12.024

Dinsmore KJ, Skiba UM, Billett MF, et al (2009) Spatial and temporal variability in CH4 and N2O fluxes from a Scottish ombrotrophic peatland: Implications for modelling and up-scaling. Soil Biol Biochem 41:1315–1323. https://doi.org/10.1016/j.soilbio.2009.03.022

Dolman AJ, Van Der Werf GR, Van Der Molen MK, et al (2018a) Effects of Flooding On Root and Shoot Production of Bald Cypress in Large Experimental Enclosures Author (s): J . Patrick Megonigal and Frank P . Day Published by : Ecological Society of America Stable URL : http://www.jstor.org/stable/1940668 EFFECTS O. Wetlands 38:1–7. https://doi.org/10.1016/j.agee.2019.02.012

Dolman AJ, Van Der Werf GR, Van Der Molen MK, et al (2018b) Effects of Flooding On Root and Shoot Production of Bald Cypress in Large Experimental Enclosures Author (s): J . Patrick Megonigal and Frank P . Day Published by : Ecological Society of America Stable URL : http://www.jstor.org/stable/1940668 EFFECTS O. Wetlands 38:1–7. https://doi.org/10.1016/j.agee.2019.02.012

Dong X, Wang H, Gu J, et al (2015) Root morphology, histology and chemistry of nine fern species (pteridophyta) in a temperate forest. Plant Soil 393:215–227. https://doi.org/10.1007/s11104-015-2484-7

Drew MC (1997) Oxygen deficiency and root metabolism: Injury and Acclimation under Hypoxia and Anoxia. Annu Rev Plant Biol 48:223–250. https://doi.org/10.1146/annurev.arplant.48.1.223

Drew MC, He C, Morgan PW (2000a) Programmed cell death and aerenchyma formation in roots. 5:123–127

Drew MC, He CJ, Morgan PW (2000b) Programmed cell death and aerenchyma formation in roots. Trends Plant Sci 5:123–127. https://doi.org/10.1016/S1360-1385(00)01570-3

Du K, Xu L, Wu H, et al (2012) Ecophysiological and morphological adaption to soil flooding of two poplar clones differing in flood-tolerance. Flora Morphol Distrib Funct Ecol Plants 207:96–106. https://doi.org/10.1016/j.flora.2011.11.002

Duan H, Ontedhu J, Milham P, et al (2019) Effects of elevated carbon dioxide and elevated temperature on morphological, physiological and anatomical responses of Eucalyptus

tereticornis along a soil phosphorus gradient. Tree Physiol 39:1821–1837. https://doi.org/10.1093/treephys/tpz094

E . G . Barrett-Lennard (2003) The interaction between waterlogging and salinity in higher plants : causes , consequences and implications Author (s): Source : Plant and Soil , June (I) 2003 , Vol . 253 , No . 1 , Waterlogging and Salinity Tolerance : Invited papers in honour of Ha. 253:35–54

EEA (2012) Climate change, impacts and vulnerability in Europe 2012: an indicator-based report.

Ellsworth DS, Thomas R, Crous KY, et al (2012) Elevated CO 2 affects photosynthetic responses in canopy pine and subcanopy deciduous trees over 10 years: A synthesis from Duke FACE. Glob Chang Biol 18:223–242. https://doi.org/10.1111/j.1365-2486.2011.02505.x

Else MA, Hall KC, Arnold GM, et al (1995) Export of abscisic acid, 1-aminocyclopropane-1-carboxylic acid, phosphate, and nitrate from roots to shoots of flooded tomato plants: Accounting for effects of xylem sap flow rate on concentration and delivery. Plant Physiol 107:377–384. https://doi.org/10.1104/pp.107.2.377

Evans CD, Peacock M, Baird AJ, et al (2021) Overriding water table control on managed peatland greenhouse gas emissions. Nature 593:548–552. https://doi.org/10.1038/s41586-021-03523-1

Evans DE (2003) Tansley review Aerenchyma formation. New Phytol 161:35–49

FAO (2020) Global Forest Resource Assessment, 2020 Main report

Farquhar GD, Hubick KT, Condon AG, Richards RA (1989) Carbon Isotope Fractionation and Plant Water-Use Efficiency. 21–40. https://doi.org/10.1007/978-1-4612-3498-2_2

Ferner E, Rennenberg H, Kreuzwieser J (2012) Effect of flooding on C metabolism of flood-tolerant (Quercus robur) and non-tolerant (Fagus sylvatica) tree species. Tree Physiol 32:135–145. https://doi.org/10.1093/treephys/tps009

Frye J, Grosse W (1992) Growth Responses to Flooding and Recovery of Deciduous Trees. Zeitschrift fur Naturforsch - Sect C J Biosci 47:683–689. https://doi.org/10.1515/znc-1992-9-1008

Gardner A, Ellsworth DS, Crous KY, et al (2022) Is photosynthetic enhancement sustained through three years of elevated CO2exposure in 175-year-old Quercus robur? Tree Physiol 42:130–144. https://doi.org/10.1093/treephys/tpab090

Gardner A, Jiang M, Ellsworth DS, et al (2023) Optimal stomatal theory predicts CO2 responses of stomatal conductance in both gymnosperm and angiosperm trees. New Phytol 237:1229–1241. https://doi.org/10.1111/nph.18618

Garnet KN, Megonigal JP, Litchfield C, Taylor GE (2005) Physiological control of leaf methane emission from wetland plants. Aquat Bot 81:141–155. https://doi.org/10.1016/j.aquabot.2004.10.003

Gartner BL, Moore JR, Gardiner BA (2004) Gas in stems: Abundance and potential consequences for tree biomechanics. Tree Physiol 24:1239–1250. https://doi.org/10.1093/treephys/24.11.1239

Gauci V, Gowing DJG, Hornibrook ERC, et al (2010a) Woody stem methane emission in mature wetland alder trees. Atmos Environ 44:2157–2160. https://doi.org/10.1016/j.atmosenv.2010.02.034

Gauci V, Gowing DJG, Hornibrook ERC, et al (2010b) Woody stem methane emission in mature wetland alder trees. Atmos Environ 44:2157–2160. https://doi.org/10.1016/j.atmosenv.2010.02.034

Geigenberger P (2003) Response of plant metabolism to too little oxygen. Curr Opin Plant Biol 6:247–256. https://doi.org/10.1016/S1369-5266(03)00038-4

George TS, Bulgarelli D, Carminati A, et al (2024) Bottom-up perspective – The role of roots and rhizosphere in climate change adaptation and mitigation in agroecosystems. Plant Soil 3:. https://doi.org/10.1007/s11104-024-06626-6

Gill CJ (1975) The Ecological Significance of Adventitious Rooting as a Response to Flooding in Woody Species, with Special Reference to Alnus glutinosa (L.) Gaertn. Flora 164:85–97. https://doi.org/10.1016/s0367-2530(17)31790-5

Gilliam FS (2016) Forest ecosystems of temperate climatic regions: from ancient use to climate change. New Phytol 212:871–887. https://doi.org/10.1111/nph.14255

Girkin NT, Turner BL, Ostle N, Sjögersten S (2018) Composition and concentration of root exudate analogues regulate greenhouse gas fluxes from tropical peat. Soil Biol Biochem 127:280–285. https://doi.org/10.1016/j.soilbio.2018.09.033

Glenz C, Schlaepfer R, Iorgulescu I, Kienast F (2006) Flooding tolerance of Central European tree and shrub species. For Ecol Manage 235:1–13. https://doi.org/10.1016/j.foreco.2006.05.065

Gravatt DA, Kirby CJ (1998) Patterns of photosynthesis and starch allocation in seedlings of four bottomland hardwood tree species subjected to flooding. Tree Physiol 18:411–417. https://doi.org/10.1093/treephys/18.6.411

Grünfeld S, Brix H (1999) Methanogenesis and methane emissions: Effects of water table, substrate type and presence of Phragmites australis. Aquat Bot 64:63–75. https://doi.org/10.1016/S0304-3770(99)00010-8

Gunderson CA, Norby RJ, Wullschleger SD (2000) Acclimation of photosynthesis and respiration to simulated climatic warming in northern and southern populations of Acer saccharum: Laboratory and field evidence. Tree Physiol 20:87–96. https://doi.org/10.1093/treephys/20.2.87

Guo D, Xia M, Wei X, et al (2008) Anatomical traits associated with absorption and mycorrhizal colonization are linked to root branch order in twenty-three Chinese temperate tree species. New Phytol 180:673–683. https://doi.org/10.1111/j.1469-8137.2008.02573.x

Hanson PJ, Wullschleger SD (2018) Seasonal and topographic patterns of forest floor co2 efflux from an upland oak forest.pdf. 1–15

Hao M, Messier C, Geng Y, et al (2020) Functional traits influence biomass and productivity through multiple mechanisms in a temperate secondary forest. Eur J For Res 139:959–968. https://doi.org/10.1007/s10342-020-01298-0

Hasper TB, Dusenge ME, Breuer F, et al (2017) Stomatal CO2 responsiveness and

photosynthetic capacity of tropical woody species in relation to taxonomy and functional traits. Oecologia 184:43–57. https://doi.org/10.1007/s00442-017-3829-0

Hazman M, Brown KM (2018) Progressive drought alters architectural and anatomical traits of rice roots. Rice 11:. https://doi.org/10.1186/s12284-018-0252-z

Heath J, Kerstiens G, Tyree MT (1997) Stem hydraulic conductance of European beech (Fagus sylvatica L.) and pedunculate oak (Quercus robur L.) grown in elevated CO2. J Exp Bot 48:1487–1489. https://doi.org/10.1093/jxb/48.7.1487

Henneberg A, Sorrell BK, Brix H (2012) Internal methane transport through Juncus effusus: Experimental manipulation of morphological barriers to test above- and below-ground diffusion limitation. New Phytol 196:799–806. https://doi.org/10.1111/j.1469-8137.2012.04303.x

Hennessy K, Fawcett R, Kirono D, et al (2008) An assessment of the impact of climate change on the nature and frequency of exceptional climatic events. Australian Government, Bureau of Meterology

Herrick JD, Maherali H, Thomas RB, Herrick JD (2004) Reduced stomatal conductance in sweetgum (Liquidambar styraciflua) sustained over long-term CO 2 enrichment. 387–396. https://doi.org/10.1111/j.1469-8137.2004.01045.x

Hidalgo CA, Klinger B, Barabási A., Hausmann R (2007) A large and persistent carbon sink in the world's forest. Science (80-) 317:4

Hirota M, Tang Y, Hu Q, et al (2004) Methane emissions from different vegetation zones in a Qinghai-Tibetan Plateau wetland. Soil Biol Biochem 36:737–748. https://doi.org/10.1016/j.soilbio.2003.12.009

Hook DD., Brown CL., Wetmore RH. (1972) Aeration in Trees. Univ Chicago Press Stable URL https//www.jstor.org/stable/2474119 Univ Chicago Press is Collab with JSTOR to Digit , Preserv 133:443–454

Hoyos-Santillan J, Craigon J, Lomax BH, et al (2016) Root oxygen loss from Raphia taedigera palms mediates greenhouse gas emissions in lowland neotropical peatlands. Plant Soil 404:47–60. https://doi.org/10.1007/s11104-016-2824-2

Hoyos-Santillan J, Lomax BH, Large D, et al (2019) Evaluation of vegetation communities, water table, and peat composition as drivers of greenhouse gas emissions in lowland tropical peatlands. Sci Total Environ 688:1193–1204. https://doi.org/10.1016/j.scitotenv.2019.06.366

Huang B, Eissenstat DM (2000) Linking hydraulic conductivity to anatomy in plants that vary in specific root length. J Am Soc Hortic Sci 125:260–264. https://doi.org/10.21273/jashs.125.2.260

Huang B, Johnson JW, NeSmith DS (1997) Responses to root-zone CO2 enrichment and hypoxia of wheat genotypes differing in waterlogging tolerance. Crop Sci 37:464–468. https://doi.org/10.2135/cropsci1997.0011183X003700020026x

Huang XF, Chaparro JM, Reardon KF, et al (2014) Rhizosphere interactions: Root exudates, microbes, and microbial communities1. Botany 92:267–275. https://doi.org/10.1139/cjb-2013-0225

Hynynen J, Niemistö P, Viherä-Aarnio A, et al (2010) Silviculture of birch (Betula pendula

Roth and Betula pubescens Ehrh.) in Northern Europe. Forestry 83:103–119. https://doi.org/10.1093/forestry/cpp035

Hyvönen R, Ågren GI, Linder S, et al (2006) The likely impact of elevated [CO2], nitrogen deposition, increased temperature and management on carbon sequestration in temperate and boreal forest ecosystems: a literature review.

IPCC (2022) Climate Change 2022, Mitigation of Climate Change Summary for Policymakers (SPM)

IPCC (2013a) Climate Change

IPCC (2013b) Climate change

IPCC (2007) Climate Change 2007:The Fourth Assessment Report of Intergovernmental Panel on Climate Change.Cambridge University

Irfan M, Hayat S, Hayat Q, et al (2010) Physiological and biochemical changes in plants under waterlogging. Protoplasma 241:3–17. https://doi.org/10.1007/s00709-009-0098-8

Iversen CM, McCormack ML, Powell AS, et al (2017) A global Fine-Root Ecology Database to address below-ground challenges in plant ecology. New Phytol 215:15–26. https://doi.org/10.1111/nph.14486

Jackson MB, Armstrong W (1999a) Formation of aerenchyma and the processes of plant ventilation in relation to soil flooding and submergence. Plant Biol 1:274–287. https://doi.org/10.1111/j.1438-8677.1999.tb00253.x

Jackson MB, Armstrong W (1999b) Formation of Aerenchyma and the Processes of Plant Ventilation in Relation to Soil Flooding and Submergence. 274–287

Jacobsen AL, Agenbag L, Esler KJ, et al (2007) Xylem density, biomechanics and anatomical traits correlate with water stress in 17 evergreen shrub species of the Mediterranean-type climate region of South Africa. J Ecol 95:171–183. https://doi.org/10.1111/j.1365-2745.2006.01186.x

Jaeger C, Gessler A, Biller S, et al (2009) Differences in C metabolism of ash species and provenances as a consequence of root oxygen deprivation by waterlogging. J Exp Bot 60:4335–4345. https://doi.org/10.1093/jxb/erp268

Jager MM, Richardson SJ, Bellingham PJ, et al (2015) Soil fertility induces coordinated responses of multiple independent functional traits. J Ecol 103:374–385. https://doi.org/10.1111/1365-2745.12366

Jens Hesselbjerg C, Bruce Hewitson (2007) Regional climate projections. Appl Geoinformatics Sustain Integr L Water Resour Manag Brahmaputra River Basin Results From Ec-Project Brahmatwinn 11–15. https://doi.org/10.1007/978-81-322-1967-5_4

Jiménez S, Fattahi M, Bedis K, et al (2020) Interactional Effects of Climate Change Factors on the Water Status, Photosynthetic Rate, and Metabolic Regulation in Peach. Front Plant Sci 11:1–18. https://doi.org/10.3389/fpls.2020.00043

Joabsson A, Christensen TR, Wallén B (1999) Vascular plant controls on methane emissions from northern peatforming wetlands. Trends Ecol Evol 14:385–388. https://doi.org/10.1016/S0169-5347(99)01649-3

Johansson T (1992) Dormant buds on Betula pubescens and Betula pendula stumps under

different field conditions. For Ecol Manage 47:245–259. https://doi.org/10.1016/0378-1127(92)90277-G

Joseph C, Vu V, Yelenosky G (1991) Photosyiitlietic responses of citrus trees to soil flooding. 7–14

Jumrani K, Bhatia VS (2019) Interactive effect of temperature and water stress on physiological and biochemical processes in soybean. Physiol Mol Biol Plants 25:667–681. https://doi.org/10.1007/s12298-019-00657-5

Jung J, Lee SC, Choi HK (2008) Anatomical patterns of aerenchyma in aquatic and wetland plants. J Plant Biol 51:428–439. https://doi.org/10.1007/BF03036065

Justin ASHFW, Armstrong W (1987) The Anatomical Characteristics of Roots and Plant Response to Soil Flooding Published by : Blackwell Publishing on behalf of the New Phytologist Trust Stable URL : http://www.jstor.org/stable/2434813 OF CHARACTERISTICS THE ANATOMICAL SOIL TO ROOTS AND PLA. New Phytol 106:465–495

Kankaala P, Käki T, Mäkelä S, et al (2005) Methane efflux in relation to plant biomass and sediment characteristics in stands of three common emergent macrophytes in boreal mesoeutrophic lakes. Glob Chang Biol 11:145–153. https://doi.org/10.1111/j.1365-2486.2004.00888.x

King GM (1994) Associations of methanotrophs with the roots and rhizomes of aquatic vegetation. Appl Environ Microbiol 60:3220–3227. https://doi.org/10.1128/aem.60.9.3220-3227.1994

Kogawara S, Yamanoshita T, Norisada M, et al (2006) Photosynthesis and photoassimilate transport during root hypoxia in Melaleuca cajuputi, a flood-tolerant species, and in Eucalyptus camaldulensis, a moderately flood-tolerant species. Tree Physiol 26:1413–1423. https://doi.org/10.1093/treephys/26.11.1413

Kong D, Wang J, Zeng H, et al (2017) The nutrient absorption–transportation hypothesis: optimizing structural traits in absorptive roots. New Phytol 213:1569–1572. https://doi.org/10.1111/nph.14344

Kozlowski TT (1997) Responses of woody plants to flooding and salinity. Tree Physiol 17:490–490. https://doi.org/10.1093/treephys/17.7.490

Kramer PJ, Jackson WT (1954) Causes of Injury to Flooded Tobacco Plants. Plant Physiol 29:241–245. https://doi.org/10.1104/pp.29.3.241

Kreuzwieser J, Fürniss S, Rennenberg H (2002) Impact of waterlogging on the N-metabolism of flood tolerant and non-tolerant tree species. Plant, Cell Environ 25:1039–1049. https://doi.org/10.1046/j.1365-3040.2002.00886.x

Kreuzwieser J, Rennenberg H (2014) Molecular and physiological responses of trees to waterlogging stress. Plant Cell Environ 37:2245–2259. https://doi.org/10.1111/pce.12310

Kuai J, Liu Z, Wang Y, et al (2014) Waterlogging during flowering and boll forming stages affects sucrose metabolism in the leaves subtending the cotton boll and its relationship with boll weight. Plant Sci 223:79–98. https://doi.org/10.1016/j.plantsci.2014.03.010

Kumar M, Saha S, Rajwar GS, Upadhaya K (2016) Litter production, decomposition and

nutrient release of woody tree species in Dhanaulti region of temperate forest in Gahwal Himalaya. Eurasian J For Sci 4:17–30. https://doi.org/10.31195/ejejfs.258622

Laanbroek HJ (2010) Methane emission from natural wetlands: Interplay between emergent macrophytes and soil microbial processes. A mini-review. Ann Bot 105:141–153. https://doi.org/10.1093/aob/mcp201

Lamba S, Hall M, Räntfors M, et al (2018) Physiological acclimation dampens initial effects of elevated temperature and atmospheric CO2 concentration in mature boreal Norway spruce. Plant Cell Environ 41:300–313. https://doi.org/10.1111/pce.13079

Lambers H, Shane MW, Cramer MD, et al (2006) Root structure and functioning for efficient acquisition of phosphorus: Matching morphological and physiological traits. Ann Bot 98:693–713. https://doi.org/10.1093/aob/mcl114

Larson JE, Funk JL (2016) Seedling root responses to soil moisture and the identification of a belowground trait spectrum across three growth forms. New Phytol 210:827–838. https://doi.org/10.1111/nph.13829

Lawson JR, Fryirs KA, Leishman MR (2017) Interactive effects of waterlogging and atmospheric CO2 concentration on gas exchange, growth and functional traits of Australian riparian tree seedlings. Ecohydrology 10:1–11. https://doi.org/10.1002/eco.1803

Lawson JR, Fryirs KA, Leishman MR (2015) Hydrological conditions explain variation in wood density in riparian plants of south-eastern Australia. J Ecol 103:945–956. https://doi.org/10.1111/1365-2745.12408

Lawson JR, Leishman MR (2017) Interactive effects of waterlogging and atmospheric CO 2 concentration on gas exchange , growth and functional traits of Australian riparian tree seedlings. 1–11. https://doi.org/10.1002/eco.1803

Leverenz JW, Bruhn D, Saxe H (1999) Responses of two provenances of Fagus sylvatica seedlings to a combination of four temperature and two CO2 treatments during their first growing season: Gas exchange of leaves and roots. New Phytol 144:437–454. https://doi.org/10.1046/j.1469-8137.1999.00541.x

Li CX, Wei H, Geng YH, Schneider R (2010) Effects of submergence on photosynthesis and growth of Pterocarya stenoptera (Chinese wingnut) seedlings in the recently-created Three Gorges Reservoir region of China. Wetl Ecol Manag 18:485–494. https://doi.org/10.1007/s11273-010-9181-3

Li J, Hu HW, Cai ZJ, et al (2019) Contrasting Soil Bacterial and Fungal Communities between the Swamp and Upland in the Boreal Forest and their Biogeographic Distribution Patterns. Wetlands 39:441–451. https://doi.org/10.1007/s13157-018-1086-6

Liu Z, Deng Z, Davis S, Ciais P (2023) Monitoring global carbon emissions in 2022. Nat Rev Earth Environ 4:205–206. https://doi.org/10.1038/s43017-023-00406-z

Long SP, Ainsworth EA, Rogers A, Ort DR (2004) Rising Atmospheric Carbon Dioxide: Plants FACE the future. Annu Rev Plant Biol 55:591–628. https://doi.org/10.1146/annurev.arplant.55.031903.141610

Luo Y, Gerten D, Le Maire G, et al (2008) Modeled interactive effects of precipitation, temperature, and [CO2] on ecosystem carbon and water dynamics in different climatic

zones. Glob Chang Biol 14:1986–1999. https://doi.org/10.1111/j.1365-2486.2008.01629.x

Lynch JP, Chimungu JG, Brown KM (2014) Root anatomical phenes associated with water acquisition from drying soil: Targets for crop improvement. J Exp Bot 65:6155–6166. https://doi.org/10.1093/jxb/eru162

Ma Q, Cui L, Song H, et al (2017) Aboveground and Belowground Biomass Relationships in the Zoige Peatland, Eastern Qinghai–Tibetan Plateau. Wetlands 37:461–469. https://doi.org/10.1007/s13157-017-0882-8

Machacova K, Bäck J, Vanhatalo A, et al (2016) Pinus sylvestris as a missing source of nitrous oxide and methane in boreal forest. Sci Rep 6:1–8. https://doi.org/10.1038/srep23410

Maier M, Machacova K, Lang F, et al (2018) Combining soil and tree-stem flux measurements and soil gas profiles to understand CH4 pathways in Fagus sylvatica forests. J Plant Nutr Soil Sci 181:31–35. https://doi.org/10.1002/jpln.201600405

McElrone AJ, Pockman WT, Martínez-Vilalta J, Jackson RB (2004) Variation in xylem structure and function in stems and roots of trees to 20 m depth. New Phytol 163:507–517. https://doi.org/10.1111/j.1469-8137.2004.01127.x

Medlyn BE, Badeck FW, De Pury DGG, et al (1999) Effects of elevated [CO2] on photosynthesis in European forest species: A meta-analysis of model parameters. Plant, Cell Environ 22:1475–1495. https://doi.org/10.1046/j.1365-3040.1999.00523.x

Medlyn BE, Barton CVM, Broadmeadow MSJ, et al (2001) Stomatal conductance of forest species after long-term exposure to elevated CO2 concentration: A synthesis. New Phytol 149:247–264. https://doi.org/10.1046/j.1469-8137.2001.00028.x

Megonigal JP, Vann CD, Wolf AA (2005) Flooding constraints on tree (taxodium distichum) and herb growth responses to elevated CO2. Wetlands 25:430–438. https://doi.org/10.1672/17

Meier IC, Leuschner C, Marini E, Fender AC (2016) Species-specific effects of temperate trees on greenhouse gas exchange of forest soil are diminished by drought. Soil Biol Biochem 95:122–134. https://doi.org/10.1016/j.soilbio.2015.12.005

Menezes-Silva PE, Loram-Lourenço L, Alves RDFB, et al (2019) Different ways to die in a changing world: Consequences of climate change for tree species performance and survival through an ecophysiological perspective. Ecol Evol 9:11979–11999. https://doi.org/10.1002/ece3.5663

Met office (2021) East Midlands weather forecast. https://www.metoffice.gov.uk/. Accessed 20 Mar 2021

Morison J, Matthews R, Miller G, et al (2012) Understanding the carbon and greenhouse gas balance of forests in Britain

Morison JIL, Lawlor DW (1999) Interactions between increasing CO2 concentration and temperature on plant growth. Plant, Cell Environ 22:659–682. https://doi.org/10.1046/j.1365-3040.1999.00443.x

Mueller KE, LeCain DR, McCormack ML, et al (2018) Root responses to elevated CO2, warming and irrigation in a semi-arid grassland: Integrating biomass, length and life

span in a 5-year field experiment. J Ecol 106:2176–2189. https://doi.org/10.1111/1365-2745.12993

Nguyen LTT, Osanai Y, Anderson IC, et al (2018) Impacts of waterlogging on soil nitrification and ammonia-oxidizing communities in farming system. Plant Soil 426:299–311. https://doi.org/10.1007/s11104-018-3584-y

Norby RJ, Ledford J, Reilly CD, et al (2004) Fine-root production dominates response of a deciduous forest to atmospheric CO2 enrichment. Proc Natl Acad Sci U S A 101:9689–9693. https://doi.org/10.1073/pnas.0403491101

Norby RJ, Wullschleger DD, Hanson P., et al (2006) 13 CO 2 Enrichment of a Deciduous Forest : The Oak Ridge FACE Experiment. 187:

Ojeda M, Schaffer B, Davies FS (2004) Flooding, root temperature, physiology and growth of two Annona species. Tree Physiol 24:1019–1025. https://doi.org/10.1093/treephys/24.9.1019

Oliveira AS De, Ferreira CS, Graciano-ribeiro D, Franco AC (2015) Anatomical and morphological modifications in response to flooding by six Cerrado tree species. 29:478–488. https://doi.org/10.1590/0102-33062014abb0035

Orsenigo S, Mondoni A, Rossi G, Abeli T (2014) Some like it hot and some like it cold, but not too much: Plant responses to climate extremes. Plant Ecol 215:677–688. https://doi.org/10.1007/s11258-014-0363-6

Osborn TJ, Hulme M, Jones PD, Basnett TA (2000) Observed trends in the daily intensity of United Kingdom precipitation. Int J Climatol 20:347–364. https://doi.org/10.1002/(SICI)1097-0088(20000330)20:4<347::AID-JOC475>3.0.CO;2-C

Palmer TN, Räisänen J (2002) Quantifying the risk of extreme seasonal precipitation events in a changing climate. Nature 415:512–514. https://doi.org/10.1038/415512a

Pan J, Sharif R, Xu X, Chen X (2021) Mechanisms of Waterlogging Tolerance in Plants: Research Progress and Prospects. Front Plant Sci 11:. https://doi.org/10.3389/fpls.2020.627331

Pangala SR (2013) Methane Emissions From Wetland Trees: Controls and Variability. 1–180

Pangala SR (2014) Methane Emissions From Wetland Trees: Controls and Variability. 1–180

Pangala SR, Gowing DJ, Hornibrook ERC, Gauci V (2014) Controls on methane emissions from Alnus glutinosa saplings. New Phytol 201:887–896. https://doi.org/10.1111/nph.12561

Pangala SR, Hornibrook ERC, Gowing DJ, Gauci V (2015) The contribution of trees to ecosystem methane emissions in a temperate forested wetland. Glob Chang Biol 21:2642–2654. https://doi.org/10.1111/gcb.12891

Pangala SR, Moore S, Hornibrook ERC, Gauci V (2013) Trees are major conduits for methane egress from tropical forested wetlands. New Phytol 197:524–531. https://doi.org/10.1111/nph.12031

Parent C, Capelli N, Berger A, et al (2008) An overview of plant responses to soil waterlogging. Plant Stress 2:20–27

Passioura JB (1988) Water Transport in and to Roots. Annu Rev Plant Physiol Plant Mol Biol 39:245–265. https://doi.org/10.1146/annurev.pp.39.060188.001333

Pate JS, Jeschke WD, Aylward MJ (1995) Hydraulic architecture and xylem structure of the dimorphic root systems of south-west australian species of proteaceae. J Exp Bot 46:907–915. https://doi.org/10.1093/jxb/46.8.907

Pawlowski K, Bergman B, Pawlowski K, Bergman B (2007) Chapter 11 Plant Symbioses with Frankia and. Elsevier B.V.

Pérez-López U, Robredo A, Lacuesta M, et al (2009) The impact of salt stress on the water status of barley plants is partially mitigated by elevated CO2. Environ Exp Bot 66:463–470. https://doi.org/10.1016/J.ENVEXPBOT.2009.03.007

Pezeshki SR (2001) Wetland plant responses to soil flooding. Environ Exp Bot 46:299–312. https://doi.org/10.1016/S0098-8472(01)00107-1

Piekielek WP, Fox RH, Toth JD, Macneal KE (1995) Use of a chlorophyll meter at the early dent stage of corn to evaluate nitrogen sufficiency. Agron J 87:403–408. https://doi.org/10.2134/agronj1995.00021962008700030003x

Pihlatie M, Ambus P, Rinne J, et al (2005) Plant-mediated nitrous oxide emissions from beech (Fagus sylvatica) leaves. New Phytol 168:93–98. https://doi.org/10.1111/j.1469-8137.2005.01542.x

Pineda-García F, Paz H, Meinzer FC, Angeles G (2015) Exploiting water versus tolerating drought: Water-use strategies of trees in a secondary successional tropical dry forest. Tree Physiol 36:208–217. https://doi.org/10.1093/treephys/tpv124

Piper F, Zúñiga-Feest A, Rojas P, et al (2008) Responses of two températe evergreen Nothofagus species to sudden and gradual waterlogging: Relationships with distribution patterns. Rev Chil Hist Nat 81:257–266. https://doi.org/10.4067/S0716-078X2008000200008

Pires HRA, Franco AC, Piedade MTF, et al (2018) Flood tolerance in two tree species that inhabit both the Amazonian floodplain and the dry Cerrado savanna of Brazil. AoB Plants 10:1–15. https://doi.org/10.1093/aobpla/ply065

Plante PM, Rivest D, Vézina A, Vanasse A (2014) Root distribution of different mature tree species growing on contrasting textured soils in temperate windbreaks. Plant Soil 380:429–439. https://doi.org/10.1007/s11104-014-2108-7

Rawat M, Singh R, Sharma J, et al (2022) An Overview of the functioning of Temperate Forest Ecosystems with Particular Reference to Himalayan Temperate Forest. Trees, For People 8:100230. https://doi.org/10.1016/j.tfp.2022.100230

Reddy KR, Patrick WH, Lindau CW (1989) Nitrification-denitrification at the plant root-sediment interface in wetlands. Limnol Oceanogr 34:1004–1013. https://doi.org/10.4319/lo.1989.34.6.1004

Reich PB, Hobbie SE, Lee TD (2014) Plant growth enhancement by elevated CO2 eliminated by joint water and nitrogen limitation. Nat Geosci 7:920–924. https://doi.org/10.1038/ngeo2284

Rice AL, Butenhoff CL, Shearer MJ, et al (2010) Emissions of anaerobically produced methane by trees. Geophys Res Lett 37:1–5. https://doi.org/10.1029/2009GL041565

Rieger M, Litvin P (1999) Root system hydraulic conductivity in species with contrasting root anatomy. J Exp Bot 50:201–209. https://doi.org/10.1093/jxb/50.331.201

Roden JS, Ball MC (1996) Growth and photosynthesis of two eucalypt species during high temperature stress under ambient and elevated [CO2]. 115–128

Rodríguez-Gamir J, Intrigliolo DS, Primo-Millo E, Forner-Giner MA (2010) Relationships between xylem anatomy, root hydraulic conductivity, leaf/root ratio and transpiration in citrus trees on different rootstocks. Physiol Plant 139:159–169. https://doi.org/10.1111/j.1399-3054.2010.01351.x

ROGERS HH, PETERSON CM, McCRIMMON JN, CURE JD (1992) Response of plant roots to elevated atmospheric carbon dioxide. Plant Cell Environ 15:749–752. https://doi.org/10.1111/j.1365-3040.1992.tb01018.x

Roulet NT (2000) Peatlands, carbon storage, greenhouse gases, and the kyoto protocol: Prospects and significance for Canada. Wetlands 20:605–615. https://doi.org/10.1672/0277-5212(2000)020[0605:PCSGGA]2.0.CO;2

Rusch H, Rennenberg H (1998) Black alder (Alnus glutinosa (L.) Gaertn.) trees mediate methane and nitrous oxide emission from the soil to the atmosphere. Plant Soil 201:1–7. https://doi.org/10.1023/A:1004331521059

Ryser P, Gill HK, Byrne CJ (2011) Constraints of Root Response to Waterlogging in Alisma Triviale Constraints of root response to waterlogging in Alisma triviale. https://doi.org/10.1007/s11104-011-0715-0

Saibo NJM, Lourenço T, Oliveira MM (2009) Transcription factors and regulation of photosynthetic and related metabolism under environmental stresses. Ann Bot 103:609–623. https://doi.org/10.1093/aob/mcn227

Saunders MJ, Kansiime F, Jones MB (2014) Reviewing the carbon cycle dynamics and carbon sequestration potential of Cyperus papyrus L. wetlands in tropical Africa. Wetl Ecol Manag 22:143–155. https://doi.org/10.1007/s11273-013-9314-6

Saunois M, Bousquet P, Poulter B, et al (2016) The global methane budget 2000-2012. Earth Syst Sci Data 8:697–751. https://doi.org/10.5194/essd-8-697-2016

Saxe H, Ellsworth DS, Heath J (1998) Tree and forest functioning in an enriched CO2 atmosphere. New Phytol 139:395–436. https://doi.org/10.1046/j.1469-8137.1998.00221.x

Schindler T, Machacova K, Mander Ü, et al (2021) Diurnal tree stem ch4 and n2o flux dynamics from a riparian alder forest. Forests 12:1–9. https://doi.org/10.3390/f12070863

Schmull M, Liebl QM, Thomas FM (2000) Morphological and physiological reactions of young deciduous trees (Quercus Morphological and physiological reactions of young deciduous trees (Quercus robur L ., Q . petraea [Matt .] Liebl ., Fagus sylvatica L .) to waterlogging. https://doi.org/10.1023/A

Schröder P (1989) Characterization of a thermo-osmotic gas transport mechanism in Alnus glutinosa (L.) Gaertn. Trees 3:38–44. https://doi.org/10.1007/BF00202399

Schuldt B, Leuschner C, Brock N, Horna V (2013) Changes in wood density, wood anatomy and hydraulic properties of the xylem along the root-to-shoot flow path in tropical rainforest trees. Tree Physiol 33:161–174. https://doi.org/10.1093/treephys/tps122

Schulze ED, Ciais P, Luyssaert S, et al (2010) The European carbon balance. Part 4: Integration of carbon and other trace-gas fluxes. Glob Chang Biol 16:1451–1469. https://doi.org/10.1111/j.1365-2486.2010.02215.x

Servais S, Kominoski JS, Davis SE, et al (2019) Effects of Nutrient-Limitation on Disturbance Recovery in Experimental Mangrove Wetlands. Wetlands 39:337–347. https://doi.org/10.1007/s13157-018-1100-z

Shimono H, Konno T, Sakai H, Sameshima R (2012a) Interactive Effects of Elevated Atmospheric CO2 and Waterlogging on Interactive Effects of Elevated Atmospheric CO 2 and Waterlogging on Vegetative Growth of Soybean (Glycine max (L .) Merr .). https://doi.org/10.1626/pps.15.238

Shimono H, Konno T, Sakai H, Sameshima R (2012b) Interactive effects of elevated atmospheric CO 2 and waterlogging on vegetative growth of soybean (Glycine max (L.) Merr.). Plant Prod Sci 15:238–245. https://doi.org/10.1626/pps.15.238

Sjögersten S, Aplin P, Gauci V, et al (2018) Temperature response of ex-situ greenhouse gas emissions from tropical peatlands: Interactions between forest type and peat moisture conditions. Geoderma 324:47–55. https://doi.org/10.1016/j.geoderma.2018.02.029

Sjögersten S, Black CR, Evers S, et al (2014) Tropical wetlands: A missing link in the global carbon cycle? Global Biogeochem Cycles 28:1371–1386. https://doi.org/10.1002/2014GB004844

Sjögersten S, Cheesman AW, Lopez O, Turner BL (2011) Biogeochemical processes along a nutrient gradient in a tropical ombrotrophic peatland. Biogeochemistry 104:147–163. https://doi.org/10.1007/s10533-010-9493-7

Sjögersten S, Siegenthaler A, Lopez OR, et al (2020a) Methane emissions from tree stems in neotropical peatlands. New Phytol 225:769–781. https://doi.org/10.1111/nph.16178

Sjögersten S, Siegenthaler A, Lopez OR, et al (2020b) Methane emissions from tree stems in neotropical peatlands. New Phytol 225:769–781. https://doi.org/10.1111/nph.16178

Soana E, Bartoli M (2013) Seasonal variation of radial oxygen loss in Vallisneria spiralis L.: An adaptive response to sediment redox? Aquat Bot 104:228–232. https://doi.org/10.1016/j.aquabot.2012.07.007

Solomon S, Qin D, Manning M, et al (2007) The Physical Science Basis. Contribution of Working Group I to the Fourth Assessment Report of the Intergovernmental Panel on Climate Change. Cambridge Univ Press 59:235. https://doi.org/10.1256/wea.58.04

Sommerville AHC (1991) Willows in the environment. Proc - R Soc Edinburgh, Sect B 98:215–224. https://doi.org/10.1017/s0269727000007570

Sorrell BK, Brix H (2015) Gas Transport and Exchange through Wetland Plant Aerenchyma. 177–196. https://doi.org/10.2136/sssabookser10.c11

Sorz J, Hietz P (2006) Gas diffusion through wood: Implications for oxygen supply. Trees - Struct Funct 20:34–41. https://doi.org/10.1007/s00468-005-0010-x

Steudle E, Peterson CA (1998) How does water get through roots? J Exp Bot 49:775–788. https://doi.org/10.1093/jxb/49.322.775

Ström L, Tagesson T, Mastepanov M, Christensen TR (2012) Presence of Eriophorum

scheuchzeri enhances substrate availability and methane emission in an Arctic wetland. Soil Biol Biochem 45:61–70. https://doi.org/10.1016/j.soilbio.2011.09.005

Tanaka K, Masumori M, Yamanoshita T, Tange T (2011) Morphological and anatomical changes of Melaleuca cajuputi under submergence. Trees - Struct Funct 25:695–704. https://doi.org/10.1007/s00468-011-0547-9

Tang ZC, Kozlowski TT (1982) Some physiological and growth responses of Betula papyrifera seedlings to flooding. Physiol Plant 55:415–420. https://doi.org/10.1111/j.1399-3054.1982.tb04521.x

Terazawa K, Ishizuka S, Sakata T, et al (2007) Methane emissions from stems of Fraxinus mandshurica var. japonica trees in a floodplain forest. Soil Biol Biochem 39:2689–2692. https://doi.org/10.1016/j.soilbio.2007.05.013

Terentieva IE, Sabrekov AF, Ilyasov D, et al (2019) Highly Dynamic Methane Emission from the West Siberian Boreal Floodplains. Wetlands 39:217–226. https://doi.org/10.1007/s13157-018-1088-4

Teskey R, Wertin T, Bauweraerts I, et al (2015) Responses of tree species to heat waves and extreme heat events. Plant Cell Environ 38:1699–1712. https://doi.org/10.1111/pce.12417

Teskey RO, Hinckley TM (1981) Influence of temperature and water potential on root growth of white oak. Physiol Plant 52:363–369. https://doi.org/10.1111/j.1399-3054.1981.tb06055.x

Teskey RO, Mcguire MA (2007) Measurement of stem respiration of sycamore (Platanus occidentalis L.) trees involves internal and external fluxes of CO2 and possible transport of CO2 from roots. Plant, Cell Environ 30:570–579. https://doi.org/10.1111/j.1365-3040.2007.01649.x

Thomas et al. (2004) Extinction risk from climate change. Nature 427 (6970). https://doi.org/10.2307/j.ctv8jnzw1.37

Thomas KL, Benstead J, Davies KL, Lloyd D (1996) Role of wetland plants in the diurnal control of CH4 and CO2 fluxes in peat. Soil Biol Biochem 28:17–23. https://doi.org/10.1016/0038-0717(95)00103-4

Topa MA, McLeod KW (1986) Aerenchyma and lenticel formation in pine seedlings: A possible avoidance mechanism to anaerobic growth conditions. Physiol Plant 68:540–550. https://doi.org/10.1111/j.1399-3054.1986.tb03394.x

Tripepi2 RR, Mitchell CA (1984) Metabolic Response of River Birch and European Birch Roots to Hypoxia’

Tsukahara H, Kozlowski TT (1986) Effect of flooding and temperature regime on growth and stomatal resistance of Betula platyphylla var. japonica seedlings. Plant Soil 92:103–112. https://doi.org/10.1007/BF02372271

Turetsky MR, Kotowska A, Bubier J, et al (2014) A synthesis of methane emissions from 71 northern, temperate, and subtropical wetlands. Glob Chang Biol 20:2183–2197. https://doi.org/10.1111/gcb.12580

TYREE MT, EWERS FW (1991) The hydraulic architecture of trees and other woody plants. New Phytol 119:345–360. https://doi.org/10.1111/j.1469-8137.1991.tb00035.x

Upton A, Vane CH, Girkin N, et al (2018) Does litter input determine carbon storage and peat organic chemistry in tropical peatlands? Geoderma 326:76–87. https://doi.org/10.1016/j.geoderma.2018.03.030

van Winden JF, Reichart GJ, McNamara NP, et al (2012) Temperature-induced increase in methane release from peat bogs: A mesocosm experiment. PLoS One 7:4–8. https://doi.org/10.1371/journal.pone.0039614

Vann CD, Megonigal JP (2003) Elevated CO2 and water depth regulation of methane emissions: Comparison of woody and non-woody wetland plant species. Biogeochemistry 63:117–134. https://doi.org/10.1023/A:1023397032331

Verhertbruggen Y, Walker JL, Guillon F, Scheller H V. (2017) A comparative study of sample preparation for staining and immunodetection of plant cell walls by light microscopy. Front Plant Sci 8:1–17. https://doi.org/10.3389/fpls.2017.01505

Vesterdal L, Elberling B, Christiansen JR, et al (2012) Soil respiration and rates of soil carbon turnover differ among six common European tree species. For Ecol Manage 264:185–196. https://doi.org/10.1016/j.foreco.2011.10.009

Visser EJW, Voesenek LACJ (2005) Acclimation to soil flooding-sensing and signal-transduction. Plant Soil 274:197–214. https://doi.org/10.1007/s11104-004-1650-0

Voesenek LACJ, Bailey-Serres J (2015) Flood adaptive traits and processes: An overview. New Phytol 206:57–73. https://doi.org/10.1111/nph.13209

Wagner D (1996) Scenarios of extreme temperature events. Clim Change 33:385–407. https://doi.org/10.1007/BF00142585

Walsh JE, Ballinger TJ, Euskirchen ES, et al (2020) Extreme weather and climate events in northern areas: A review. Earth-Science Rev 209:103324. https://doi.org/10.1016/j.earscirev.2020.103324

Walther G, Post E, Convey P, et al (2002) Ecological response to recent climate cnahge. Nature 416:389–395

Wang A-F, Roitto M, Sutinen S, et al (2015a) Waterlogging in late dormancy and the early growth phase affected root and leaf morphology in Betula pendula and Betula pubescens seedlings. Tree Physiol 36:86–98. https://doi.org/10.1093/treephys/tpv089

Wang AF, Roitto M, Lehto T, et al (2017) Photosynthesis, nutrient accumulation and growth of two Betula species exposed to waterlogging in late dormancy and in the early growing season. Tree Physiol 37:767–778. https://doi.org/10.1093/treephys/tpx021

Wang AF, Roitto M, Lehto T, et al (2013) Waterlogging under simulated late-winter conditions had little impact on the physiology and growth of Norway spruce seedlings. Ann For Sci 70:781–790. https://doi.org/10.1007/s13595-013-0325-5

Wang D, Heckathorn SA, Wang X, Philpott SM (2012) A meta-analysis of plant physiological and growth responses to temperature and elevated CO 2. Oecologia 169:1–13. https://doi.org/10.1007/s00442-011-2172-0

Wang KY, Kellomaki S (1997) Stomatal conductance and transpiration in shoots of Scots pine after 4-year exposure to elevated CO2 and temperature. Can J Bot 75:552–561. https://doi.org/10.1139/b97-061

Wang X, Taub DR (2010) Interactive effects of elevated carbon dioxide and environmental stresses on root mass fraction in plants: A meta-analytical synthesis using pairwise techniques. Oecologia 163:1–11. https://doi.org/10.1007/s00442-010-1572-x

Wang Y, Dong X, Wang H, et al (2015b) Root tip morphology, anatomy, chemistry and potential hydraulic conductivity vary with soil depth in three temperate hardwood species. Tree Physiol 36:99–108. https://doi.org/10.1093/treephys/tpv094

Warren JM, Hanson PJ, Iversen CM, et al (2015) Root structural and functional dynamics in terrestrial biosphere models - evaluation and recommendations. New Phytol 205:59–78. https://doi.org/10.1111/nph.13034

Warren JM, Norby RJ, Wullschleger SD (2011) Elevated CO 2 enhances leaf senescence during extreme drought in a temperate forest. 117–130. https://doi.org/10.1093/treephys/tpr002

Weiss J V., Emerson D, Megonigal JP (2005) Rhizosphere Iron (III) Deposition and Reduction in a Juncus effusus L.-Dominated Wetland . Soil Sci Soc Am J 69:1861–1870. https://doi.org/10.2136/sssaj2005.0002

Whiting GJ, Chanton JP (1996) Control of the diurnal pattern of methane emission from emergent aquatic macrophytes by gas transport mechanisms. Aquat Bot 54:237–253. https://doi.org/10.1016/0304-3770(96)01048-0

Wiens JJ (2016) Climate-Related Local Extinctions Are Already Widespread among Plant and Animal Species. PLoS Biol 14:1–18. https://doi.org/10.1371/journal.pbio.2001104

Wright EL, Black CR, Cheesman AW, et al (2013a) Impact of simulated changes in water table depth on ex situ decomposition of leaf litter from a neotropical peatland. Wetlands 33:217–226. https://doi.org/10.1007/s13157-012-0369-6

Wright EL, Black CR, Turner BL, Sjögersten S (2013b) Environmental controls of temporal and spatial variability in CO2 and CH4 fluxes in a neotropical peatland. Glob Chang Biol 19:3775–3789. https://doi.org/10.1111/gcb.12330

Wright IJ, Reich PB, Westoby M, et al (2004) The worldwide leaf economics spectrum. Nature 428:821–827. https://doi.org/10.1038/nature02403

Yamamoto F, Sakata T, Terazawa K (1995) Physiological, morphological and anatomical response of Fraxinus mandshurica seedlings to flooding. Tree Physiol 15:713–719. https://doi.org/10.1093/treephys/15.11.713

Yamauchi T, Abe F, Tsutsumi N, Nakazono M (2019) Root cortex provides a venue for gas-space formation and is essential for plant adaptation to waterlogging. Front Plant Sci 10:. https://doi.org/10.3389/fpls.2019.00259

Yamauchi T, Nakazono M (2022) Mechanisms of lysigenous aerenchyma formation under abiotic stress. Trends Plant Sci 27:13–15. https://doi.org/10.1016/j.tplants.2021.10.012

Yamori W, Hikosaka K, Way DA (2014) Temperature response of photosynthesis in C3, C4, and CAM plants: Temperature acclimation and temperature adaptation. Photosynth Res 119:101–117. https://doi.org/10.1007/s11120-013-9874-6

Zhao X, Tian Q, Michelsen A, et al (2023) The effect of experimental warming on fine root functional traits of woody plants: Data synthesis. Sci Total Environ 894:165003. https://doi.org/10.1016/j.scitotenv.2023.165003

Zhen B, Li H, Niu Q, et al (2020) Effects of combined high temperature and waterlogging stress at booting stage on root anatomy of rice (oryza sativa L.). Water (Switzerland) 12:1–14. https://doi.org/10.3390/w12092524

Zhou M, Bai W, Li Q, et al (2021) Root anatomical traits determined leaf-level physiology and responses to precipitation change of herbaceous species in a temperate steppe. New Phytol 229:1481–1491. https://doi.org/10.1111/nph.16797

Zhou M, Wang J, Bai W, et al (2019) The response of root traits to precipitation change of herbaceous species in temperate steppes. Funct Ecol 33:2030–2041. https://doi.org/10.1111/1365-2435.13420

Zúñiga-Feest A, Bustos-Salazar A, Alves F, et al (2017) Physiological and morphological responses to permanent and intermittent waterlogging in seedlings of four evergreen trees of temperate swamp forests. Tree Physiol 37:779–789. https://doi.org/10.1093/treephys/tpx023